

Curtin Medical School

**Understanding the Relationship between Iron and Lipid Metabolism in
Non-alcoholic Fatty Liver Disease**

Abhishek Kumar Singh

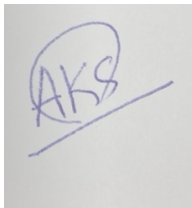
**This thesis is presented for the Degree of
Doctor of Philosophy
at
Curtin University**

August 2022

Declaration

To the best of my knowledge and belief this thesis contains no material previously published by any other person except where due acknowledgment has been made. This thesis contains no material which has been accepted for the award of any other degree or diploma in any university.

The research presented and reported in this thesis was conducted in compliance with the National Health and Medical Research Council Australian code for the care and use of animals for scientific purposes 8th edition (2013). The proposed research study received animal ethics approval from the Curtin University Animal Ethics Committee, Approval Number # **AEC_2015_40**



Signature:

Date: 31/08/2022

Acknowledgements

“**Arise, awake, stop not till the goal is reached,**” said **Swami Vivekananda**. I am delighted to have reached so far after years of hurdles and persistence that my PhD thesis is seeing the light of the day. I am indebted to **Almighty SAI** for being the invisible force, which kept me going through out my PhD journey. This journey would not have been possible without the unconditional love and support of my parents, Mr **KNP Singh** and Mrs **Mamta Singh** who gave me the freedom to do and choose what I like. Mom and Dad have been the reason for everything which I have achieved so far, and I am sure they will be proud that I am finishing my PhD. I cannot forget all the sacrifices which they have made for me to reach where I am today.

Any academic journey is not possible without the support and guidance of excellent mentors. I am, fortunate, to have had **Professor Nagini Siddavaram & Professor Balraj Mittal** who supported, mentored, and introduced me to the world of biomedical research so that I was able to start my PhD journey. I would like to thank the lab members of both the labs especially **Dr Priydarshini & Dr Sonam Tulsyan** who helped me with my undergraduate and postgraduate research in the respective labs which paved the way for my PhD.

My PhD journey would not have been successful if it was not for the guidance and support of my supervisors, **Dr Ross Graham, A/Prof Cyril Mamotte** and **Prof Leon Adams**. Ross has been one of the best supervisors anyone can have. He has supported me both personally and professionally and his knowledge in the field of iron biology has been of immense help and has made me much more knowledgeable and competent since starting my PhD. Cyril has been a valuable supervisor with his vast knowledge and experience in clinical biochemistry. Leon with his clinical expertise has always helped whenever I approached him. I would be failing in my duty if I do not acknowledge the help of **A/Prof Vincent Williams** and **Miss Sarah Loi**, Senior Scientific Officer in helping me out with histology. In fact, Vin has helped me with one of the novel findings in my thesis. I would also like to thank my past thesis chair **Professor Elizabeth Watkin** for the immense help and guidance during challenging times. I also acknowledge the help of **Dr Kylie Munyard** in some very tough times during my PhD.

During the mid-years of my PhD, I met a wonderful lady **Shubhika Lal** who is my wife now. I started my PhD journey due to my passion for research and science but if it is seeing the final light it is due to Shubhika. I am sure I will not be able to find someone better to be a life partner. She made sure that I had food to eat when I was working late, she checked on me every day to make sure I was alright. She kept me motivated whenever I was down and checked my progress

every day. She has given me the support whenever I needed it and has been by my side during the most challenging times of my PhD. I know words are not enough to describe everything she has done for me, but I will cherish it for a lifetime. I dedicate this thesis to **Shubhika**.

I would also like to acknowledge the **School of Medicine, CHIRI and Graduate Research School** for providing me the financial and research support during my PhD. My special thanks to **Dr Rob Steuart, Mr Sam Siem and Ms Winnie Pun** in CHIRI. I would also like to thank **Dr Beng Chua & Dr Tara Pike** for helping me conduct my animal studies. I would also like to thank **Dr Kevin Keane & Dr Rodrigo Carlessi** for helping me with some *in vitro* experiments.

PhD journey cannot be fun without some wonderful lab members. I am fortunate to have very understanding and helpful lab mates. I would like to thank **Dr Dorji Dorji, Rob Harvey, Sara McGeough, Clinton Kidman, James Chasland, Keea Inder-Smith, Bryce Tremethick and Gorcin Kurejsepi** for all the help and support in the lab and for helping me out with optimisations and animal work. Special mention goes to **Dorji, Clinton and James** who helped me with some experiments and looked after my mice when I was away.

I am very lucky to have some wonderful friends who have become family. I would like to acknowledge **Dr Thiru Sabapathy, Dr Himel Nahreen Khaleque, Mr Raihan Shafique, Dr Imran Khan, Dr Abhijeet Deshmukh, Dr Ratish Permala and Dr Homayoun Fathollahzadeh**, who have been a strong support and motivated me to keep going when I was down. Thiru has been very supportive, and I acknowledge his help in setting up experiments and helping me with various discussions around the results and has kept me motivated throughout my PhD journey. Imran has been a big brother offering advice and suggestions every time I needed one. Himel has been a wonderful friend and a constant support throughout. I am indebted to all these wonderful friends who have helped me come a long way. I would also like to acknowledge all my colleagues in the school and CHIRI who have helped me in some way or the other during my PhD especially **Dr Gaewyn Ellison** and the lab members of **Tirnitz-Parker** lab at CHIRI.

I would also like to acknowledge my younger brother, **Ankit** who has always believed in me and supported me throughout my journey. He made sure that I was fine even though he is miles away in India and always told me how proud he is of my journey. The support from family cannot be ignored and I am lucky to have a wonderful extended family. I would like to thank my father-in-law **Dr Murari Lal** who has always checked my progress and shared with me his life experiences which has kept me going through the testing times. I thank him for all the support and guidance. My mother-in-law, **Poonam Lal** needs a special mention for all the belief

and faith she has shown in me and all the support she has given me as a family. My brother in-law **Dr Nikhil Lal** a budding surgeon has been in constant touch with me to make sure I was doing fine. In the end, I am thankful to everyone who was directly or indirectly involved in making this thesis a success.

Abbreviations

ACAT	Acyl-CoA cholesterol acyltransferase
ATP	Adenosine triphosphate
DNA	Deoxy ribonucleic acid
DNL	De novo lipogenesis
ER	Endoplasmic reticulum
ETC	Electron transport chain
FA	Fatty acid
FAC	Ferric ammonium citrate
FAO	Fatty acid oxidation
FC	Free cholesterol
FCCP	Carbonyl cyanide-4-phenylhydrazon
FFA	Free fatty acid
FPN	Ferroportin
H&E	Haematoxylin and eosin
HFD	High fat diet
HSC	Hepatic stellate cell
IL	Interleukin
IMM	Inner mitochondrial membrane
IR	Insulin resistance
IRE	Iron responsive element
IRP	Iron responsive protein
LPC	Liver progenitor cell
MUFA	Mono unsaturated fatty acid

NAFLD	Non-alcoholic fatty liver disease
NASH	Non-alcoholic steatohepatitis
NHI	Non-haem iron
NTBI	Non transferrin bound iron
OA	Oleic acid
OCR	Oxygen consumption rate
OCT	Optimal cutting temperature
OMM	Outer mitochondrial membrane
ORO	Oil Red O
PA	Palmitic acid
PUFA	Poly unsaturated fatty acid
RNA	Ribonucleic acid
ROS	Reactive oxygen species
RT PCR	Real time polymerase chain reaction
SEM	Standard error of mean
TF	Transferrin
TFR	Transferrin receptor
TG	Triglyceride
TNF	Tumour necrosis factor
UTR	Untranslated region
VLDL	Very low-density lipoprotein
α -SMA	Alpha smooth muscle actin

Table of Contents

Declaration.....	2
Acknowledgements.....	3
Abbreviations.....	6
Table of Contents.....	8
List of Figures.....	11
List of Tables.....	12
Abstract.....	13
Chapter 1 Literature Review.....	16
1.0. General introduction.....	16
1.1 Non-Alcoholic Fatty Liver Disease.....	17
1.2. NAFLD Pathogenesis.....	18
1.3. Iron and NAFLD.....	19
1.3.1. Iron Biology.....	19
1.3.2 Hepatic Iron Metabolism.....	20
1.4. Genes Involved in Liver Iron Homeostasis.....	21
1.5. Iron Overload and NAFLD.....	24
1.6. Hepatic Lipid Metabolism.....	26
1.6.1 Hepatic Cholesterol and NAFLD.....	26
1.7. Iron Overload and Hepatic Lipid Metabolism.....	28
1.8. Mitochondria and NAFLD.....	29
1.9. Hepatic Fatty Acid Oxidation.....	30
1.10. Mitochondrial Dysfunction and NAFLD.....	31
1.11. Iron and Mitochondria.....	32
1.12. Iron Transport to the Mitochondria.....	33
1.13. Fatty Acids and Mitochondria.....	35
1.15. Objectives of this Thesis.....	36
Chapter 2 Materials and Methods.....	38
2.1. Cell Culture Methods.....	38
2.1.1. Cell Culture.....	38
2.1.2. Cell Viability Assay.....	38
2.1.3. Iron Loading.....	38
2.1.4. Free Fatty Acid Loading.....	38
2.1.5. Oil Red-O Staining.....	39
2.2. Mitochondrial Bioenergetics.....	39
2.2.1. Assay Media Preparation.....	40
2.2.2. Mitochondrial Stress Reagents.....	40
2.2.3. Mitochondrial Bioenergetics Assay Day Preparations.....	40
2.3. Animal Studies.....	41
2.3.1. Animal Maintenance.....	41
2.3.2. Diet Preparation.....	41
2.3.3. Sample Collection.....	42
2.3.4 RNA Extraction.....	42
2.3.5. RNA Quantification.....	43
2.3.6. cDNA Synthesis.....	43
2.3.7. Real Time- Quantitative Polymerase Chain Reaction (RT-qPCR).....	43
2.3.8. Non-haem Iron Assay.....	44
2.3.9. Histology.....	44
2.4. Haematoxylin and Eosin (H&E) Staining.....	46

2.4.1. Perls' Prussian Blue Staining.....	46
2.4.2. Oil Red O Staining for Liver Tissue	46
2.4.3. Isolation of Mouse Liver Mitochondria	47
2.4.4. Immunohistochemistry of Mouse Liver.....	47
2.4.5. Statistical Analysis.....	48
Chapter 3 Effect of Iron and Free Fatty Acid Loading on Mitochondrial Bioenergetics	49
3.1. Background.....	49
3.2. Methods.....	49
3.3. Results	50
3.3.1. Cell Viability & Oil Red O Staining.....	50
3.3.2. Effect of Iron and Free Fatty Acid Loading on Oxygen Consumption Rate	52
3.3.2.1. Basal Respiration	53
3.3.2.2. Proton Leak.....	53
3.3.2.3. Maximal Respiration.....	53
3.3.2.4. Spare Respiratory Capacity.....	53
3.3.2.5. Non-mitochondrial Respiration.....	54
3.3.2.6. ATP Production	54
3.4. Discussion.....	56
Chapter 4 Determination of Iron Concentration to Induce Dietary Iron Loading	61
4.1. Background.....	61
4.2. Methods.....	62
4.3. Results.....	64
4.3.1 Hepatic iron concentration.....	64
4.3.2. Effect of iron loading on mitochondrial cholesterol	67
4.3.3. Body Weight	68
4.3.4. Genes involved in hepatic iron homeostasis	69
4.3.5. Genes involved in mitochondrial and peroxisomal fatty acid oxidation.....	71
4.4. Discussion.....	73
Chapter 5 Hepatic Gene Expression in Dietary Iron Loading	77
5.1. Background.....	77
5.2. Methods.....	78
5.3. Results.....	80
5.3.1. Mouse body weight and hepatic iron concentration	80
5.3.2. Expression of hepatic iron homeostasis genes	82
5.3.3. Expression of mitochondrial and peroxisomal fatty acid metabolism genes	83
5.3.4. Effect of iron loading on iron homeostasis genes in the spleen	85
5.3.5. Effect of iron loading on iron homeostasis genes in the duodenum	86
5.3.6. Liver morphology	88
5.3.7. Iron loading and hepatic cholesterol crystals.....	90
5.3.8. Hepatic injury markers.....	92
5.4. Discussion.....	94
Chapter 6 Hepatic Changes Associated with High fat and High Iron diet.....	101
6.1. Background.....	101
6.2. Methods.....	102
6.3. Results.....	103
6.3.1. Mouse hepatic iron concentration and liver histology	103
6.3.2. Mouse body and liver weight.....	106
6.3.3. Expression of hepatic iron homeostasis genes	107
6.3.4. Expression of mitochondrial and peroxisomal fatty acid metabolism genes	108
6.3.5. Effect of high fat and high fat plus iron on iron homeostasis genes in the spleen.....	111
6.3.6. Effect of high fat and high fat plus iron on iron homeostasis genes in the duodenum	112

6.3.7. Differences in hepatic cholesterol crystals associated with high fat and high fat plus iron.....	113
6.3.8 Markers of hepatic injury.....	115
6.4. Discussion.....	117
Chapter 7 General Discussion.....	121
7.1 Background.....	121
7.2 Effect of iron and lipid loading on mitochondrial respiration.....	121
7.3. Effect of varying dietary iron concentration on hepatic gene expression.....	122
7.4. Hepatic changes associated with dietary iron overload and high fat diet.....	126
7.5. Effect of Iron Overload on Hepatic Cholesterol Crystal.....	129
7.6. Conclusion.....	131
7.7. Limitations.....	131
7.8. Future Directions.....	132
Publications and Presentations.....	134
References.....	135
Appendix A.....	150
Appendix B.....	151

List of Figures

Figure 1.1	Overview of systemic iron homeostasis.	24
Figure 1.2	Representation of mitochondrial fatty acid oxidation	31
Figure 2.1.	Animal dietary plan	42
Figure 3.1	Effect of FFA and iron on cell viability	50
Figure 3.2	Oil Red O stained AML12 cells for neutral lipids	51
Figure 3.3	Measurement of mitochondrial bioenergetics in real-time using a Seahorse XF96 analyser	52
Figure 3.4	Changes in mitochondrial respiration upon iron and fatty acid loading in AML12 cells for 12 h	55
Figure 4.1	Influence of Dietary Iron Loading on Non-Haem Iron	65
Figure 4.2	Influence of Iron Loading on Hepatic Iron	66
Figure 4.3	Influence of Iron Loading on Mitochondrial Cholesterol Content	67
Figure 4.4	Effect of Iron Loading on Body Weight	68
Figure 4.5	Influence of Iron Loading on Hepatic Iron homeostasis genes	70
Figure 4.6	Influence of Iron Loading on Mitochondrial and Peroxisomal Fatty Acid Oxidation Genes	72
Figure 5.1	Mouse body weight	80
Figure 5.2	Hepatic non-haem iron concentration	81
Figure 5.3	Hepatic expression of iron homeostasis genes	82
Figure 5.4	Hepatic expression of mitochondrial fatty acid oxidation genes	83
Figure 5.5	Hepatic expression of peroxisomal lipid metabolism genes	84
Figure 5.6	Splenic expression of iron homeostasis genes	85
Figure 5.7	Duodenal expression of iron homeostasis genes	87
Figure 5.8	Liver histology	89
Figure 5.9	Hepatic cholesterol crystals	91
Figure 5.10	Markers of hepatic inflammation	93

Figure 6.1	Hepatic non-haem iron concentration	104
Figure 6.2	Liver histology & neutral lipid staining	105
Figure 6.3	Mouse body and liver weight	106
Figure 6.4	Hepatic expression of iron homeostasis genes	107
Figure 6.5	Hepatic expression of mitochondrial fatty acid oxidation genes	109
Figure 6.6	Hepatic expression of peroxisomal lipid metabolism genes	110
Figure 6.7	Splenic expression of iron homeostasis genes	111
Figure 6.8	Duodenal expression of iron homeostasis genes	112
Figure 6.9	Hepatic cholesterol crystals	114
Figure 6.10	Immunohistochemistry of mouse liver	116
Figure 7.1	Hepatic non-haem iron concentration	125

List of Tables

Table 2.1	Primer details	42
Table 5.1	List of primary and secondary antibodies.	79

Abstract

Non-alcoholic fatty liver disease (NAFLD) is recognised as a leading cause of liver related mortality in Australia and worldwide. The prevalence of NAFLD related liver deaths is set to increase to 85% of total liver related deaths in Australia by 2030. NAFLD is defined as the presence of excess fat in the liver in the absence of significant alcohol consumption. There are several risk factors which are associated with NAFLD including iron overload and dysregulated lipid metabolism. It is estimated that around 30% of NAFLD patients present with altered iron parameters. Iron has long been associated with the progression to late-stage liver diseases such as fibrosis and hepatocellular carcinoma but the role of iron in initial NAFLD development is not completely understood.

In the present study, I investigated the role of iron in initial fat accumulation and its role in altering lipid metabolism using an *in vitro* and an animal model of NAFLD. The *in vitro* study investigated the role of iron and fatty acid loading and its effect on mitochondrial bioenergetics. AML12, a mouse hepatocyte cell line, was used to investigate how iron and fatty acid loading alters parameters associated with mitochondrial bioenergetics such as basal respiration, proton leak, spare respiratory capacity, non-mitochondrial respiration, and ATP production. The results show that iron and fatty acid loading increases mitochondrial bioenergetic parameters. Importantly, iron on its own as well, as in the presence of saturated (palmitic acid) and unsaturated (oleic acid) fatty acids, was found to be the key driver of the increased changes observed across all the parameters. The results indicate that iron and free fatty acid loading may increase energy production in the mitochondria.

C57BL/6 mice were used as the dietary model of NAFLD to investigate the role of iron by narrowing down on a concentration of carbonyl iron which is sufficient to load the liver and mimic initial iron loading. Changes in gene expression associated with iron homeostasis, and mitochondrial and peroxisomal fatty acid oxidation were investigated in the livers of mice fed different concentrations of carbonyl iron. Liver morphology, along with hepatic and mitochondrial non-haem iron (NHI), was also examined. The results indicated an increased iron deposition in the liver with increasing iron concentration which was reflected by the increased expression of *Hamp1* and was visible in the histological examination for iron staining as well as the liver and mitochondrial NHI results. The liver iron concentration ranged from $3.9 \pm 0.3 \mu\text{mol} / \text{g}_{\text{liver}}$ in mice fed 0.25% carbonyl iron to $15 \pm 2.6 \mu\text{mol} / \text{g}_{\text{liver}}$ in mice fed 2% carbonyl iron. The presence of inflammatory cells was also detected in the livers of mice fed iron diet.

To investigate the interaction between iron and fatty acid loading, another group of mice were fed a control, iron loaded, high fat, or high fat + iron diet. It was interesting to note that the high fat diet was able to reduce liver NHI compared to mice which were fed high fat plus iron. Further results obtained from these studies indicated that iron and high fat diet had a differential effect on iron metabolism, mitochondrial, and peroxisomal fatty acid oxidation genes. Mitochondrial fatty acid oxidation genes (*Acadm* & *Hadha*) were downregulated in mice fed an iron loaded control diet, but no significant change was observed in genes associated with peroxisomal fatty acid oxidation whereas, in mice fed a combination of iron and high fat, peroxisomal fatty acid oxidation genes (*Acaa1a* & *Slc27a2*) were upregulated. To investigate the reason for the decreased liver NHI in the presence of high fat, gene expression of iron homeostasis genes was investigated in the spleen and the duodenum. In the spleen, *Hamp1* was downregulated in the mice fed the control plus iron diet compared to control, but the other genes did not show any significant differences. In the duodenum, the control plus iron diet led to a decrease in *Dmt1* with *Fpn* exhibiting a decreasing trend. In the mice fed high fat plus iron, *Dmt1* and *Tfr1* were upregulated compared to mice fed high fat alone.

The present study shows that cholesterol crystals form in the liver as early as the steatosis phase in mice fed a high fat diet and there are significantly fewer when iron is present in the diet. To my understanding, this is the first report linking iron to a decrease in cholesterol crystals in the liver. This finding may have important clinical and therapeutic significance as cholesterol crystals may drive inflammation and cause damage to the cell. Previous studies have linked cholesterol crystals to non-alcoholic steatohepatitis, the more advanced form of NAFLD, but not to steatosis which is the initial stage of NAFLD. The important and novel findings arising from this project was the reduction of hepatic NHI by high fat diet and the presence of cholesterol crystals in the liver of these mice.

In conclusion, the results obtained from this study indicate differential regulation of mitochondrial, peroxisomal fatty oxidation and iron metabolism genes in the duodenum by high fat, iron and high fat plus iron diet, presence of inflammatory cells in the liver of mice fed iron loaded diet and a decrease in hepatic cholesterol crystals in the presence of high hepatic iron. These findings are important because they manifest in the initial stage of NAFLD as compared to the late stages which have been the focus of the majority of pre-clinical and clinical studies. Iron and high fat driving changes in the early stages of NAFLD give an insight into changes which may be clinically relevant to treating NAFLD. In addition, this study has led to new questions such as the mechanism by which cholesterol crystals are reduced in the

presence of iron in high fat diet, reduction of hepatic iron by high fat diet which will require further investigation and are included as potential future directions.

Chapter 1 Literature Review

1.0. General introduction

Non-alcoholic fatty liver disease (NAFLD) is predicted to be the next global epidemic given the increasing incidence of obesity worldwide [1]. NAFLD consists of a spectrum of liver-related disorders from simple steatosis to non-alcoholic steatohepatitis (NASH) to cirrhosis and end-stage liver disease [2]. The prevalence of NAFLD in western populations is estimated to be between 20 and 30%, [3] which increases to 90% in obese people [4]. NAFLD is considered to be the hepatic manifestation of the metabolic syndrome, a set of four metabolic risk factors: obesity, glucose intolerance, dyslipidaemia (including altered cholesterol) and hypertension [5].

The liver is the metabolic centre of the body and an essential site for iron and lipid metabolism and the main site for any potential interaction between them. Even a slight iron imbalance can have serious clinical consequences, as there is no specialised mechanism for iron excretion. Iron overload has been linked to the pathogenesis and progression of NAFLD, and although the mechanism of action is not clearly understood, redox cycling is considered to be of central importance [6, 7].

Hepatic lipid metabolism is crucial to a healthy liver. Any imbalance in the uptake, synthesis or breakdown of fatty acids can lead to hepatic steatosis, which is the first stage of NAFLD. Both iron deficiency and overload can affect hepatic lipid metabolism. In rats, iron deficiency has been shown to increase hepatic lipogenesis leading to triglyceride (TG) accumulation and steatosis [8]. Reduced beta-oxidation of fatty acids is proposed to be the reason for the TG accumulation; this then, can be linked to reduced expression of the hepatic long-chain fatty acid fusion molecule, acyl-carnitine, in the iron deficient state, as two hydroxylases which are involved in carnitine synthesis require iron [9].

Iron overload has been linked to progression of NAFLD [10], often attributed to increased oxidative stress and lipid peroxidation [11]. In non-alcoholic steatohepatitis (NASH), oxidative stress has been linked to cell death by depletion of adenosine triphosphate (ATP), nicotinamide adenine dinucleotide (NAD) and glutathione, and further by damaging DNA, lipids and proteins within hepatocytes [11]. The level of oxidative stress has been found to be reduced in rats fed an iron-deficient diet [12]. In human biopsies from NAFLD patients, increased hepatic iron has been associated with increased lipid peroxidation [13].

In summary, both iron deficiency and overload have clinical consequences and affect liver metabolism. Moreover, iron overload has been linked to the pathogenesis and progression of NAFLD. Different animal models have been used to study the effect of iron and fat overload and deficiency in NAFLD. However, conflicting results have been obtained due to a variety of factors, including differences in strain, sex and feeding duration [14, 15] which will be discussed in detail in the coming chapters. The present study looks into the relationship between iron and lipid metabolism in NAFLD using both *in vitro* and *in vivo* models.

1.1 Non-Alcoholic Fatty Liver Disease

Non-alcoholic fatty liver disease (NAFLD) is a collective term for a spectrum of chronic liver disorders. It starts with an initial fatty deposition in hepatocytes (hepatic steatosis) where histologically a minimum of 5% of the hepatocytes contain fat [16] exceeding 5-10% of the liver weight [17] and may progress to NASH in which hepatocyte fat deposition is associated with liver injury and fibrosis. The increase in the prevalence of NAFLD has occurred in parallel with the rise in cases of obesity and diabetes [18], thus making it the most common cause of chronic liver disease in western countries [19, 20]. The prevalence of NAFLD in the western population is estimated to be between 30 and 40% in males, and 15 and 20% in females [20], increasing to 90% in obese people [4]. The clinically significant form, NASH, has a lower prevalence rate of about 2-3% in the general population [21] rising to 37% in the obese population [22]. It is important to note that the burden of NAFLD is on the rise in children and young adults, reported to be 3% in the general paediatric population rising significantly to 53% in obese children [22, 23]. Recent evidence suggests that NAFLD takes the form of a multisystem disease affecting not only the liver but other organs and regulatory pathways [24]. Metabolic syndrome and NAFLD share many factors including, among other things, high circulating low-density lipoprotein (LDL)-cholesterol and triglycerides (TG), low high-density lipoprotein (HDL)-cholesterol and insulin resistance (IR) [25].

As mentioned, iron has also been linked to NAFLD but interestingly, clinical trials on NAFLD patients where phlebotomy was performed to deplete iron have yielded conflicting results. Some studies [26-28] have reported improvement in liver enzymes and IR in patients with steatosis, classified based on the NAFLD activity score, whereas a randomised, controlled trial found iron removal by phlebotomy had no association with any significant changes in IR, liver injury, assessed based on alanine aminotransferase (ALT), hepatic steatosis, lipid peroxidation, or quality of life [29]. It is argued that some of these studies were single-arm or non-randomised

and, therefore, prone to bias, not least by way of occurrence of “regression to the mean” [29]. Despite conflicting results in several human studies, the role of disordered iron metabolism in NAFLD cannot be ignored. A recent study in two independent cohorts of European NAFLD patients demonstrated that hepatic iron is a strong predictor of serum ferritin levels compared to non-NAFLD controls [30]. Elevated serum ferritin has also been shown to be an independent predictor of histologic severity in steatosis and NASH; moreover, it showed strong association with fibrosis and NAFLD activity score, a widely used grading measure [31]. In summary, there is a clear association of hepatic iron deposition with NAFLD, although the nature of this association remains ambiguous.

1.2. NAFLD Pathogenesis

The pathogenesis of NAFLD is explained based on a two-hit hypothesis where the first hit is the initial fat accumulation (steatosis). The progression from steatosis to NASH is not a sudden change but develops over time where several insults sensitize the liver causing liver damage due to the release of inflammatory cytokines/adipokines, mitochondrial dysfunction and oxidative stress which contribute to NASH and/or fibrosis and fall under the second hit [32, 33]. Recently, with many more factors being linked to the pathogenesis and progression of NAFLD, a new multiple hit theory has been proposed [34] which takes into account the multiple insults. The current multiple-hit theory considers factors such as dietary habits, environmental and genetic factors. These factors can lead to development of insulin resistance, obesity and an altered gut microbiome. IR results in increased *de novo* lipogenesis (DNL) which is linked to increased FA influx in the liver. Changes in gut flora are associated with increased FA production in the bowel and thus increasing bowel permeability leading to increased FA absorption. Genetic and epigenetic factors have been thought to affect hepatocyte fat content, enzymatic processes and inflammation leading to progression of NAFLD [34].

The role of genetic factors in NAFLD pathogenesis has been linked to a number of single nucleotide polymorphisms (SNPs) which have been associated with FFA flux, and cytokine production [35]. Epigenetic modifications such as DNA methylation, histone modification and changes in microRNA (miRNA) activities have also been linked to NAFLD pathophysiology [36]. miRNAs have been found to influence biological processes such as glucose and lipid metabolism which are also epigenetically altered in NAFLD [37, 38]. The progression of NAFLD to NASH is also considered to be influenced by DNA methylation [39]

The change in dietary habits of the world's population has led to an increased prevalence of obesity and IR [1]. The rise in the number of cases of obesity along with the development of IR and environmental and genetic factors has proven to play an important role in the pathogenesis of NAFLD [34].

IR has been linked to hepatic lipid accumulation [40]. As a consequence of fat accumulation, there is a chain of events which include structural, morphological, ultrastructural, and functional alterations leading to mitochondrial dysfunction along with oxidative and reactive endoplasmic reticulum (ER) stress. All these parameters play an important role in the progression of NAFLD [41]. The mechanisms involving these changes and their roles in NAFLD are discussed in subsequent sections.

Intestinal absorption of monosaccharides has been linked to the gut microbiota, also leading to increased DNL, and suppression of fasting-induced adipocyte factor, leading to the accumulation of triglycerides in adipocytes [42]. Interestingly, it has been reported that the gut microbiota are involved in choline metabolism, and dysregulation of choline metabolism can lead to hepatic inflammation and damage [43]. The gut microbiota convert choline into toxic dimethylamine and trimethylamine, which are rapidly absorbed by the liver and converted into trimethylamine oxide (TMAO) causing hepatic inflammation [43]. Choline is an important component of cell membrane phospholipids, and plays a crucial role in lipid metabolism preventing abnormal hepatic lipid accumulation [44]. The mechanism behind this is thought to be the activation of nuclear receptor, liver receptor homologue 1 (LRH-1) for which dilauroyl phosphatidylcholine (DLPC) is an endogenous ligand. The activation of LRH-1 increases bile acid biosynthesis lowers triglycerides and decreases serum glucose [45].

Apart from the various multiple-hits discussed above, data from our laboratory suggests that iron plays an important role in the pathogenesis of NAFLD where it may act as part of the first hit by increasing the initial lipid accumulation. It has been shown in mice that dietary iron loading leads to up-regulation of the cholesterol biosynthesis pathway [46] and that iron loading leads to increased fat accumulation in AML12 cells [227].

1.3. Iron and NAFLD

1.3.1. Iron Biology

Iron is an essential trace element and an important structural and functional component of many physiological systems. Iron plays pivotal roles in oxygen transport and other biological

processes such as DNA synthesis. Due to the redox properties of iron, its entry and storage in mammalian systems are very tightly regulated.

The amount of iron entering the circulation is regulated at the level of duodenal enterocytes to maintain a balance between iron absorption and loss. Absorption of non-haem iron is dependent on the body's requirements and existing iron stores. When the body has enough iron stored, absorption is low. Irrespective of tight regulation, iron deficiency and iron overload can occur and may have serious clinical consequences [47].

1.3.2 Hepatic Iron Metabolism

The liver plays a pivotal role in iron metabolism and is the primary storage site for iron. It expresses a wide range of molecules which play an important role in iron transport and homeostasis. Iron is crucial for all life forms due to its role in numerous cellular processes including synthesis of DNA, cell proliferation and differentiation, gene regulation and drug metabolism. Mammals, including humans, have limited ability to excrete iron [48] which means iron balance has to be maintained completely through regulated iron absorption from the diet [49, 50]. At physiological pH, iron, in its free form, is insoluble and also toxic. Therefore, iron is always bound to specific ligands to render it soluble and non-toxic. The toxicity of iron arises due to its ability to cycle between its oxidation states. The uncontrolled release of an electron from ferrous iron may lead to the formation of reactive oxygen species (ROS) which can oxidise lipids, proteins and DNA [51]. At the same time, biological systems take advantage of the oxidation states and redox potential of iron and adjust the chemical reactivity of iron to meet physiological needs [52].

In mammalian systems, iron is transported bound to the plasma glycoprotein, transferrin, which is predominantly produced in the liver [53] but small amounts can also be synthesised in the brain and testes [54, 55]. Transferrin concentration in normal human plasma is between 25 and 50 $\mu\text{mol/L}$ and is about one-third saturated with iron [56]. The buffering capacity is provided by the remainder of the unoccupied binding sites on transferrin to counter any increase in plasma iron, which is important given the toxicity of free iron. Upon uptake by the tissues, iron is transferred to the cytosolic pool where it is stored in the form of ferritin or incorporated into molecules such as haem or iron-sulphur clusters. About 80% of hepatic iron is in the form of ferritin, 2-3% is haem and the remainder is in the transit pool (a pool of chelatable and redox active iron) or bound to transferrin [57].

The liver is responsible for three main functions in regard to iron homeostasis. It is the major storage site of iron, it plays a very important role in the transport of iron from hepatocytes to the circulation based on biological demand, and it is very important in regulation of iron homeostasis by regulating the level of the iron regulatory hormone, hepcidin, which will be discussed in detail in the next section. It has been confirmed histologically that iron is distributed around the portal region of the liver and decreases in concentration towards the central vein region. Under conditions of hepatic iron overload, this feature becomes very prominent [58]. Hepatocytes are the most loaded cell type with lesser loading detected in Kupffer cells [59]. Any dysregulation in the liver's ability to maintain iron homeostasis paves the way for iron-related disorders. Anaemia and iron overload are the most prominent iron-related disorders affecting the global population [60]. Excess hepatic iron plays an important role in the pathogenesis and progression of steatohepatitis, fibrosis, cirrhosis and hepatocellular carcinoma [61].

1.4. Genes Involved in Liver Iron Homeostasis

The liver expresses a wide range of molecules which function in maintaining iron homeostasis, including a complex range of genes that have been associated with iron-related functions. An overview of systemic iron homeostasis is shown in figure 1.1. Transferrin receptor 1 (TFR1) is a cell surface receptor which mediates cellular iron uptake by receptor-mediated endocytosis. Diferric transferrin binds to TFR1 and is endocytosed [58]. The pH of the extracellular fluid is more conducive to the binding of diferric transferrin than monoferric or apo- transferrin [59]. Acidification of the resulting endosome reduces the affinity of transferrin for iron, leading to the detachment of iron [62], which is transported out of the endosome and into the cytosol by DMT1.

Iron regulates the expression of TFR1 by post-transcriptional modifications by iron regulatory proteins (IRP1 and IRP2). These are cytoplasmic proteins which bind to iron-responsive elements (IRE) present in the untranslated region (UTR) of mRNAs of several genes associated with iron metabolism [63, 64]. The IRPs bind to the five IRE motifs in the 3' UTR of TFR1 mRNA [65]. The activity of IRPs is regulated by cellular iron. During low cellular iron levels, the binding of IRPs protects the TFR1 transcript from degradation by nucleases allowing for more translation and leading to increased TFR1 protein levels and subsequent iron uptake. The opposite happens during cellular iron abundance, decreased IRP binding leads to the degradation of TFR1 mRNA. Apart from IRPs, TFR1 mRNA has been thought to be regulated

by endogenous ribonucleases [66, 67]. Recently, regnase-1, an endoribonuclease, has been identified which targets the 3' UTR of TFR1 mRNA [68]. Regnase-1 has been found to be a critical regulator of iron homeostasis by destabilizing mRNAs involved in iron homeostasis including TFR1 and has also been found to facilitate duodenal iron uptake due to the ribonuclease activity of Regnase-1 which destabilises prolyl-hydroxylase-domain-containing proteins (PHD3) [68]. TFR1 expression is also regulated by other mechanisms including hypoxia response element, where iron scarcity stimulates TFR1 gene transcription through HIF-1 α , a transcriptional activator of hypoxia-sensitive genes [69], cytokines, mitogens and growth factors [69-72].

Iron endocytosed by TFR1 is transported from the endosome to the cytosol following reduction to its ferrous state by the ferrireductase, six-transmembrane epithelial antigen of the prostate 3 (STEAP3), through divalent metal transporter 1 (DMT1), which is a transmembrane glycoprotein [73]. DMT1 is also known as natural resistance-associated macrophage protein 2 (NRAMP2), divalent cation transporter 1 (DCT1) and SLC11A2. It has four known isoforms: 1A/IRE(+), 1A/IRE(-), 1B/IRE(+) and 1B/IRE(-) which differ in their N and C termini arising from mRNA transcripts. The 1A/B denote the exon position of the isoforms at the 5'-end or 3'-end, respectively, giving rise to mRNAs containing (+) or lacking (-) the IRE [74]. It has been found that DMT1 operates as a metal-proton cotransporter depending on cell membrane potential and at lower pH [75]. Apart from Fe²⁺ there are several other divalent metal ions which compete with iron for transport including Mn²⁺, Cd²⁺ and Co²⁺ [75, 76]. It has been shown that iron levels regulate DMT1 (+IRE) expression. The expression of the four isoforms is organ specific. The 1A isoform is present in the polarised cells of the duodenum and kidney, and the expression of the 1B isoform is ubiquitous. It should be noted that despite being present in different cell types, all four isoforms transport Fe²⁺ at the same rate.

In diseases of iron overload such as hereditary haemochromatosis and thalassaemia major there is an unregulated supply of iron which is directed to the liver and thus the iron-carrying capacity of transferrin is overwhelmed. This results in circulating non-transferrin bound iron (NTBI) which is redox active and may prove to be toxic [77]. DMT1 has been found to be a major transporter of NTBI in hepatocytes [78]. Increased uptake of NTBI has been shown in cells with upregulated DMT1 mRNA and protein expression [78]. The first evidence of NTBI uptake by DMT1 was provided by Trinder et al. [79] who showed that DMT1 was present on the rat hepatocyte plasma membrane and was elevated in iron overloaded conditions. DMT1 functions optimally at an acidic pH and this is important because the duodenum and the endosome, which

is formed from the plasma membrane, share a similar acidic environment which is optimal for hydrolases and other enzyme activities [80]. A study in *Xenopus* oocytes has shown that DMT1 mediated modest H⁺- uncoupled facilitative Fe²⁺ transport at pH 7.4 suggesting NTBI uptake at the plasma membrane.

Export of iron from hepatocytes is solely via the iron export protein ferroportin (FPN), which is under the control of hepcidin, the central regulator of systemic iron homeostasis. FPN has been shown to be the receptor for hepcidin [81]. FPN is also regulated at the post transcriptional level by IRE/IRP signalling, where iron overload promotes FPN transcription and deficiency represses it [64, 82] but there also exists an isoform for FPN called FPN1B which lacks a 5'IRE and is not post-transcriptionally regulated by iron [82]. In macrophages, FPN is also regulated by hypoxia-inducible factor 2 (HIF2 α), nuclear factor erythroid (NRF2) and metal regulatory transcriptional factor 1 (MTF-1) at the transcriptional level [83-85]. Additionally, oestrogen has been linked to iron metabolism through the regulation of FPN signalling. Oestrogen has been shown to have an inhibitory effect on FPN expression through a functional oestrogen response element (ERE) within its promoter region [86], which may explain some of the sex-based differences seen in animal models of iron overload.

FPN is also known as solute carrier family 40 member 1 (SLC40A1), IREG1 or metal transporter protein 1 (MTP1). Three groups reported it independently in 2000 [87-89]. It has been confirmed that FPN is highly expressed in cells and tissues involved with iron transport such as duodenal enterocytes, liver macrophages, splenic red pulp macrophages, periportal hepatocytes and placental syncytiotrophoblasts [90]. FPN-mediated iron transport requires ferroxidase activity [82] which is provided by the multicopper oxidase, caeruloplasmin (CP). Studies conducted between 1950 and 1970 demonstrated that copper deficiency in animals was accompanied by iron deficiency and copper was essential for the release of iron from macrophages and hepatocytes [91-93]. The importance of an oxidase in iron transport is highlighted by two important factors, the first being that the reaction does not generate oxygen radicals in contrast to spontaneous oxidation of iron and second, under low oxygen conditions, when the oxidation of iron is low, the oxidase enhances iron oxidation [94]. In glioma cells and astrocytes, it has been shown that the absence of oxidase impairs iron transport [95, 96].

Hepcidin is a key iron regulator in vertebrates [97]. It is a 25 amino acid peptide hormone and regulates plasma iron concentration [98] by binding to FPN and decreasing iron release. Hepatocytes are the main source of circulating hepcidin, but other cell types such as macrophages and adipocytes express hepcidin mRNA albeit at much lower levels [99, 100].

Hepcidin production is regulated by iron and erythropoietic demand for iron [101]. Therefore, during iron overload hepatocytes produce more hepcidin which in turn promotes internalisation and degradation of FPN, limiting further iron absorption from the duodenum, whereas during conditions of iron deficiency, the opposite occurs, allowing more iron to enter the plasma [90]. Hepcidin production is suppressed during active erythropoiesis, making iron available for haemoglobin synthesis [102, 103]. Hepcidin production is regulated at the transcriptional level. In humans, there is only one hepcidin gene but in mice, there are two: hepcidin antimicrobial peptide-1 (Hamp1) and hepcidin antimicrobial peptide-2 (Hamp2), which share 68% similarity at the peptide level but have distinct functions where only Hamp1 plays a role in iron metabolism [104-108].

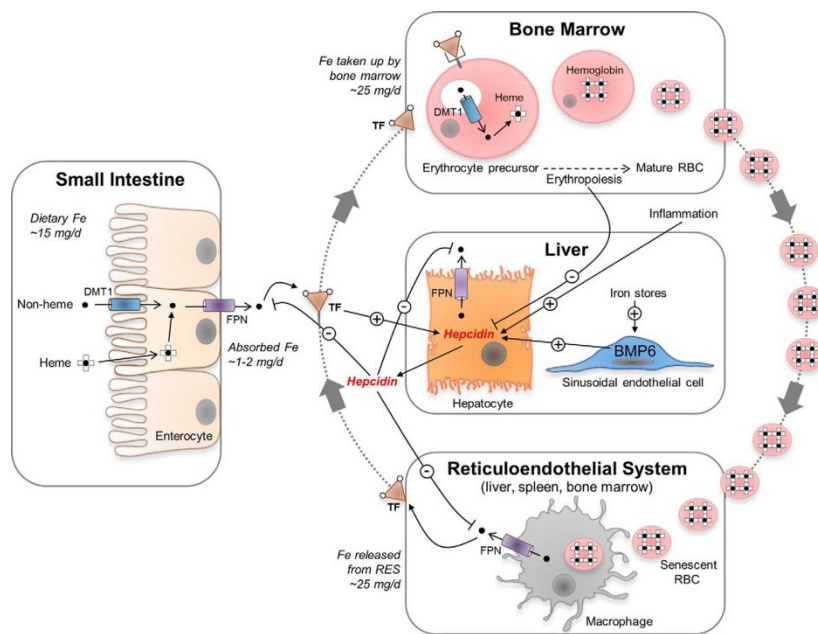


Figure 1.1. Overview of systemic iron homeostasis. Adapted from Knutson MD. Iron transport proteins: Gateways of cellular and systemic iron homeostasis. *J Biol Chem.* 2017 Aug 4;292(31):12735-12743. Used under the terms of Creative Commons CC-BY licence.

1.5. Iron Overload and NAFLD

The worldwide rise in obesity has led to an increase in cases of NAFLD [1]. It is recognised that NAFLD has emerged as an independent risk factor for type II diabetes mellitus,

cardiovascular complications, and hepatocellular carcinoma [2, 109, 110]. The risk factors leading to the pathogenesis and progression of NAFLD have been discussed in section 1.3. Apart from these, there is new evidence which shows a modest iron overload to be associated with liver injury in NAFLD but the mechanism remains unclear [6] and this has been shown in two studies where NAFLD patients had 35% and 50% hepatic iron deposition, respectively [111, 112]. Previous data from the laboratory on hepatic iron loading in mice has shown that hepatic iron loading increases liver cholesterol synthesis and hints at an additional mechanism whereby iron contributes to the initial lipid accumulation in the liver, thus contributing to the development of NAFLD [46].

The role of hepatic iron in NAFLD pathogenesis has traditionally centred on the generation of oxidative stress due to the redox nature of iron and subsequent generation of ROS. Oxidative stress has been found to be an important factor in the pathogenesis of NASH [11]. Free radicals have an unpaired electron and are redox active. They are a product of natural cell metabolism and are beneficial when they play a cytotoxic role against pathogens including bacteria. On the other hand, when the normal anti-oxidant mechanism of the cells fails to counter free radicals, they may cause damage to normal cells and tissues. Therefore, a balance between antioxidants and prooxidants is paramount to a healthy system. Anything which favours prooxidants can lead to oxidative stress. Iron is a well-known pro-oxidant and so it is not surprising that it may cause oxidative stress and lipid peroxidation in NAFLD patients [113, 114]. Other mechanisms by which oxidative stress plays a role in the pathogenesis of NASH include increased production of pro-inflammatory cytokines and the fibrogenic response [11]. Iron overload has been shown to activate hepatic stellate cells which in turn promotes fibrogenesis and also polarises macrophages leading to release of pro-inflammatory cytokines [115, 116]. Oxidative stress not only enhances steatohepatitis but also increases steatosis by degrading apolipoprotein B100 (ApoB100) resulting in decreased secretion of very low-density lipoprotein (VLDL) [117] and thus increasing retention of its major lipid load.

Oxidative stress was considerably reduced in rats fed an iron-deficient diet and after phlebotomy [12]. In patients with NAFLD, liver biopsies revealed an increased hepatic iron store which was associated with increased lipid peroxidation [13]. Increased serum thioredoxin, a marker of oxidative stress, has been observed in NASH patients and, in cultured AML12 cells, iron leads to the generation of oxidative stress and impaired insulin signalling [118, 119]. Hepatic iron has been shown to activate hepatic macrophages and hepatic stellate cells [120]

as *in vitro* studies have shown that iron activates inflammatory signalling through hepatic macrophages [121].

In summary, hepatic iron overload has been associated with the pathogenesis of NAFLD through several mechanisms including oxidative stress, reduced VLDL export, macrophage activation, stellate cell activation, ER stress and increased cholesterol synthesis. The current study is based on the hypothesis that iron plays an important role in the initial insults in NAFLD as well as its later progression to NASH.

1.6. Hepatic Lipid Metabolism

Impairment of fatty acid metabolism results in the development of hepatic steatosis, the initial stage of the NAFLD spectrum [122]. Free fatty acids (FFA) for TG synthesis are derived from plasma FFA and DNL [14]. The amount of FFA uptake from the plasma by the liver is not regulated and depends on the concentration of FFA in the plasma; the major contributor to the plasma pool is TG lipolysis from adipose tissue. Peripheral lipolysis of lipoproteins and dietary FFA further contribute to the FFA pool [14]. Fatty acid binding proteins and fatty acid translocase facilitate the hepatic uptake of fatty acids. Fatty acids undergo esterification with glycerol or cholesterol to form TGs or cholesteryl esters, respectively, once in the hepatocyte. These esters are then secreted as VLDL into the plasma and any excess is stored as lipid droplets in the cytoplasm.

Segregation of TG into different pools under normal dietary conditions is controlled by hormonal and metabolic regulatory mechanisms. Insulin is a major metabolic factor involved in the regulation of fat metabolism. Hepatic insulin increases TG synthesis in hepatocytes and directs TG to the cytosol [123]. Additionally, insulin inhibits hepatic lipolysis [124] and reduces the assembly of VLDL by reducing the intracellular association of ApoB100 with TG [125]. This, in turn, has been shown to inhibit translation of ApoB100 mRNA in HepG2 cells [126] leading to the degradation of ApoB [127], which decreases VLDL-TG secretion. All the above events, along with insulin-related expression of the adipose differentiation-related protein (ADRP) [128], which is involved in cytosolic lipid storage, promote lipid droplet accumulation [129].

1.6.1 Hepatic Cholesterol and NAFLD

Hepatic inflammatory responses in NAFLD are thought to be a key step in the pathogenesis of the disease as it eventually promotes liver damage leading to fibrosis, cirrhosis and liver cancer

[110]. The absorption of dietary phytosterol and cholesterol is tightly regulated in the gastrointestinal (GI) tract. The absorption efficiency of other lipids such as TG is about 98% compared to the absorption efficiency of cholesterol which is 50% [130]. Altered hepatic cholesterol homeostasis and free cholesterol (FC) accumulation have been linked to the pathogenesis of NASH both clinically and experimentally [131, 132].

In 2006, the classical mechanism of cholesterol-induced NASH was proposed which was based on the claim that mitochondrial FC loading leads to precipitation of NASH [133]. The authors explained this based on changes in the mitochondrial membrane fluidity which led to the oxidation of mitochondrial glutathione which promoted hepatocyte death by the activation of tumour necrosis factor (TNF) α and Fas-dependent signalling [133]. In a diet-induced NASH rodent model, cholesterol has been found to alter the metabolic and inflammatory status of the liver [134]. Redox signalling and oxidative stress mediated mechanisms have been thought to play a role in the development of inflammation and apoptosis/necrosis in hepatocytes and non-parenchymal cells due to cholesterol. All these factors point to mitochondrial [133] mediated progression of NAFLD to NASH by a mechanism involving cholesterol.

In a recent study, cholesterol crystallization within hepatocyte lipid droplets, and aggregation and activation of Kupffer cells around these lipid droplets, was proposed as a mechanism for the progression of simple steatosis to NASH [135]. The addition of dietary cholesterol to high fat diet (HFD) in C57BL/6J mice caused the progression of steatosis to steatohepatitis [136]. The authors found an association between the presence of cholesterol crystals and NASH. They reported that hepatocyte lipid droplets were seen in both simple steatosis and NASH, but cholesterol crystals were present only in the lipid droplets of patients and mice with NASH [135, 137]. The mechanism proposed by the authors is based on the interpretation that Kupffer cells took up free cholesterol and cholesterol crystals, esters and TG from the lipid droplets of necrotic hepatocytes. This was followed by the hydrolysis of the cholesteryl esters and TG by the Kupffer cells and oxidation of the released fatty acids. Further metabolism of free cholesterol derived from any of the above sources was not possible and it accumulated in the small lipid droplets within Kupffer cells. The Kupffer cells that ingested the cholesterol crystals were transformed into activated foam cells which in turn activated the inflammatory pathway leading to NAFLD progression [135]. Macrophages have been shown to be activated on exposure to excess free cholesterol and cholesterol crystals [138].

1.7. Iron Overload and Hepatic Lipid Metabolism

The role of iron overload in the development and progression of NAFLD is clearly evident from several studies [10, 139-141]. Iron overload has been associated with oxidative stress and lipid peroxidation [11] which, in turn, may modify the fatty acid profile of the cell membrane, leading to cellular damage and impaired mitochondrial oxidation [142]. The free radicals formed may reduce the ratio of saturated to unsaturated membrane phospholipids, leading to reduced membrane fluidity [143], in turn affecting the function of the embedded enzymes [144, 145]. Peroxidation products formed by hepatocytes increase in the presence of unsaturated fatty acids and it is believed that in the presence of iron overload, polyunsaturated fatty acids (PUFA) may exert a repressive effect on lipogenic genes due to cytotoxicity caused by peroxidation [146]. It is possible that iron overload may result in decreased fatty acid synthesis and also play a part in decreased fatty acid catabolism.

It has been shown that iron overload has a direct effect on hepatic lipid metabolism [14], but conflicting results have been reported based on different experimental models. In a study investigating cholesterol metabolism conducted on rats with dietary iron overload, it was shown that there was an increase in the activity of acyl-CoA cholesterol acyltransferase (ACAT) whereas there was a reduction in the activity of HMG-CoA reductase and 7- α -hydroxylase [147]. In another study conducted in our laboratory on mice, dietary iron overload was found to be associated with increase in hepatic cholesterol content but not circulating cholesterol and genes involved in cholesterol biosynthesis were upregulated [46]. The differences observed in the two studies may be due to the amount and time of iron loading. The study conducted on rats used a 3% carbonyl iron diet for 12 weeks compared to 2% carbonyl iron for 3 weeks in the study conducted on mice. The study conducted on rats concluded that the changes related to cholesterol were due to oxidative damage caused to membranes which housed enzymes involved in cholesterol metabolism but this may not be true as the study conducted on mice showed increases liver cholesterol with iron loading, and a recent *in vitro* study conducted on endothelial cells found no differences in oxidation of membrane phospholipids upon iron loading but found increased cholesterol biosynthesis [46, 148]. These observations suggest that iron overload can lead to cholesterol biosynthesis in rodents and cell lines without causing membrane damage at least in experimental models of short-term iron overload.

The rate of cholesteryl ester formation has been linked to the amount of VLDL cholesterol secreted which can be explained by increased activity of ACAT [147, 149]. Investigation of

the biliary pool size showed less cholesterol and bile acid which can be linked to the decreased activity of cholesterol 7- α -hydroxylase [147]. Since bile acids are major products of cholesterol catabolism, their diminished yield can lead to increased plasma cholesterol. These results point to the effect of free radicals generated due to iron overload on the physical properties of the membrane in which these enzymes are embedded, including alteration of the unsaturation/saturation ratio of membrane phospholipids, fatty acid chain length, distribution of fatty acids and the formation of covalent cross-links between lipid radicals [144]. A previous study performed in our laboratory has shown that transcripts of seven enzymes, including the rate-limiting enzyme HMG CoA reductase, were up-regulated with increasing hepatic iron with an increase in cholesterol biosynthesis observed [46]. A recent study in a mouse model of juvenile haemochromatosis indicated that feeding a high-fat diet modulated iron metabolism by affecting the expression of genes involved in maintaining iron homeostasis [150]. It is interesting to note the differences in the studies discussed here but they are not surprising because of the differences in experimental models of iron loading, the species used, level and duration of iron overload, type of diet and feeding regime and sex of the animals [151]. For example, Graham et al [46] used 2% carbonyl iron supplementation for 3 weeks whereas Brunet et al [147] fed rats 3% carbonyl iron for 12 weeks. It may be argued that feeding higher percentage of carbonyl iron for a longer duration can lead to higher levels of oxidative stress compared to shorter term feeding with a lower percentage of carbonyl iron.

1.8. Mitochondria and NAFLD

Mitochondria generate ATP using substrates derived from fat and glucose. The number of mitochondria present in a specific cell or tissue depends on the function it performs. The liver is the metabolic centre of the body and it is known that hepatocytes are rich in mitochondria with each hepatocyte containing, on average, 800 mitochondria, accounting for about 18% of the total liver cell volume [152]. Mitochondria are the primary site for oxidation of fatty acids and oxidative phosphorylation and, therefore, are integral to hepatic metabolism. They consist of inner and outer mitochondrial membranes which are made up of phospholipid bilayers and membrane proteins [152]. They also contain their own genome in the form of mitochondrial DNA (mtDNA). mtDNA has unique features including high copy numbers in cell, maternal inheritance and a high mutation rate due to the lack of error correction mechanisms during replication [153]. Mitochondrial membrane transport proteins aid in the active transport of larger molecules across the mitochondrial outer membrane, whereas the inner mitochondrial

membrane lacks porins, rendering the matrix impermeable to larger molecules. Hence, the inner membrane requires special transporters. The proteins of the inner mitochondrial membrane serve important functions which include oxidation reactions of the respiratory chain. The matrix of the mitochondria contains enzymes which perform important functions including oxidation of pyruvate and fatty acids, as well as many citric acid cycle enzymes [152].

The mitochondrial respiratory chain (MRC) is essential for aerobic energy production. Its components are encoded both by nuclear DNA and mtDNA. mtDNA lacks histones and is bound to the inner membrane. Protection of mtDNA is very important as it encodes many proteins involved in oxidative phosphorylation and damage to hepatic mtDNA may lead to reduced ATP production and β -oxidation leading to necrosis and microvesicular steatosis which is a common feature in NAFLD [154].

1.9. Hepatic Fatty Acid Oxidation

Fatty acid oxidation (FAO) is the major energy source for skeletal and cardiac muscle, whereas liver oxidises fatty acids under conditions of extended fasting, illness, or heavy physical activity. The process of FAO takes place in three different places, β -oxidation in the mitochondria and peroxisomes, and ω -oxidation in the endoplasmic reticulum [155, 156]. A representation of mitochondrial fatty acid oxidation is shown in figure 1.2. Among these three, mitochondrial β -oxidation is the most important pathway for the breakdown of fatty acids under normal conditions and is involved in the oxidation of short, medium, and long chain fatty acids, resulting, eventually, in production of acetyl-CoA. The electrons generated are donated to the mitochondrial respiratory chain coupling mitochondrial fatty acid oxidation to ATP production. Short and medium chain fatty acids can enter the mitochondria on their own, but the entry of long chain fatty acids is regulated by carnitine palmitoyltransferase 1 (CPT1). The activity of CPT1 is inhibited by high malonyl-CoA (an initial substrate of fatty acid synthesis) leading to decreased FAO and thereby reducing the entry of fatty acids into the mitochondria. Therefore, in the case of high caloric intake, there is increased deposition of fatty acids and decreased oxidation. The opposite happens in the fasting state leading to the entry of long-chain fatty acids into the mitochondria and increased β -oxidation. A different form of β -oxidation takes place in the peroxisomes in which the electrons generated are donated to O_2 , leading to the formation of hydrogen peroxide and then water. Very long chain fatty acids are oxidised by this mechanism until they are short enough to be transferred to the mitochondria for complete oxidation. Branched chain fatty acids, obtained from the diet, cannot be oxidised

by β -oxidation due to the presence of 3-methyl groups. Therefore, the terminal carboxyl group is first removed by a process called α -oxidation, which also takes place in the peroxisomes [157].

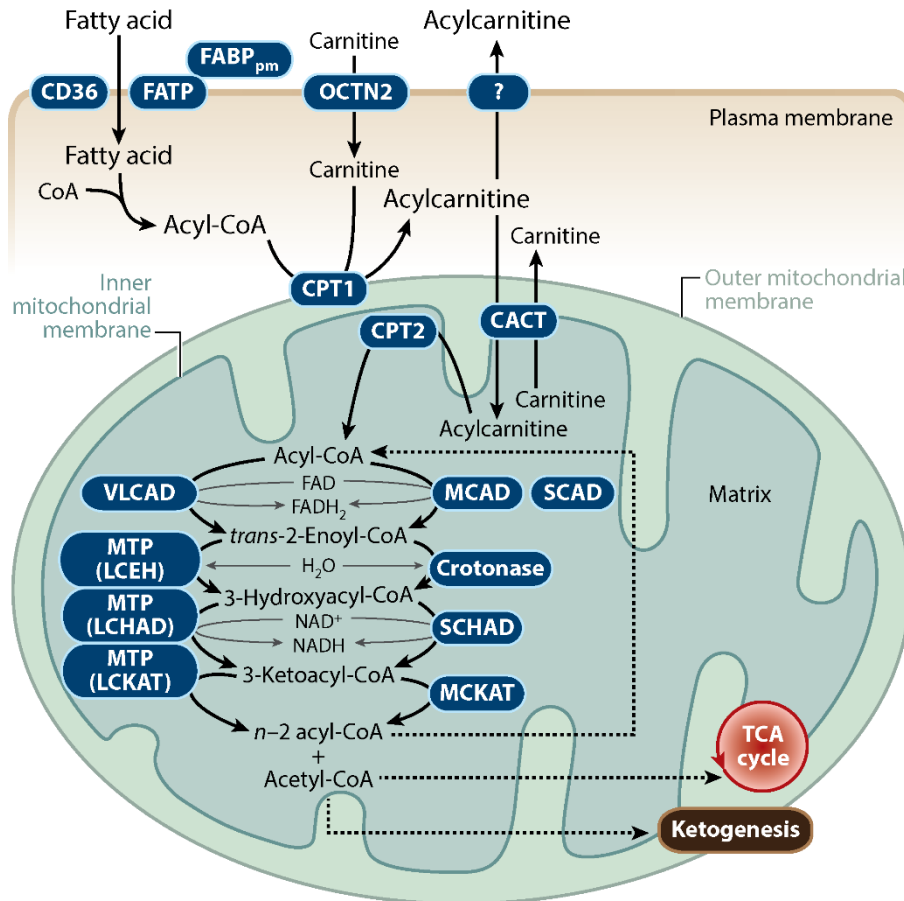


Figure 1.2. Representation of mitochondrial fatty acid oxidation. Adapted from Houten SM, et al. 2016. Annu. Rev. Physiol. 78:23-44. Permission received through Copyright Clearance Centre, Inc. Order Licence ID 1333375-1

1.10. Mitochondrial Dysfunction and NAFLD

NAFLD is associated with numerous mitochondrial changes, including ultrastructural lesions such as paracrystalline inclusions in the matrix, reduced activity of the respiratory chain complexes and impaired β -oxidation, suggesting that mitochondrial dysfunction is closely associated with NAFLD [152, 158, 159]. Similar ultrastructural lesions have been observed in the liver mitochondria of patients and animal models with NASH [41, 159]. Images of livers from a mouse model of NAFLD obtained through electron microscopy depicted swollen and scarce mitochondria with paracrystalline inclusions in the matrix [159]. The present study

hypothesises that iron loading leads to iron being targeted towards the mitochondria, potentially leading to the production of ROS, and initiating a chain of events leading to mitochondrial dysfunction. A recent study in an animal model of NASH has shown that liver specific deletion of retinoic acid receptor-related orphan receptor α (ROR α), which is associated with regulation of genes involved in lipid metabolism and inflammation, aggravates diet-induced NASH by promoting mitochondrial dysfunction [160] due to the loss of mitochondrial membrane potential and structural integrity. This change in the mitochondria may be due to impairment of mitochondrial fission followed by mitophagy and also due to reduced oxygen consumption [161]. It was shown that core machineries of mitochondrial dynamics which include dynamin-1-like protein (Drp1) and BCL2/adenovirus E1B 19 kDa interacting protein 3 (Bnip3) were downregulated in the hepatocytes of ROR α -LKO mice [160]. The hepatic expression of ROR α was significantly reduced in NAFLD patients and NASH animal models [162, 163] suggesting the role of ROR α in pathogenesis of the disease by the mechanisms discussed above. There is evidence to suggest that the expression of ROR α was diminished in NASH patients and a loss of function of ROR α in mice promoted NASH. ROR α has been shown to prevent mitochondrial dysfunction by balancing mitochondrial membrane potential and integrity thus inhibiting NAFLD progression [162, 164].

1.11. Iron and Mitochondria

The most important function of mitochondria in a cell is energy production. In addition, mitochondria also play a crucial role in the metabolism of trace elements, especially iron. The redox properties of iron make it a valuable component of enzymes and proteins [165]. However, this property makes iron a double-edged sword as it can participate in harmful reactions leading to the generation of ROS, which can lead to cell death [165]. Cells have evolved mechanisms to minimise the toxicity of iron and at the same time utilise it for the biological functioning of the system [166].

Iron-sulphur cluster formation occurs in the mitochondria, providing a necessary cofactor for proteins in mitochondria as well as elsewhere in the cell. Some of these proteins are involved in respiratory chain function. The presence of iron-containing proteins in the mitochondria signifies the important role of iron in mitochondrial function. In the case of lung carcinoma, around 20% of total cellular iron was found in the mitochondria [167]. There have been several studies that have shown that chelatable iron is not present in the cytosol but rather other cellular compartments including nuclei, mitochondria, and lysosomes [168-170]. It is interesting to

note here that, out of all these organelles, mitochondria in liver cells had a very high concentration of chelatable iron [168, 169]. In isolated rat hepatocytes, the concentration of chelatable iron in the mitochondria was higher than in the cytosol [168, 169].

Mitochondria are the site of oxidative phosphorylation and oxygen consumption, therefore, the role of chelatable iron in the mitochondria becomes important. It may act as a catalyst for ROS generation, making the mitochondria more susceptible to oxidative stress, thus bringing down their energy producing capacity. Mitochondrial iron has been linked to development of cardiovascular disease [171]. Decreases in the mitochondrial chelatable iron pool have been shown to play a protective role in cardiomyopathy by reducing ischaemia/reperfusion damage [171]. In NAFLD, the chelatable iron pool in the mitochondria can also alter the enzyme activity of genes involved in FA oxidation, potentially leading to increased deposition of fat in the hepatocyte [172, 173].

1.12. Iron Transport to the Mitochondria

The mechanism of iron transport to the mitochondria is still not very clear. Ferrous iron may be transported to the mitochondria through the inner mitochondrial membrane to the mitochondrial matrix, where it is used for haem synthesis, iron-sulphur cluster biogenesis or stored in mitochondrial ferritin [174]. It is thought that several mechanisms act in coordination, including direct delivery of extracellular iron to the mitochondria and uptake of cytosolic iron [174].

The first mechanism proposes that iron enters the mitochondria from a transient cytosolic pool of labile iron known as the transit pool or the labile iron pool (LIP) which is largely composed of ferrous iron [175]. In rat hepatocytes and yeast, it has been shown that ferrous iron is taken from the cytosol by the mitochondria in a membrane potential-dependent manner [176, 177].

Direct entry of endosomal iron into the mitochondria without entering the cytosol is proposed to be through a “Kiss and Run” mechanism. The transferrin receptor (TFR)-transferrin (TF) complex is endocytosed from the extracellular milieu and ferric iron is reduced to ferrous iron. The “Kiss and Run” mechanism involves the docking of endosomes and lysosomes with the mitochondria, with direct passage of Fe^{2+} to the mitochondria [178]. This mechanism has only been demonstrated in erythroid cells [178, 179].

Iron may also be routed to the mitochondria by high molecular weight complexes such as metallochaperones [180], proteins that bind to metal ions and deliver them to enzymes and

transporters by protein-protein interaction. Metallochaperones involved in copper transport have been known for many years [181] but iron chaperones are still being investigated and some potential candidates such as human poly (rC)-binding protein 1 (PCBP1) have emerged as a result [182, 183].

Irrespective of the method employed by any cell to acquire mitochondrial iron, the iron has to traverse first the outer mitochondrial membrane (OMM) and then the IMM. The exact mechanism is still not completely deciphered; however, it is hypothesised that porins are involved in the movement of iron across the OMM [184]. Alternatively, a recent study has shown that DMT1 plays an important role in the mitochondrial uptake of iron and manganese [185]. The authors conducted this study to further explain their previous finding of localisation of DMT1 in the OMM suggesting its role in mitochondrial iron acquisition [186, 187]. Wolff et al observed an increased uptake of Fe^{2+} and Mn^{2+} in mitochondria from HEK293 cells overexpressing DMT1 [185] using three independent techniques: radioisotope uptake, inductively coupled plasma optical emission spectroscopy (ICPOES) and metal-induced quenching of the indicator dye Phen GreenTM SK (PGSK) preloaded into the mitochondria [188].

The mechanism proposed by Wolff et al suggests that there are two mitochondrial iron influx systems. The DMT1-dependent system contributes substantially over time whereas the other, DMT1-independent system, contributes substantially to initial Fe^{2+} uptake. The role of DMT1 in iron accumulation in the mitochondria was confirmed by optical emission spectroscopy, where incorporation of mitochondrial DMT1 expression increased non-haem iron. The authors suggested that a proton gradient was the driver for Fe^{2+} uptake by DMT1-overexpressing HEK293 mitochondria. It has been shown that plasma membrane DMT1 is able to mediate metal ion uptake, including Fe^{2+} [189], in the absence of a proton gradient; however, the iron uptake is very small. This is consistent with the results obtained by Wolff et al, who have shown that DMT1-dependent uptake of metal ions is higher and more rapid at acidic pH than neutral pH which highlights DMT1's proton dependence.

The mitochondrial matrix is the major site for iron metabolism; therefore, iron has to be transported across the IMM. This is an active process facilitated by mitoferrin1 (Mfrn1) and its homologue mitoferrin 2 (Mfrn2), which are members of the solute carrier family of proteins. The mechanism is still not very clear [190, 191] but the interaction between Mfrn1 and Abcb10, which is an IMM ATP-binding cassette transporter, increases Mfrn1 stability leading to iron import [192]. Apart from this mechanism, ferrochelatase, an enzyme involved in haem

synthesis, complexes with both Mfn1 and Abcb10 and this complex formation directs iron to ferrochelatase leading to increased haem synthesis [193].

Iron overload has a negative impact on mitochondrial function mainly due to the production of ROS catalysed by iron bound to its binding partners with low affinity. Iron loading in rat cardiomyocytes *in vitro* led to mitochondrial DNA damage and reduced respiratory function [194]. It is interesting to note that iron overload due to hereditary haemochromatosis (HH) resulted in the accumulation of cytosolic iron but not mitochondrial iron in hepatocytes but led to decreased mitochondrial oxygen consumption [195].

1.13. Fatty Acids and Mitochondria

Most tissues and blood plasma contain a proportion of FFA. The majority of the long chain fatty acids are bound either specifically or non-specifically to fatty acid binding proteins [196]. Most of the FFA is associated with the cellular membrane and only a very small part remains free [197]. Apart from being oxidised by the mitochondria and supplying electrons to the respiratory chain, FFA also interact with the mitochondrial membrane playing a role in the energy-coupling process as weak uncouplers [198]. It has to be noted that long chain fatty acids are natural uncouplers of oxidative phosphorylation due to their protonophoric properties whereas short and medium chain fatty acids lack protonophoric abilities. The reason for this difference is the trans bilayer movement of undissociated fatty acid in one direction and its anion in the opposite direction. This transfer is thought to be due to the action of adenine nucleotide translocase in at least some mitochondria. This has been reported in several *in vitro* studies with isolated mitochondria and evidence also suggests the occurrence of protonophoric uncoupling *in vivo* after hypoxia/reperfusion or high fat diet [199, 200]. Such uncoupling processes lead to mitochondrial dysfunction and impaired ATP production [199].

FFA also play an important role on the IMM by increasing proton conductance and promoting opening of the permeability transition pore (PTP) [201], a conductance channel through which mitochondrial apoptogenic proteins can be released into the cytosol. It has been shown that saturated fatty acids have minimal effects on mitochondrial membrane potential and show negligible short-term cytotoxicity. The presence of double bonds increased both depolarization and cytotoxicity in an experiment which tested the effect of mitochondrial depolarization by fatty acids but was offset by the hydrocarbon chain length, and higher unsaturation was required to see an effect [202]. However, it was found that the number of unsaturated bonds was an important factor in causing any depolarizing effects. Stearic (C18:0) and oleic (C18:1)

acids were ineffective, whereas linolenic acid (C18:3) caused complete depolarization and an intermediate effect was seen on addition of linoleic acid (C18:2) [202]. In another study conducted on HepG2 cells, oleic acid (OA) induced significantly higher TG accumulation compared to palmitic acid (PA; C16:0) upon treating cells with equimolar concentrations of each fatty acid [203]. Interestingly, PA but not OA was found to induce apoptosis in three different cell lines in contrast to equimolar concentrations of OA [203]. It was also observed that in the presence of OA and PA, apoptosis was significantly reduced compared to PA alone [203]. This observation suggests that OA plays a protective role in PA induced apoptosis; this was further confirmed by measuring the activity of caspases 3/7 which are fully operative during cell death. OA did not have any effect on caspase activity whereas PA significantly increased caspase activity [203]. The effects of OA and PA correlated with gene expression: OA was found to increase the expression of peroxisome proliferator activated receptor gamma (PPAR γ), whereas the expression of PPAR α was increased by PA. The lower steatosis and increased apoptosis seen may have been due to the activation of PPAR α leading to enhanced β -oxidation and oxidative stress [204].

1.15. Objectives of this Thesis

The work carried out in this thesis principally focuses on the role of iron and lipid metabolism in NAFLD. It is evident from the literature that imbalanced iron and lipid metabolism play an important role in the development of steatosis and its progression to more severe stages including NASH and cirrhosis. Most of the studies discussed in the literature review focussed on the role of iron in NAFLD progression and investigated NASH and fibrosis. Previous work carried out in our group has shown that initial iron accumulation in NAFLD can not only lead to the progression of the disease but also in initial fat accumulation or steatosis. The various results discussed in the following chapters shed light into the mechanisms by which iron loading contributes to initial fat accumulation in the liver. There is strong evidence linking mitochondrial dysfunction and NAFLD and the results discussed in the present study further elucidate the mechanism by which iron and high fat diet affect mitochondrial function, leading to NAFLD. The role of cholesterol and hepatic cholesterol crystals in NAFLD has gained a lot of importance and therefore, I investigated the role of iron and high fat diet on cholesterol crystallisation as there is no evidence in the literature on the role of iron in the formation hepatic cholesterol crystals. Therefore, to address some of the gaps identified in the literature review this study aimed to:

1. Investigate rates of mitochondrial activity *in vitro* in cells loaded with iron and/or lipids.
2. Investigate hepatic gene expression associated with iron and fatty acid metabolism in mice fed control or Western-style, high-fat diet, with or without iron.
3. Investigate the interaction of iron and fat and their role in hepatic cholesterol crystal formation.

Chapter 2 Materials and Methods

2.1. Cell Culture Methods

2.1.1. Cell Culture

AML12 cells (alpha mouse liver 12) obtained from ATCC were used for all *in vitro* studies. Cells were cultured in DMEM:F12 (1:1) medium supplemented with 10% foetal bovine serum (FBS), insulin (1.0 g/L)-transferrin (0.55 g/L)-selenium (0.00067 g/L) (ITS) (Gibco™ - ThermoFisher, Australia) and 40 ng/ml dexamethasone. Cells were maintained in a 5% CO₂/95% air incubator at 37 °C. The medium was replaced 1-2 times a week, depending on cell confluency.

The cell seeding density for all experiments was 10,000 cells/well, 50,000 cells/well or 100,000 cells/well for 96, 24 and 12 well plates, respectively. Cells were incubated overnight following seeding prior to experimental treatments. All experiments were carried out in duplicate or triplicate.

2.1.2. Cell Viability Assay

Cell viability was assessed using the AlamarBlue® cell viability assay (Thermo Fisher Scientific, Australia). Briefly, 10,000 cells/well were plated in a 96 well plate and incubated at 37 °C overnight after which cells were treated for 12 h with iron or fatty acids (Sections 2.1.3 and 2.1.4). After 12 h, 10 µl of 1x AlamarBlue® solution was added to each well containing the cells. The plate was incubated for 3 h at 37 °C and absorbance was measured at 570 nm using an EnSpire Multimode Plate Reader (PerkinElmer, Australia).

2.1.3. Iron Loading

Ferric ammonium citrate (FAC) (Sigma-Aldrich, Australia) was used to iron load AML12 cells. A stock concentration of 3 mg/ml of FAC in 0.01 M HCl was prepared. Cells were incubated in cell culture medium (Section 2.1.1.) containing a final concentration of 30 µg/ml FAC for 12 h before the experiment [205]. This concentration was found suitable to iron load the cells [206].

2.1.4. Free Fatty Acid Loading

Both saturated and unsaturated fatty acids were used to fat load cells and investigate their differential effects on AML12 cells. Oleic acid (C18:1) conjugated to bovine serum albumin (BSA) (Sigma-Aldrich, Australia) and palmitic acid (C16:0) (Sigma-Aldrich, Australia) conjugated to BSA were used at a concentration 100 µM (FA). Cells were pre-incubated for 12

h in a CO₂/95% air incubator before the experiment. Oleic acid was supplied as a ready to use solution (100 mg/ml BSA) and 1 mM sodium palmitate/0.17 mM BSA solution (6:1 molar ratio palmitate:BSA) was prepared in-house using instructions from Seahorse Biosciences. Briefly, 100 ml of BSA solution (0.17mM) was prepared in 150 mM NaCl along with 44 ml of sodium palmitate (1 mM) in 150 mM NaCl. From this 50 ml of BSA was mixed with 40 ml of sodium palmitate, stirred for 1 h at 37 °C and final volume was adjusted to 100 ml and pH to 7.4. The BSA-palmitate conjugate was stored at -20°C in aliquots; 0.17mM BSA was used as control.

2.1.5. Oil Red-O Staining

The presence of fat was detected using Oil Red-O (ORO; Sigma-Aldrich, Australia). This is a lipophilic dye which stains triglycerides and other neutral lipids red. Following incubation, cells incubated with free fatty acids as described above were washed twice with 500 µl of phosphate buffered saline (PBS) and fixed with 500 µl of 10% neutral buffered formalin (Amber Scientific, Western Australia) at room temperature (RT) for 30 minutes. Cells were washed twice at RT with 1 ml of double distilled water, then once with 60% isopropanol for 5 minutes. The isopropanol was removed, and the cells were left to air dry completely. The ORO stock was made up in 100% isopropanol, which was stirred overnight, and stored at RT. The working solution was prepared fresh by mixing 3 parts of stock to 2 parts of double distilled water. Each well was incubated with 500 µl of ORO working solution for 10 minutes at RT. Cells were washed with double distilled water and counterstained with Gill's #2 haematoxylin, 0.5% haematoxylin (Amber Scientific, Western Australia) after which they were washed 3-4 times in tap water until the water ran clear. Images were acquired using a Nikon-Eclipse TS 100 microscope (Nikon, Australia).

2.2. Mitochondrial Bioenergetics

The effect of iron and FFA loading on mitochondrial bioenergetics was studied using a Seahorse XF96 analyser (Agilent Technologies). AML12 cells were seeded at a density of 10,000 cells/well in XF96 cell culture microplates (Agilent Technologies, Australia). The cells were incubated overnight and were iron and fat loaded the next day as described in sections 2.2.3 and 2.2.4. The Seahorse XF^e 96 extracellular flux assay kit (Agilent Technologies) was hydrated with 200 µl of Seahorse XF calibrant (provided in the kit) by incubation at 37°C in an air incubator attached to the Seahorse XF96 system 24 h prior to the assay.

2.2.1. Assay Media Preparation

Base Dulbecco's minimal essential medium (DMEM) was purchased in powdered form from Sigma-Aldrich, Australia, and was dissolved in 1L of double distilled water, and glucose (2.5 mM), alanyl glutamine (2 mM) and sodium pyruvate (1 mM) added to the medium. The pH was adjusted to 7.35 ± 0.05 at 37°C and the medium filter-sterilised before being stored at 4°C . This assay medium did not contain FBS or bicarbonate as they would provide buffering capacity and mask the small changes in pH measured in the mitochondrial bioenergetics assay.

2.2.2. Mitochondrial Stress Reagents

The following reagents were purchased from Sigma-Aldrich, Australia, and stock and working solutions prepared in dimethyl sulphoxide (DMSO).

- A. Oligomycin. A solution of 5 mM was aliquoted and stored at -20°C until use. A final concentration of 2 μM was used for the assay. It is an ATP synthase inhibitor (complex V).
- B. Carbonyl cyanide-4-phenylhydrazone (FCCP) was reconstituted in the assay media to give a stock concentration of 20 mM. A working solution was prepared in DMSO to give a concentration of 5 mM which was aliquoted and stored at -20°C until use. A final concentration of 0.5 μM in experimental medium (as described in section 2.2.2.1.) was used for the assay. FCCP acts as an uncoupler of mitochondrial oxidative phosphorylation.
- C. Rotenone was reconstituted in the assay media to give a stock concentration of 20 mM and diluted in DMSO to give a working concentration of 5 mM which was aliquoted and stored at -20°C until use. A final concentration of 1 μM in experimental medium was used for the assay. It is a complex I inhibitor.
- D. Antimycin A was reconstituted in the assay media to give a stock concentration of 20 mM. A working solution was prepared in DMSO to give a concentration of 5 mM which was aliquoted and stored at -20°C until use. A final concentration of 1 μM was used for the assay. It is a complex III inhibitor.

2.2.3. Mitochondrial Bioenergetics Assay Day Preparations

On the day of the assay, the change of medium was performed as per the manufacturer's protocol. Briefly, the initial serum-containing medium was replaced by serum-free medium as described in section 2.2.2.1. The medium change cycle involved 3 wash cycles leaving a final volume of 175 μl per well. The cell culture microplate was incubated in an air incubator for 1 h at 37°C . Blank wells contained medium only.

In the meantime, reagents prepared (using assay media) from the stock as described in section 2.2.2.1 were added (25 µl) to the respective injection ports in the hydrated cartridge. Each blank well contained the same volume of medium instead of the reagents.

2.3. Animal Studies

2.3.1. Animal Maintenance

Female C57BL/6J wild type mice were purchased from the Animal Resource Centre (ARC) Murdoch, Western Australia and housed at the Life Sciences Research Facility, Curtin University, in a temperature-controlled environment with a 12-hour light-dark cycle. The mice had *ad libitum* access to food and water. The animal study was approved by the Animal Ethics Committee, Curtin University (AEC_2015_40).

Mice were three weeks old on arrival and were acclimatised for a week before the start of the study. The animals were monitored three times a week to ensure their wellbeing.

2.3.2. Diet Preparation

Diets were purchased from Speciality Feeds, Glen Forrest, Western Australia. All diets were supplied as a powder and were mixed with sterile water as per the supplier's instructions to make a dough. The dough was then moulded into pellets in sterile silicone trays and the pellets used to feed the mice. A quality control was maintained for each batch of the diets prepared to ensure sterility. This was done by maintaining a small amount of diet from each batch in a sealed Petri dish at 37°C which was monitored for microbial growth.

An iron-replete diet (SF01-017) was used as the control diet for the iron loading study. A diet containing 2% carbonyl iron (SF07-082) was purchased and used to prepare intermediate concentrations of 0.25%, 0.5% and 1% carbonyl iron diet by mixing the desired amount of SF07-082 diet with SF01-017. Animals were then fed these diets. In the second study, a Western-style, high fat diet (SF00-219) was used along with the control diet (SF15-106). In this study, 1% carbonyl iron was used to iron load the mice and a combination of 1% carbonyl iron diet and high fat diet to induce fat and iron loading. A flow chart showing the dietary intervention is shown (Figure 2.1).

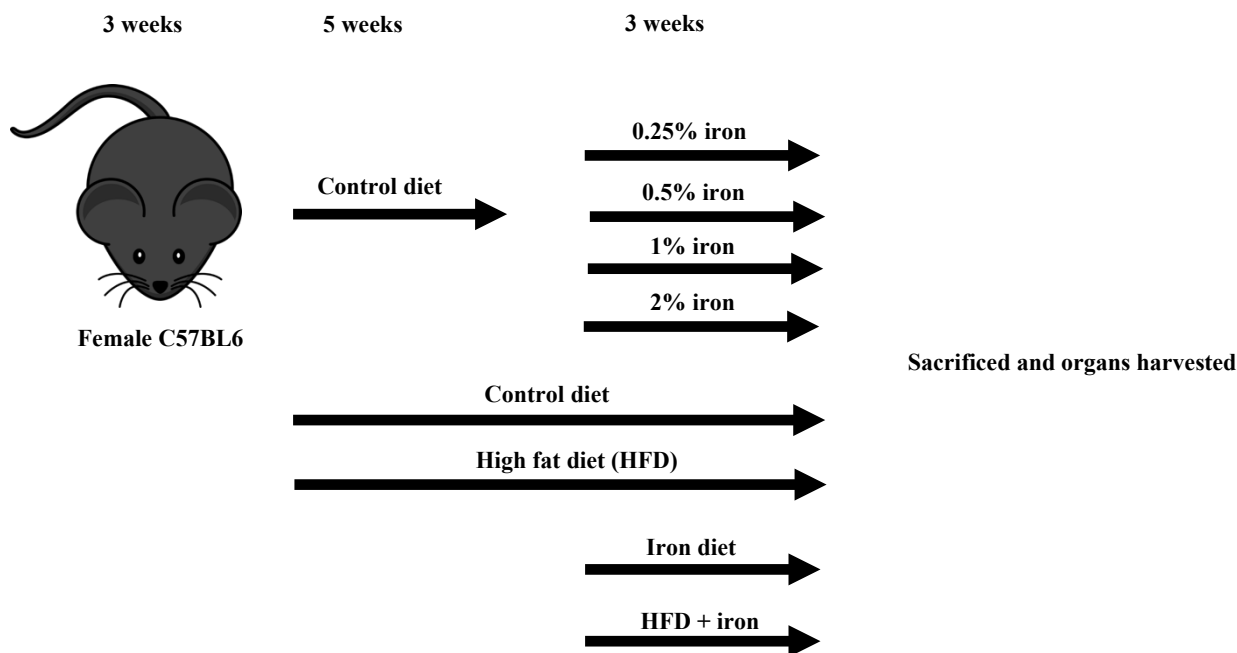


Figure 2. 1 Animal Dietary Plan

2.3.3. Sample Collection

All mice were fasted overnight prior to sacrifice. They were anaesthetized in an isoflurane chamber (2% isoflurane and 0.8-1 L/min O₂) followed by cardiac perfusion with 150 mM NaCl to exsanguinate the tissues. Tissues including liver, spleen and duodenum were collected in microfuge tubes and a part of the liver was embedded in optimal cutting temperature (OCT) compound in a plastic cryomould and stored in aluminium foil to be used for histology. All tissues were snap frozen in liquid nitrogen and stored at -80°C until further use.

2.3.4 RNA Extraction

Total RNA extraction from liver, spleen and duodenum was carried out using TriReagent[®] (Sigma, Australia). Briefly, 50 mg of tissue was homogenised in 500 µl of Tri Reagent[®] using a plastic pestle until it was completely disrupted. A further 300 µl of Tri Reagent[®] was added to the homogenate and mixed. To this mixture 80 µl of 1-bromo-3-chloropropane (Sigma, Australia) was added and mixed vigorously for 15-30 seconds. The mixture was then incubated at room temperature (RT) for 10 minutes followed by centrifugation at 14000 g for 15 minutes

at 4°C. The top (aqueous) phase was transferred to a new microfuge tube and care was taken to avoid contact with the interphase or the bottom layer. A volume of isopropanol equal to the volume of the aqueous phase was added to the tube and gently mixed to precipitate the RNA. After an incubation of at least 10 minutes, RNA was pelleted at 14000 g for 15 minutes at 4°C. The supernatant was carefully removed, and the pellet was washed twice with 75% molecular-grade ethanol (~200 µl depending on the size of the pellet). The supernatant was completely removed, and the pellet allowed to air dry for approximately 30 minutes, after which the RNA was dissolved in nuclease-free water, 15-50 µl depending on the pellet size. This was then incubated for 10 minutes at 55-60 °C. The RNA was then aliquoted in duplicate and stored at -80°C until further use.

2.3.5. RNA Quantification

RNA was quantified using a NanoDrop™ 1000 spectrophotometer (Thermo Scientific). Briefly, 1.5 µl of the extracted RNA was applied to the pedestal of the spectrophotometer and absorbance measured at 260 and 280 nm. The purity of the RNA was evaluated using the 260/280 nm ratio. RNA with a ratio between 1.8 and 2.0 was used for further experiments.

2.3.6. cDNA Synthesis

cDNA was synthesised using the SensiFast™ cDNA kit (Bioline, Australia). The master mix was prepared on ice and consisted of 1 µg of RNA, 1x TransAmp buffer, 1 µl of reverse transcriptase and DNase/RNase free water to make a total reaction volume of 20 µl. The reaction mix was incubated using the following conditions: primer annealing at 25 °C for 10 minutes, reverse transcription at 42 °C for 15 minutes, enzyme inactivation at 85 °C for 5 minutes with a final hold at 4 °C as per the manufacturer's instructions. The cDNA was either used immediately for gene expression studies or was stored at -80 °C until required.

2.3.7. Real Time- Quantitative Polymerase Chain Reaction (RT-qPCR)

Real-time, quantitative PCR was performed using a SensiFAST™ SYBR Lo-Rox (Bioline, Australia) kit with the following conditions: 2 minutes denaturation at 95°C followed by 45 cycles of 95°C for 15 seconds, 57-64.5°C (depending on primer optimisation) for 15 seconds and 72°C for 15 seconds. Melt curve analysis was performed by raising the temperature from 74 to 95°C in increments of 0.5°C. Aliquots of cDNA from each sample were pooled and used to generate standard curves by serial dilution. β-actin was used as the reference gene. Primer sequences and annealing temperatures are listed in Table 2.1.

2.3.8. Non-haem Iron Assay

Liver non-haem iron was measured as described by Crowe et al [207] with some modifications. Briefly, liver tissue homogenates were prepared diluted 1:8 (w/v) using double distilled water. Equal volumes (100 μ l) of the homogenate and protein precipitation solution (7.5% trichloroacetic acid, 0.75 M HCl) were mixed in a 0.5 ml micro-centrifuge tube and heated in heating block at 90°C for 1 h. The contents were then cooled at 4°C for 5-10 minutes, mixed and then centrifuged at 12000 g for 10 minutes. Supernatant (50 μ l) was then transferred into a 96 well plate. 2 ml of 1.5% thioglycolic acid was added to complete the stock ferrozine solution (0.508 mM ferrozine and 1.5 M sodium acetate). This was followed by addition of 50 μ l ferrozine solution to all the samples and the solutions allowed to react for 30 minutes after which absorbance was read at 562 nm using an EnSpire Multimode Plate Reader (PerkinElmer®).

Standard curves were prepared using iron (III) nitrate standards (1 mg/ml in 0.5% HNO₃) (AJAX chemicals, Australia). The standards contained 0, 1, 2, 4, 6, 8, 10, 15 and 20 μ g/ml of iron. The standard curves were linear throughout the tested range.

2.3.9. Histology

OCT embedded liver tissue was used for histological studies. A Leica CM1520 cryostat was used to cut 5 μ m sections at -14 °C which were then mounted on to glass slides. The cut sections were used within an hour or were stored at -80°C until further use

Gene	Forward primer (5'- 3')	Reverse primer (5'- 3')	Annealing Temp
<i>Hamp1</i> ¹	AGAGCTGCAGCCTTTGCAC	ACACTGGGAATTGTTACAG CATTTA	59°C
<i>Tfr1</i>	GAGGGAAATCAATGATCGTA TTATG	CTCCACTAAGCTGAGAGAG TGTG	62°C
<i>Dmt1</i>	CTCTACTCTGGCTGTGGACAT CT	CAGTCATGGTGGAGCTCTG A	62°C
<i>Fpn1</i>	GGAACAGCCTTCTCTTGACA	TGACGTCTGGGCCACTTT	59°C
<i>Acads</i>	ATGGTGACAAAATCGGCTGT	TTTGGTGCCGTTGAGGAC	64.5°C
<i>Acadvl</i>	TCTCTGCCCAGCGACTTTAT	GCAAAGGACTTCGATTCTG C	61.4°C
<i>Acadm</i>	CCCGGGAATACATATTGGAA	TGCTCCTTCACCGATTAACA	57°C
<i>Hadha</i>	TTCTTAAAGACACCACAGTGA CG	CTTCTTCACTTTGTCGTTCA GC	57°C
<i>Ech1</i>	ATGAACAGGGCTTTCTGGAG	GCCATGTCCATGAGGTCAA	57°C
<i>Acca1</i>	GGAGGCTTCAAGAACACCAC	CCTGGCTCAAGAACATTGC	64.5°C
<i>Slc27a2</i>	GATCTGGCTGGGACTGCTC	CCTCCTCCACAGCTTCTTGT	63.3°C
<i>β-actin</i> ²	CTGGCACCACACCTTCTA	GGTGGTGAAGCTGTAGCC	60.4°C

Table 2.1 Primer Details

¹ Wallace et al. 2009, Hepatology

² Graham et al. 2010, Hepatology

2.4. Haematoxylin and Eosin (H&E) Staining

Sections cut as stated in section 2.3.9 were stained in Gill's haematoxylin (Amber Scientific, Australia) for 1 minute after which they were rinsed in running tap water for 1 minute. The slides were dehydrated by rinsing in 95% histology grade non-denatured ethanol for 1 minute followed by rinsing twice in 100% ethanol. The slides were then counterstained in 1% alcoholic eosin (Amber Scientific, Australia) for 20-30 seconds followed by rinsing three times in 95% ethanol for 1 minute each time. Slides were cleared by rinsing in xylene thrice for 1 minute each and then mounted using entellan and cover slipped. Images were acquired using an Olympus BX51 upright microscope (Olympus, Australia).

2.4.1. Perls' Prussian Blue Staining

Iron was detected in liver sections using Perls' Prussian Blue stain as described previously by McDonald et al with some modifications [208]. Briefly, sections were fixed in 4% formalin at room temperature for 5 minutes, rehydrated in distilled water for 5 minutes and incubated in Perls' solution (comprising equal parts of 2% potassium ferrocyanide and 0.2 M HCl) for 30 minutes. They were washed in several changes of distilled water for 5 minutes and counterstained with filtered neutral red stain (1% solution in distilled water) for 1 minute followed by rinsing in distilled water. The sections were then rapidly dehydrated in absolute alcohol, cleared with xylene, mounted using entellan and cover slipped. Images were acquired using an Olympus BX51 upright microscope.

2.4.2. Oil Red O Staining for Liver Tissue

Liver sections were cut as described in section 2.3.8 and air dried for 60 minutes. ORO staining was performed as described by Kohn-Gaone et al [209] with some modifications. The sections were fixed in ice cold 4% formalin after which they were air dried again for 30 minutes. The slides were then placed in absolute propane-1,2-diol (VWR, Brisbane, Australia) to avoid carrying water into Oil Red O. The slides were stained in pre-warmed 0.5% ORO (Sigma) solution in propane-1,2-diol for 8 minutes in a 60 °C oven after which they were differentiated in 85% propane-1,2-diol for 5 minutes and then rinsed in 2 changes of distilled water. Slides were then dipped in Gill's haematoxylin for 30 seconds, thoroughly washed under running tap water until clear and mounted using glycerine jelly. Images were acquired using Olympus BX51 upright microscope. The slides were also imaged under polarised light for the presence of cholesterol crystals.

2.4.3. Isolation of Mouse Liver Mitochondria

Mitochondria from mouse liver were isolated using the protocol established by Frezza et al [210]. Briefly, liver tissue was collected as outlined in the section 2.3.3. All processes were carried out on ice. Liver tissue was rinsed 3-4 times using ice cold buffer for cell and mouse liver mitochondrial isolation (IBc: 10 mM Tris-MOPS pH 7.4, 0.1 mM EGTA, 200 mM sucrose) and cut into small pieces using scissors. The tissue was homogenised in 5 ml of fresh IBc using glass Potter Elvehjem homogenisers. The homogenate was transferred to 50 ml polypropylene tubes and centrifuged at 600 g at 4°C for 10 minutes. The supernatant was transferred to a high-speed centrifuge tube and centrifuged at 7000 g for 110 minutes at 4°C. The supernatant was discarded, and the pellet was washed with ice cold IBc followed by centrifugation at 7000 g for 10 minutes at 4°C. The supernatant was discarded and the pellet containing mitochondria was suspended in 2 ml of IBc and stored in microfuge tubes.

2.4.4. Immunohistochemistry of Mouse Liver

To determine whether the diets used in the study caused any hepatic injury, immunohistochemistry was performed on the sample from each group that contained the highest number of cholesterol crystals. The antibodies (CD45- BD, NSW, Australia; α SMA- Sigma-Aldrich, NSW, Australia; panCK- Dako, NSW, Australia) were kindly provided by Professor Nina Tirnitz-Parker, Curtin University. Briefly, OCT-embedded liver samples were sectioned at 5 μ m thickness and air dried at RT for 5 minutes. Sections were fixed in 4% paraformaldehyde at RT for 20 minutes and washed three times in PBS for 5 minutes. Slides were blocked using antibody blocking solution (Dako, NSW, Australia) for 20 minutes and incubated with primary antibodies for 1h at RT. Slides were then washed three times in PBS for 5 minutes and incubated with fluorescently labelled secondary antibodies in the dark under humidified conditions, overnight at 4°C. Slides were again washed three times in PBS for 5 minutes; air dried and mounted using ProLong Gold Antifade Reagent with DAPI (Life Technologies) to counterstain the nuclei. Slides were covered with a coverslip, dried in the dark and imaged using a fluorescence microscope. The details of primary and secondary antibodies used are listed in Table 5.1.

2.4.5. Statistical Analysis

Statistical analyses were performed using GraphPad Prism v8.0. Results are expressed as mean \pm standard error (SE). Comparison between means was performed using Fisher's Least Significant Difference test. Relationships between hepatic parameters of interest and non-haem iron were investigated using linear regression analysis. Significance was inferred at the nominal $\alpha = 0.05$ value. Outliers were identified using Interquartile Range (IQR) [211].

Chapter 3 Effect of Iron and Free Fatty Acid Loading on Mitochondrial Bioenergetics

3.1. Background

The role of mitochondria in the development and progression of NAFLD has gained much attention in the past few years [172]. Mitochondrial dysfunction has been found to be an important factor in the development of NAFLD [211] and the role of iron and FFA in mitochondrial abnormalities and dysfunction has been discussed in Chapter 1 (Section 1.14 and 1.15). The main role of mitochondria is energy production in the form of ATP, but this is not their only function. They are also an important site for metabolic activity, containing pathways including beta-oxidation of fatty acids. It is interesting to note that both iron and mitochondria can contribute to ROS generation independently and, therefore, combined ROS generation from both these components, if uncontrolled, may enhance damage caused to living systems.

The liver is rich in mitochondria and plays a central role in carbohydrate, lipid and iron metabolism along with maintaining ROS homeostasis [212]. Mitochondria themselves are susceptible to injury due to iron and fatty acid accumulation. In this chapter, I investigated the *in vitro* effect of iron and FFA loading on mitochondrial bioenergetics in real time using a Seahorse XF96 flux analyser. This study was performed to investigate the immediate effects of iron and FFA loading on hepatocytes in contrast to other studies which have investigated the long-term effects of iron and FFA loading on NAFLD progression [213].

3.2. Methods

The experiments described in this chapter were conducted using AML12 cells. Cells were incubated with 100 μ M FFA conjugated to BSA and 30 μ g/ml ferric ammonium citrate (FAC) for 12 hours at 37°C in order to lipid- and iron- load cells (Section 2.1.3 and 2.1.4), and extracellular acidification and oxygen consumption rates were measured. Wave software 2.6.0 (Agilent Technologies) was used to set up assay parameters and analyse the results. The results were normalised to DNA content [214] per well ($n = 5$ per condition) as per manufacturer's instructions. Briefly, cells were washed with RIPA buffer (Astral Scientific, Sydney, Australia) and total DNA was quantified by adding 100 μ l of Quanti-iT PicoGreen (Life Technologies, Gaithersburg, MD, USA) to 100 μ l of sample and fluorescence was measured (excitation \sim 480 nm, emission \sim 520 nm). Data are presented as mean \pm SEM. The cell viability assay was carried out as described in section 2.2.2.

3.3. Results

3.3.1. Cell Viability & Oil Red O Staining

Cell viability of all the treatment groups was compared to control (untreated cells) as shown in **Figure 3.1**. There was no drop in viability in cells incubated with OA or BSA alone compared to control; however, there was a small, but significant, reduction in cell viability in cells incubated with iron (4%; $P < 0.05$), PA (16%; $P < 0.0001$), OA + iron (14%; $P < 0.0001$) and PA + iron (22%; $P < 0.0001$). Higher concentrations of PA (200 μM) led to an even larger reduction (20%) in cell viability (data not shown).

AML12 cells treated with iron and FFA were stained for neutral lipids using ORO (**Figure 3.2**). All the groups including control showed the presence of red colour with varying intensity confirming the presence of lipids in the cells. ORO was not quantified and was performed to confirm the presence of lipids.

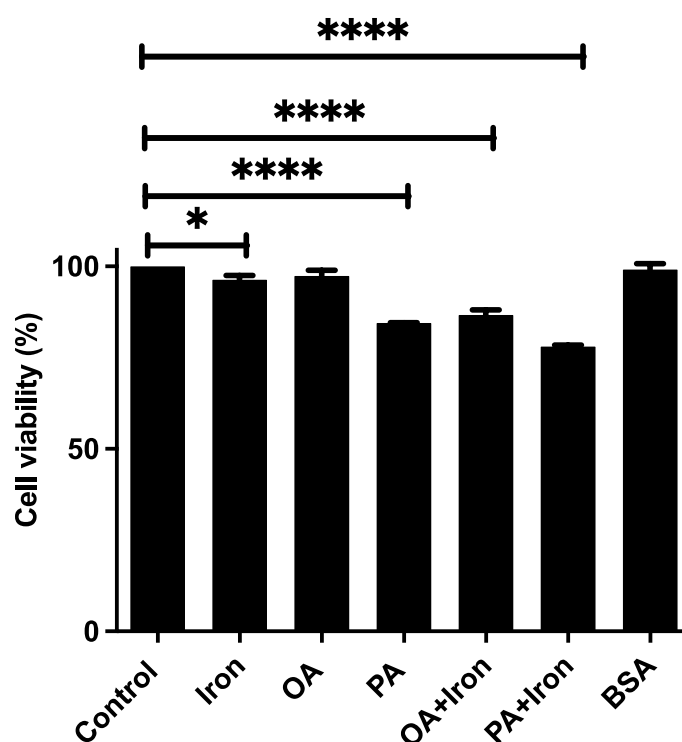


Figure 3.1. **Effect of FFA and iron on cell viability.** AML12 cells were treated with (OA; 100 μM), (PA; 100 μM) and/or iron (30 $\mu\text{g/ml}$) for 12 hours. Cell viability was determined using AlamarBlue[®]. Data were normalised to control. Three independent experiments were conducted in triplicate and data from one representative experiment is shown. All data are presented as mean \pm SEM. * $P < 0.05$, **** $P < 0.0001$.

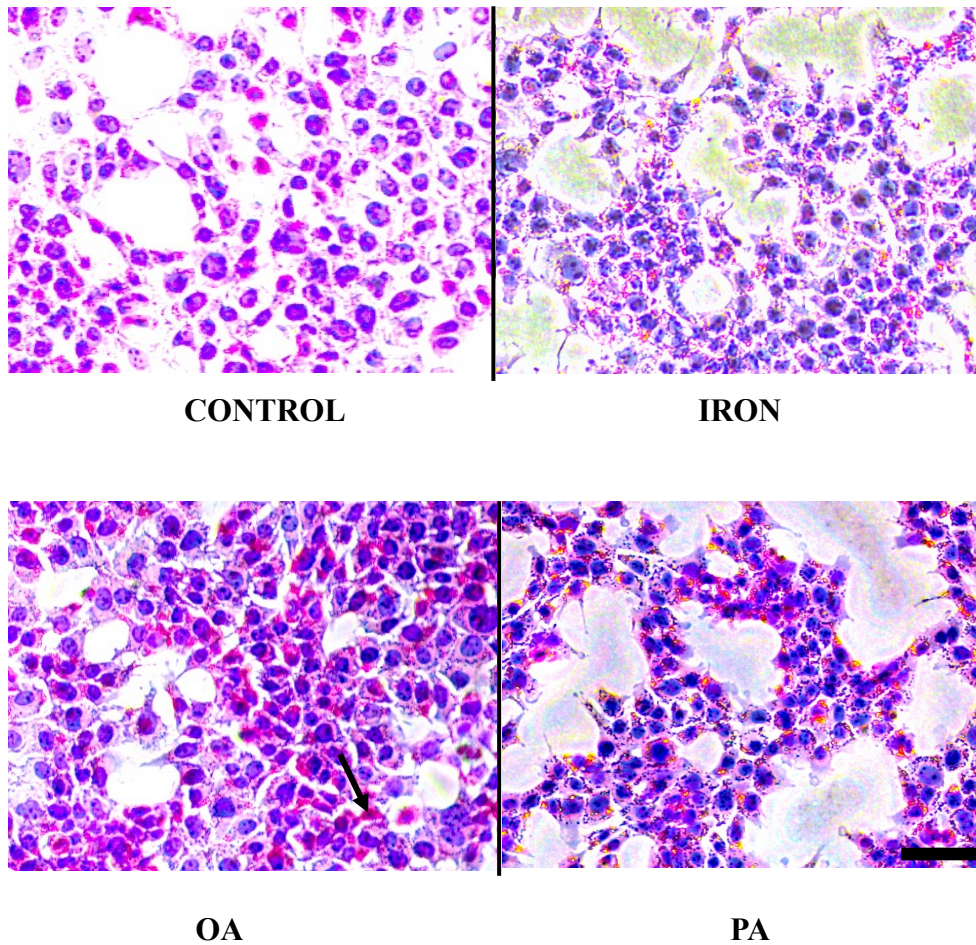


Figure 3.2 **Oil Red O stained AML12 cells for neutral lipids.** Cells were treated with FFA or iron for 12 hours as described in section 2.1.3 and 2.1.4, stained for neutral lipids (red colour) and counter-stained with haematoxylin. Images were analysed using a NIKON-ECLIPSE TS 100 microscope. Scale bar is 100 μm .

3.3.2. Effect of Iron and Free Fatty Acid Loading on Oxygen Consumption Rate

The effect of iron and FFA loading on mitochondrial bioenergetics was determined by measuring OCR. OCR is an indicator of mitochondrial respiration. It gives information about the physiological state of the cells and specifically the health of the mitochondria. Mitochondrial respiration was measured by evaluating different parameters (Figure 3.3) which were measured by addition of various reagents which act as modulators of mitochondrial respiration at different points as shown in the figure 3.3.

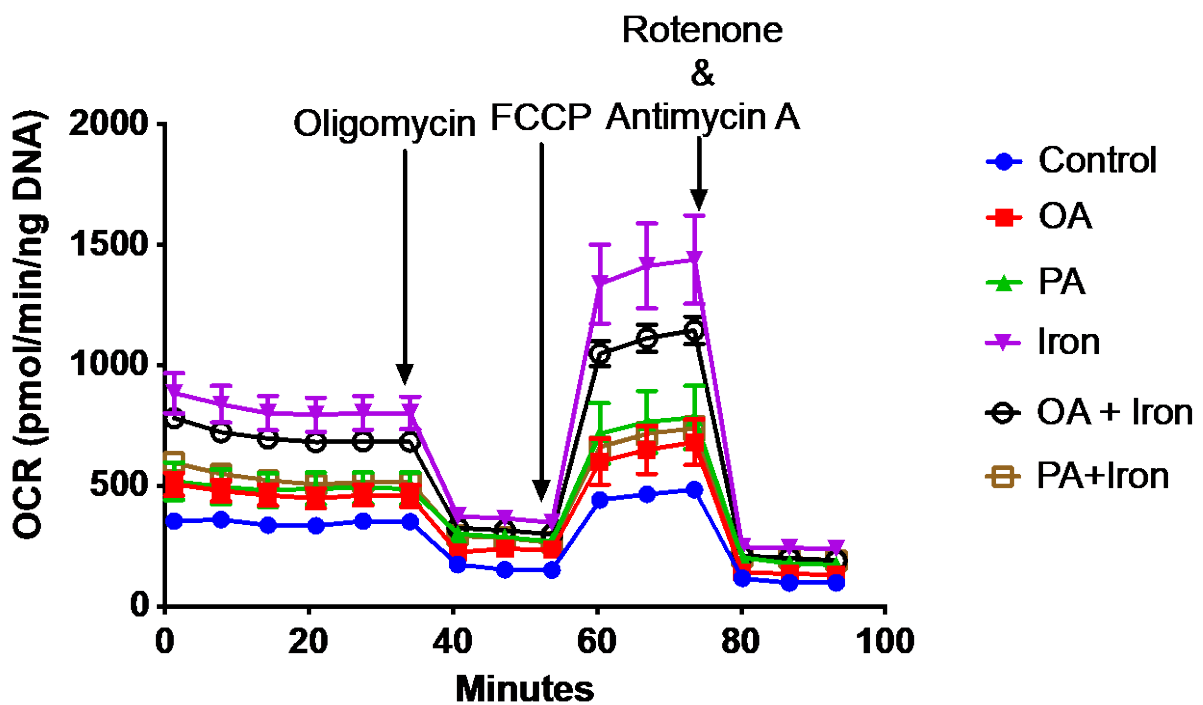


Figure 3.3 Measurement of mitochondrial bioenergetics in real-time using a Seahorse XF96 analyser. AML12 cells were used for studying mitochondrial function in real-time using oxygen consumption rate (OCR) to calculate basal respiration, ATP production, maximal respiration, proton leak, non-mitochondrial respiration and spare respiratory capacity. OCR values were normalised to DNA content per well. Three independent experiments were carried out in triplicate and the figure shows a representative result. Data are presented as mean \pm SEM.

3.3.2.1. Basal Respiration

Basal respiration is used to meet the energy demand of the cell under baseline conditions. Basal respiration is calculated after removing non-mitochondrial oxygen consumption and is measured following addition of oligomycin, which is an ATP synthase inhibitor. The slower the ATP production, the lower the rate of respiration driving it. A significant increase in basal respiration was observed in cells treated with iron (413 ± 49 pmol / min/ ng DNA; $P < 0.05$) compared to control (255 ± 18 pmol / min/ ng DNA; **Figure 3.4 A**). A significant increase was also observed in cells treated with OA+iron (383 ± 50 pmol / min/ ng DNA; $P < 0.05$; **Figure 3.4 A**). Addition of iron may have increased basal respiration by increasing the ATP turnover in the cells. Other groups did not show any significant difference compared to control.

3.3.2.2. Proton Leak

Proton leak can be defined as a reduction of protonmotive force. This is induced in the presence of the ATP synthase inhibitor oligomycin in both intact cells and isolated mitochondria [215]. Measurement of proton leak can help in identifying molecular mechanisms involved in altering proton conductance across the mitochondrial inner membrane [216]. The results indicate that there was a significant increase in proton leak in cells treated with iron (93 ± 8 pmol / min/ ng DNA; $P < 0.01$), OA (94 ± 8 pmol / min/ ng DNA; $P < 0.01$) and OA+iron (87 ± 13 pmol / min/ ng DNA; $P < 0.05$) compared to control (55 ± 5 pmol / min/ ng DNA). Other groups did not change as seen in **Figure 3.4 B**.

3.3.2.3. Maximal Respiration

Maximal respiration is induced by the addition of the protonophore, FCCP, which acts as an uncoupler of oxidative phosphorylation and leads to rapid substrate oxidation. It is a measure of the maximum respiration rate which a cell can attain. The maximal respiration was significantly higher in cells treated with iron (724 ± 118 pmol / min / ng DNA; $P < 0.05$) and OA+iron (661 ± 109 pmol / min/ ng DNA; $P < 0.05$) compared to control (388 ± 13 pmol / min/ ng DNA). No significant change was observed in other groups as seen in **Figure 3.4 C**.

3.3.2.4. Spare Respiratory Capacity

Spare respiratory capacity is the difference between basal and maximal respiration. The existence of spare respiratory capacity is linked to the capacity of a cell to respond to increased ATP demand under conditions of stress, and reduced spare respiratory capacity is seen as an indicator of mitochondrial dysfunction [217]. A significant increase in cells treated with iron

(311 ± 69 pmol / min/ ng DNA; $P < 0.05$), OA+iron (278 ± 61 pmol / min/ ng DNA; $P < 0.05$) and PA (294 ± 65 pmol / min/ ng DNA; $P < 0.05$) led to a significantly higher OCR compared to control (133 ± 9 pmol /min / ng DNA) as seen in **Figure 3.4 D**. No other groups exhibited significant differences from control.

3.3.2.5. Non-mitochondrial Respiration

Non-mitochondrial respiration is driven by non-mitochondrial oxidases such as NADPH oxidases [217] and is measured following the addition of rotenone and antimycin A, which block mitochondrial respiratory function. A significant increase was seen in cells treated with iron (164 ± 20 pmol / min/ ng DNA; $P < 0.05$), OA+iron (179 ± 16 pmol / min/ ng DNA; $P < 0.01$) and PA (173 ± 13 pmol / min/ ng DNA; $P < 0.01$) compared to control (97 ± 18 pmol / min/ ng DNA). There were no significant differences in non-mitochondrial respiration between control and the other treatment groups as seen in **Figure 3.4 E**.

3.3.2.6. ATP Production

ATP production here indicates ATP produced by the mitochondria to meet the energy requirements of the cell. It is the difference between cellular basal respiration and respiration measured in the presence of the ATP synthase inhibitor, oligomycin. ATP production was significantly higher in cells treated with iron (320 ± 41 pmol / min / ng DNA; $P < 0.05$) and OA+iron (296 ± 38 pmol / min/ ng DNA; $P < 0.05$) compared to control (200 ± 17 pmol / min/ ng DNA; **Figure 3.4 F**). The other groups showed no significant variation in ATP production.

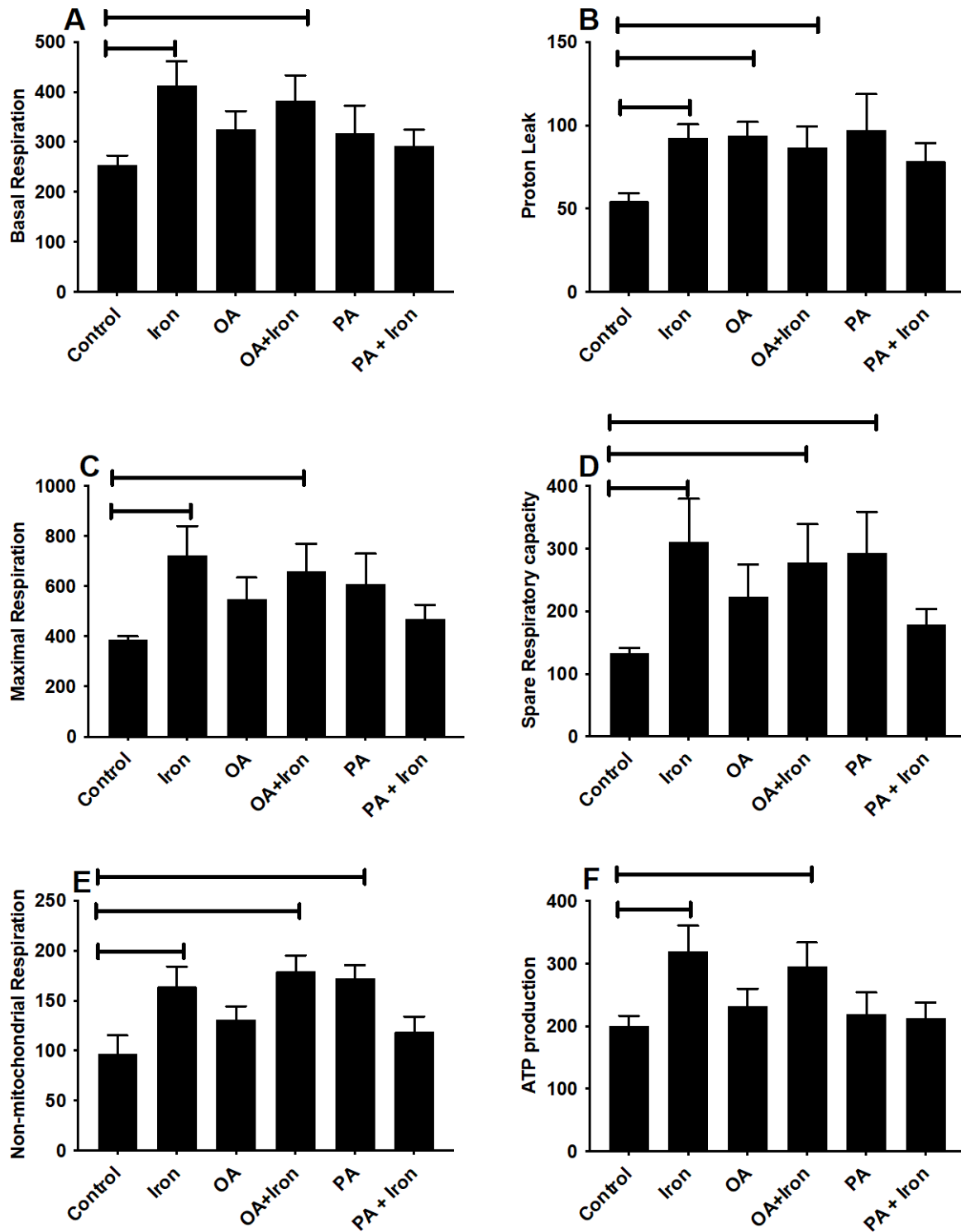


Figure 3.4 **Changes in mitochondrial respiration upon iron and fatty acid loading in AML12 cells for 12h.** Mitochondrial respiration was measured in terms of oxygen consumption rate (OCR). (A) Basal respiration, (B) proton leak, (C) maximal respiration, (D) spare respiratory capacity, (E) non-mitochondrial respiration and (F) ATP production. Data are presented as mean ± SEM. *P<0.05, **P<0.01 between the indicated measurements.

3.4. Discussion

Iron loading has been associated with NAFLD [218] and, given that liver is rich in mitochondria and an important site of iron metabolism [56], investigating the effect of iron loading on mitochondrial respiration may give us an important insight in to the role of iron in NAFLD pathogenesis. The addition of fatty acids alone or in combination with iron may shed light on how either iron or fatty acids modulate the electron transport chain (ETC) as there are several enzymes involved in the pathway that require iron as a co-factor [174]. The advantages of using intact cells instead of isolated mitochondria to study bioenergetics include avoiding artefacts associated with mitochondrial isolation. It also offers greater physiological relevance [217] as metabolism is supported by glycolysis. In addition, mitochondrial function can be manipulated and many aspects of mitochondrial respiration can be measured simultaneously [217].

Mitochondria have been implicated in the development and progression of NAFLD [172] which has led to a focus on understanding the mechanism involved in mitochondrial dysfunction [211]. To investigate the role of iron and lipid loading on mitochondrial oxidative phosphorylation, mitochondrial bioenergetics was measured in AML12 cells. The concentrations of iron and fatty acids, and the incubation time were designed to study the early stages of iron and fatty acid loading on mitochondrial respiration. The modulators used in the assay target the ETC and affect the OCR: oligomycin targets ATP synthase (complex V) and leads to a decrease in OCR, FCCP dissipates the proton gradient across the inner mitochondrial membrane, uncoupling oxidative phosphorylation and ATP synthesis, leading to an increase in OCR, and rotenone/antimycin A target complexes I and III and decrease OCR as shown in Figure 3.3.

Iron loading AML12 cells for 12 hours led to a significant reduction in cell viability which is partly in line with the observation made in a study by Messner et al [119] which showed cell viability to decrease upon iron loading and increase upon loading with oleic acid. It should be noted that Messner et al [119] loaded with 50 μM (approximately 13 $\mu\text{g}/\text{mL}$) ferric ammonium citrate for 2 h, although it is not entirely clear from the paper whether this was 50 μM iron or 50 μM ferric ammonium citrate, and iron delivery was mediated by 8-hydroxyquinoline, which is a lipophilic iron chelator, compared to 30 $\mu\text{g}/\text{mL}$ ferric ammonium citrate for 12 hours without hydroxyquinoline in the present study. Additionally, the present study used 100 μM OA for 12 hours, half the concentration used by Messner et al. A decrease in cell viability (**Figure 3.1**) was detected in cells treated with PA alone or in combination with iron. PA has

previously been shown to reduce cell viability in hepatocytes [219]. There was a larger (22%) decrease in cell viability in the group treated with PA and iron together. This is likely to be due to the combined cytotoxic effect of both the compounds given that iron has been linked with oxidative stress and it enhances the effects of PA as, on its own, iron had only a very small effect on cell viability. Iron has been shown to induce cell death in rat primary hepatocytes related to ferroptosis along with changes in mitochondria such as reduction in mitochondrial number and contracted cristae [220]. In another study in HepG2 cells, PA treatment led to an intense mitochondrial fragmentation and reduction in overall mitochondrial volume [221]. It can be argued that given both iron and PA lead to mitochondrial damage their combined effect may also lead to a lower cell viability. A similar effect was seen in another study where iron was found to be more cytotoxic in the presence of saturated fatty acids [119] compared to mono-unsaturated fatty acids. It has been shown that PA causes apoptosis in cultured hepatocytes [203] whereas OA promotes more steatosis but not apoptosis. A study using HepG2 cells found there was no substantial decrease in cell viability in the presence of iron alone suggesting that ROS generation was low and / or that ROS were detoxified by the inherent cellular anti-oxidant response [222]. This protective response appears to be only partially capable of protecting against insults by PA as well as iron and therefore led to a reduction in cell viability.

ORO staining for neutral lipids confirmed the presence of lipids (red colour) across all the groups including control. The presence of lipids in the control group is not surprising as hepatocytes contain neutral lipids which can be stored in lipid droplets [223]. There were some differences in the colour intensity of the stained lipids across the groups treated with different FFA and this may be due to the presence of different lipid classes, but this will need further investigation.

The measurement of basal respiration indicated a high OCR in cells treated with iron and OA+iron compared to the untreated cells. Addition of fatty acids has been shown to increase basal respiration in hepatocytes [224]. However, this was not observed across all the groups treated with FFA in the present study. It is possible that longer incubation times may lead to observable changes associated with mitochondrial respiration. ATP turnover, substrate oxidation and proton leak can control basal respiration therefore, it may change based on ATP demand [217]. A similar observation was made in iron loaded HepG2 cells which led to an increased mitochondrial respiration characterised by increased oxygen consumption and ATP formation [225]. This has been explained based on iron deficient cells, which show reduced

activity of citrate synthase and aconitase resulting in decreased formation of NADH. This results in a decreased capacity of the cell to produce ATP by oxidative phosphorylation. There have been reports of increased basal respiration due to fatty acid addition [224] by increasing the production of protonmotive force by acting as substrates for oxidative phosphorylation and thus increasing the NADH/NAD⁺ ratio. In the present study, the various treatments applied to the cells did not have any effect on basal respiration except for the groups treated with iron and OA+iron. It should also be noted that cells treated with PA showed a reduced cell viability compared to iron or OA treated cells, but it is unlikely that this would have an effect on the measurements made as they were normalised to DNA.

Substrate oxidation in mitochondria leads to generation of protonmotive force. Some of the protons leak back across the mitochondrial inner membrane and reduce the activity of the respiratory chain [216]. A large proton leak may indicate severely damaged (uncoupled) mitochondria, whereas a slight leak rate may indicate change in protonmotive force caused by altered substrate oxidation [217]. Iron, OA, and OA+iron treated cells showed significant increases in proton leak. The proton leak observed here may be a result of increased substrate oxidation. A similar observation was made in a study conducted on HepG2 to investigate the differential effect of OA and PA on lipid droplet and mitochondrial interaction. It was shown that the mitochondrial transmembrane potential was maximal at 6h after OA incubation and came down at 18h, whereas cells treated with PA peaked at 2h post incubation and then dropped down at 6 and 18h peaking further at 24h. It should be noted that the study used double the concentration of OA and PA compared to the present study [221]. Based on these observations it can be speculated that PA may have brought about a change in proton leak which could not be captured at 12h in the present study and a longitudinal study may give further insights into the role of OA and PA on mitochondrial bioenergetics.

Maximal capacity helps to estimate the substrate oxidation giving insight into the role of various compounds on cellular metabolism [216]. The groups that showed a significant increase in maximal respiration were iron and OA+iron treated cells. It can be argued that iron acted as a driver for substrate oxidation, increasing the maximal respiration as previous studies have shown that iron deficiency is associated with decreased mitochondrial function linked to reduced oxidative substrate metabolism [226-228]. The reason for PA not showing a similar increase to the iron and OA+iron groups may be attributed to its apoptotic nature [203] as evidenced by a decrease in cell viability.

In order to meet increased energy demand, a cell can increase its spare respiratory capacity [217]. Spare respiratory capacity is the difference between basal and protonophore induced respiration and is an indication of how close a cell is to its bioenergetic limit. Cells loaded with iron, OA+iron or PA showed significant increases in spare respiratory capacity. A decrease in spare respiratory capacity may hint at mitochondrial dysfunction [217] which was not the case in the present study. This signifies that neither FFA nor iron were able to induce an insult on mitochondrial health and did not contribute to mitochondrial dysfunction.

Non-mitochondrial OCR increased in cells treated with iron, OA+iron and PA. Redox cycling compounds, such as iron, have been shown to increase the rate of non-mitochondrial respiration [229] which is the case here. It is possible that an increase in non-mitochondrial respiration may be due to increased cytosolic ROS [230] generation. Iron and stearic acid have been shown to increase oxidative stress in AML12 cells where ROS generation was two-fold higher in cells treated with stearic acid+iron compared to iron alone [119]. Therefore, it is possible that addition of PA would have caused a similar response as it is a saturated fatty acid just like stearic acid. Saturated and unsaturated FFA act differently in mitochondrial dysfunction. OA has been shown to readily accumulate in lipid droplets and reduce its toxicity whereas PA stimulates mitochondrial oxidative damage leading to liver damage [221]. It is surprising that cells treated with PA+iron did not show any significant change in non-mitochondrial OCR, and this cannot be due to the reduced cell viability as the results were normalised to the DNA content.

ATP linked respiration can be influenced by ATP utilisation, ATP synthesis, and substrate supply and oxidation [216]. In the present experimental set up, cells treated with iron and OA+iron exhibited a higher OCR associated with ATP production. Cells treated with PA had reduced cell viability compared to control cells in contrast to OA treated cells, which did not exhibit any significant decrease in viability. A longer term (24 h) iron loading study using 100 μ M iron chloride in the erythroleukaemic cell line, K-562, has shown that high iron availability led to increased oxygen consumption and increased ATP production [225] as iron supplementation leads to increased NADH formation by citric acid cycle which can be linked to increased oxygen consumption and ATP formation by oxidative phosphorylation.

In a recent study conducted on patients with mitochondrial encephalopathy, addition of PA led to a 30% reduction in ATP production and addition of OA led to an increased ATP production compared to PA [231]. It is possible that the biochemical changes observed here may have led to decreased cell viability as PA has been shown to induce apoptosis and reduce cell viability

[232] and it is possible that a longer incubation may lead to much more pronounced changes associated with cell viability and apoptosis. Work carried out in the laboratory as part of another project using synchrotron imaging (data not shown) has revealed that iron loading results in changes associated with lipid profiles in AML12 cells upon a longer incubation time than used in the current experiments (more than 16 h) [205]. This suggests that to detect more pronounced changes in mitochondrial bioenergetics, a longer incubation with iron and FAs may be required. In conclusion, saturated and unsaturated fatty acids exert differential effect on mitochondrial respiration where PA is more cytotoxic than OA, thereby reducing ATP production. Both saturated and unsaturated fatty acids stimulate mitochondrial bioenergetics but with varying profiles. Based on the results discussed in this chapter, the role of iron in mitochondrial function and bioenergetics is very important as mitochondrial dysfunction is implicated in NAFLD [211]. Iron here has been shown to enhance the effects of OA which is interesting given that OA has been shown to be protective against cell lipotoxicity. These results also indicate that the treatments in the present study increased mitochondrial function which also means that the mitochondria were healthy.

Chapter 4 Determination of Iron Concentration to Induce Dietary Iron Loading

4.1. Background

Iron is an important trace element, as evidenced by its role in biological processes such as cellular respiration, oxygen transport and erythropoiesis [151, 190]. Very tight regulation of iron metabolism is required, as either iron deficiency or overload can have serious clinical implications. Iron overload has been found to be associated with NAFLD [6, 10, 46]. Animal models, including normal, transgenic, and knockout mice, have proved to be a valuable tool in understanding iron metabolism and regulation. Nevertheless, there have been reports of sex, strain, diet and feeding pattern influencing the outcomes of iron overload studies [151, 233, 234]. A 2% carbonyl iron has been used by many groups, including our laboratory, to study the effect of iron loading and its subsequent effect on iron regulated metabolic pathways, including gene expression and signalling [46, 235, 236]. The aim of this study was to find a favourable concentration that would induce iron loading in mice liver. It is interesting to note that most mouse studies have made use of male mice using 2% or higher iron concentrations to induce iron loading and have focussed on NASH/fibrosis rather than steatosis. Different studies have also used different strains, which may be a contributing factor for the observed differences as different strains have been shown to have different basal iron levels [237]. Other investigators have fed the animals for different time periods to load them. Strain had a significant effect on plasma hepcidin, the key iron regulator (Section 1.6), whereas sex did not show any such significance in mice fed a control diet, but had a significant effect on mice fed a high iron diet, including the C57BL/6J strain used in the present study [151]. A study on male C57BL/6J mice indicated that 0.25% carbonyl iron is sufficient to induce maximal hepcidin response [238] although mice were only fed the high iron diet for 2 weeks and were only 6 weeks of age at the time of sacrifice. It has been reported that there is an increase in hepatic iron concentration [239] with age in mice fed high iron which means hepcidin response is also likely to increase with age [240].

The investigation of mitochondria and peroxisomal fatty acid genes in NAFLD is important because they play an important role in the breakdown of fatty acids and any dysregulation may lead to NAFLD [241]. Mitochondria play an important role in small, medium and long chain fatty acid β -oxidation whereas peroxisomes are involved in very long chain fatty acid β -oxidation which cannot be performed by the mitochondria [241]. It is also known that increased mitochondrial iron can lead to mitochondrial dysfunction and oxidative stress [242] and

therefore the gene expression of both mitochondrial and peroxisomal fatty acid genes were investigated to understand how increased iron can modulate mitochondrial and fatty acid oxidation.

In the present study, female C57BL/6J mice were used to study the effect of varying iron concentration on hepatic gene expression of iron, mitochondrial and peroxisomal fatty acid oxidation genes. Mice were iron loaded with varying carbonyl iron concentrations for 3 weeks as previously described [46]. The control diet used in this study was the correct nutritional control for the high fat diet and contained calories in the form of carbohydrate rather than fat. The present study was undertaken to determine a favourable concentration to induce dietary iron loading and investigate the response of mitochondrial and peroxisomal fatty acid oxidation genes and mitochondrial cholesterol accumulation to this iron loading.

4.2. Methods

Diets were prepared as described in section 2.3.2. Briefly, the powdered diet was used to make dough which was then placed in silicone moulds to give a shape to the diet. A regular quality control was maintained to make sure the diet remained free from any contamination. The mice were divided into 5 groups: control (0.02% iron; n=5), 0.25% iron (n=4), 0.5% iron (n=4), 1% iron (n=4) and 2% iron (n=4). Mice were fed the diets for 3 weeks from 8 weeks of age after which they were fasted overnight before sacrifice. Livers were harvested; a sample from the tissue was used for embedding in OCT for histology and the remainder immediately frozen in liquid nitrogen until processing for RNA isolation, NHI assay and mitochondrial isolation.

RNA was isolated from liver as described in section 2.3.4 followed by cDNA synthesis using a SensiFast™ cDNA kit (Bioline) as described in section 2.3.6. Real-time, quantitative PCR was performed using SensiFAST™ SYBR Lo-Rox chemistry (Bioline) as described in section 2.3.7. Results were quantified as previously described by Graham et al [46] using β -actin as the house-keeping gene. Primer details are provided in Table 2.1.

Histology was performed on OCT embedded tissues as described under section 2.3.9. The NHI assay was performed on liver tissue as well as isolated mitochondria as described in section 2.3.8. Mitochondrial NHI was measured as described in Section 2.4.3.

An Amplex Red Cholesterol assay kit (Life Technologies) was used to quantify the cholesterol content of the isolated mitochondria. Mitochondrial fractions were dissolved 1:10 in the reaction buffer provided in the kit. Cholesterol standards (8, 4, 2, 1, 0.5, 0.25 and 0 μ g/ml) were prepared from the 2 mg/ml cholesterol stock provided in the kit. Finally, 50 μ l of diluted mitochondrial fraction was mixed with 50 μ l of working reagent (300 μ M) which consisted of

4.82 ml of 1x reaction buffer, 75 μ l of Amplex Red stock solution (20 mM), 50 μ l of horseradish peroxidase (HRP) stock solution (200 U / ml) and cholesterol oxidase stock solution (200 U / ml) and 5 μ l of cholesterol esterase stock solution (200 U / ml). The cholesterol content in isolated mitochondria (see section 2.4.3) was normalised to protein content, determined using a bicinchoninic acid (BCA) assay (Pierce).

4.3. Results

4.3.1 Hepatic iron concentration

There was an increase in the concentration of NHI in the livers of mice fed diets with increasing concentrations of dietary iron (**Figure 4.1 A**). A significant difference in NHI was observed across all the groups with increasing iron concentration starting with 0.25% ($3.9 \pm 0.3 \mu\text{mol} / \text{g}_{\text{liver}}$), 0.5% ($6.3 \pm 0.8 \mu\text{mol} / \text{g}_{\text{liver}}$), 1% ($8.4 \pm 0.4 \mu\text{mol} / \text{g}_{\text{liver}}$) and 2% ($15 \pm 2.6 \mu\text{mol} / \text{g}_{\text{liver}}$) compared to control ($1.6 \pm 0.2 \mu\text{mol} / \text{g}_{\text{liver}}$; $P < 0.001$). The increase in liver iron with increasing dietary iron concentration was mirrored in the liver tissues stained for iron using Perls' stain (**Figure 4.2 A-E**). Iron loading showed a peri-portal distribution (blue colour) in line with observations made by others [238].

Mitochondria were isolated from all the treated groups and NHI measured. Mitochondrial iron increased with increasing dietary iron (**Figure 4.1 B**). The measured NHI concentrations were control ($78 \pm 9 \text{ nmol} / \text{g}_{\text{liver}}$), 0.25% ($139 \pm 27 \text{ nmol} / \text{g}_{\text{liver}}$), 0.5% ($250 \pm 28 \text{ nmol} / \text{g}_{\text{liver}}$), 1% ($410 \pm 78 \text{ nmol} / \text{g}_{\text{liver}}$) and 2% ($641 \pm 214 \text{ nmol} / \text{g}_{\text{liver}}$). Significant differences were observed between all the groups, 0.25% ($P < 0.05$), 0.5% ($P < 0.01$), 1% ($P < 0.01$) and 2% ($P < 0.05$) compared to control. When liver NHI content was plotted against mitochondrial NHI (**Figure 4.1 C**), a strong positive correlation was observed ($R^2 = 0.822$, $P < 0.0001$).

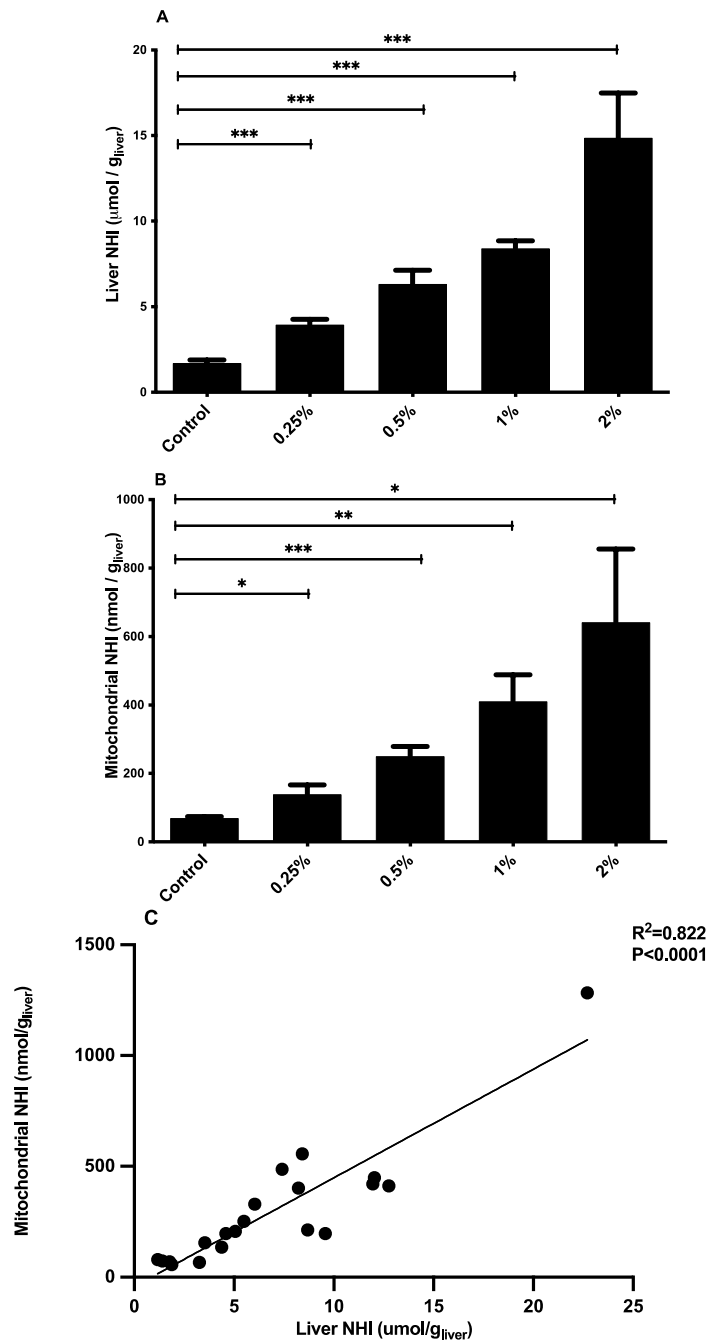


Figure 4.1. **Influence of Dietary Iron Loading on Non-Haem Iron.** (A) Hepatic and (B) mitochondrial non-haem iron were measured in mice fed control diet (n = 5), or 0.25%, 0.5%, 1% or 2% carbonyl iron diet (n = 4 in each group). (C) Relationship between mitochondrial and liver NHI. Non-haem iron was measured as described in section 2.3.8. Data in (A) and (B) are presented as mean ± SEM.

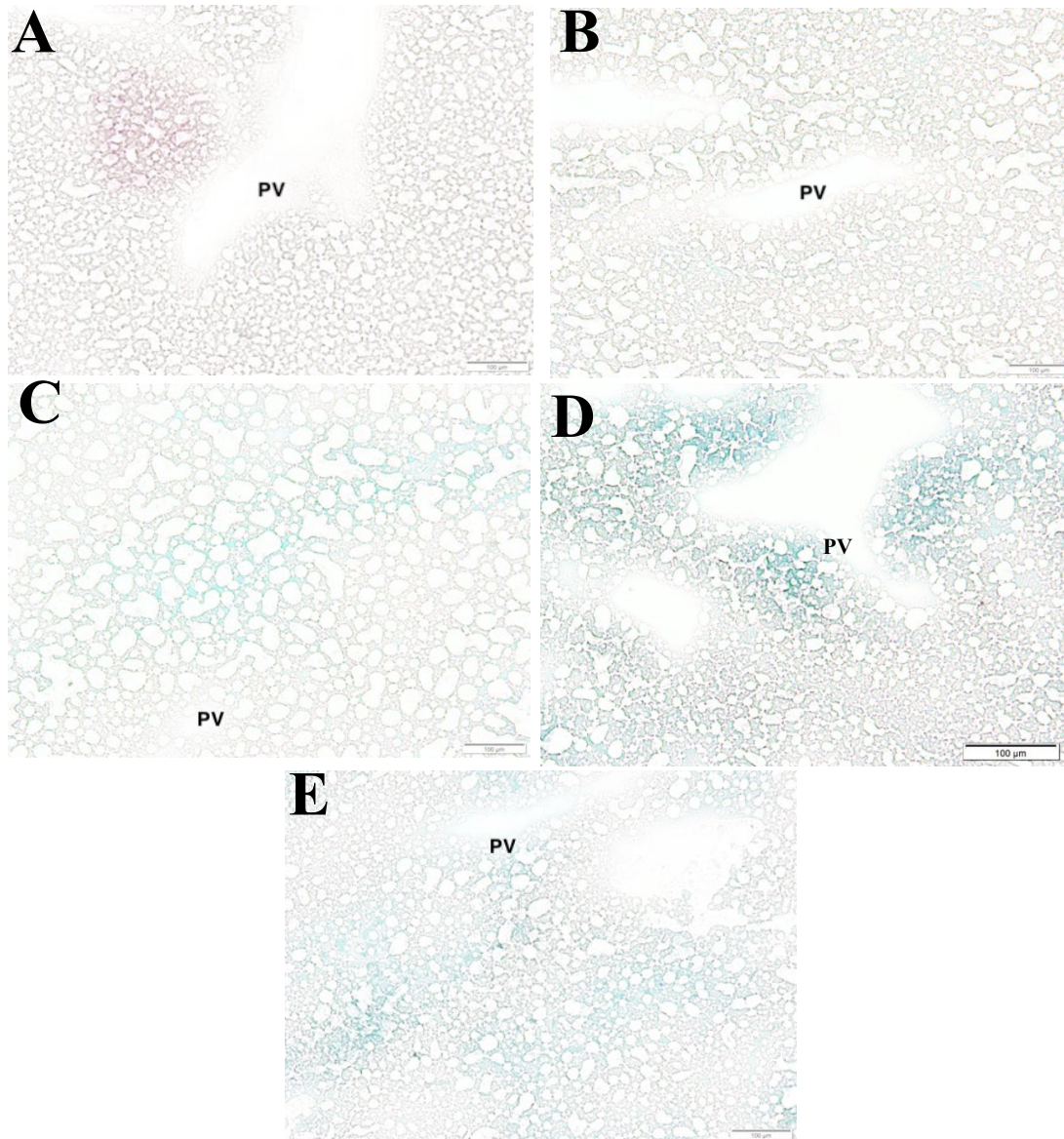


Figure 4.2. **Influence of Iron Loading on Hepatic Iron.** Liver tissues from mice fed (A) control diet, or (B) 0.25%, (C) 0.5%, (D) 1% or (E) 2% carbonyl iron were stained for iron using Perls' Prussian blue. Blue colour represents iron deposition. PV- portal vein.

4.3.2. Effect of iron loading on mitochondrial cholesterol

To investigate if iron loading in mice led to increased mitochondrial cholesterol, total cholesterol was measured in isolated mitochondria (**Figure 4.3**). Total cholesterol content in the mitochondria was not significantly different between any of the groups: control (3.07 $\mu\text{g} / \text{mg}$ protein), 0.25% (2.95 $\mu\text{g} / \text{mg}$ protein), 0.5% (3.35 $\mu\text{g} / \text{mg}$ protein), 1% (3.35 $\mu\text{g} / \text{mg}$ protein) and 2% (2.97 $\mu\text{g} / \text{mg}$ protein).

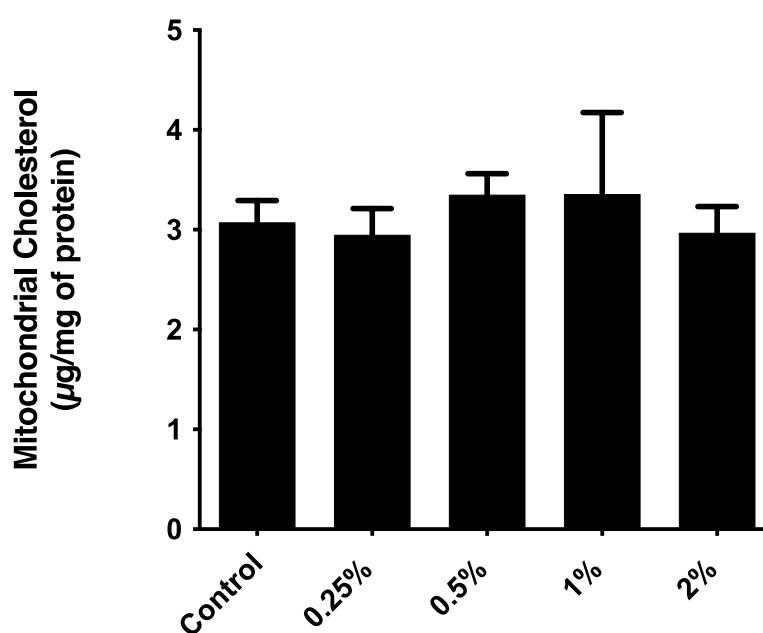


Figure 4.3. **Influence of Iron Loading on Mitochondrial Cholesterol Content.** Total cholesterol in isolated mitochondria was measured in mice fed control diet (n = 4), or 0.25% (n = 3), 0.5% (n = 4), 1% (n = 3) or 2% (n = 4) carbonyl iron diet. The assay was performed as described in section 4.2. Data presented are mean \pm SEM.

4.3.3. Body Weight

Mice fed control, 0.25%, 0.5%, 1% or 2% carbonyl iron were weighed prior to sacrifice (**Figure 4.4**). The control group weighed 19.6 ± 0.7 g compared to the 0.25% (18.5 ± 0.4 g), 0.5% (17.5 ± 0.2 g), 1% (18.4 ± 0.2 g) and 2% (18.6 ± 1.0 g) iron groups. Despite increasing iron concentration in the diet, the mice did not show any significant differences within groups in their body weights which suggests that the diets were well-tolerated. All mice were monitored twice a week for weight, coat, activity, breathing, movement, eating/drinking, presence or absence of barbering, diarrhoea, and the observations noted in the monitoring sheet. All these parameters were found to be normal during the study, indicating that interpretation of results will not be complicated by the health status of the mice.

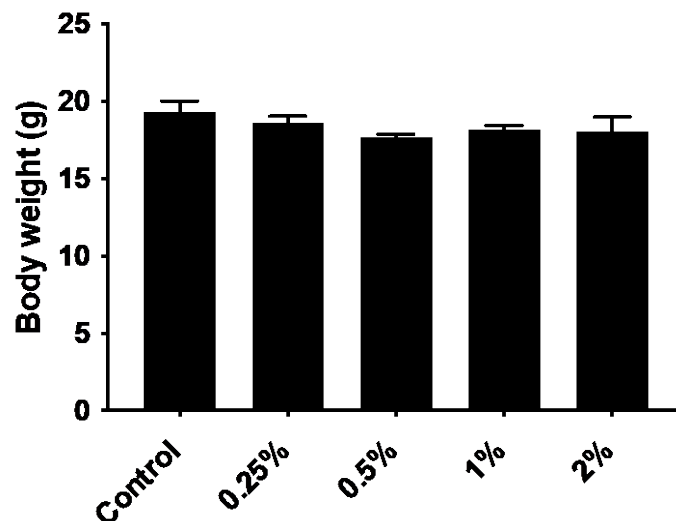


Figure 4.4. **Effect of Iron Loading on Body Weight.** Mice fed the control diet (n = 5), 0.25%, 0.5%, 1% or 2% carbonyl iron (n =4 per condition) diet was measured immediately prior to sacrifice. Data presented are mean \pm SEM.

4.3.4. Genes involved in hepatic iron homeostasis

Hepatic expression of genes involved in iron homeostasis, *Hamp1* (hepcidin), divalent metal transporter 1 and transferrin receptor 1 was examined in mice fed control, 0.25%, 0.55, 1% and 2% carbonyl iron diets (**Figure 4.5**). The expression of the mRNA for *Hamp1*, which regulates cellular and body iron homeostasis, exhibited a significant positive relationship with liver non-haem iron ($R^2= 0.547$, $P<0.003$). *Dmt1* expression did not show any significant relationship with liver non-haem iron ($R^2= 0.038$, $P<0.4$). The same was observed for *Tfr1* ($R^2= 0.005$, $P<0.76$). In summary, hepcidin expression increased with increasing hepatic iron concentration but the genes involved in iron transport, *Dmt1* and *Tfr1*, did not.

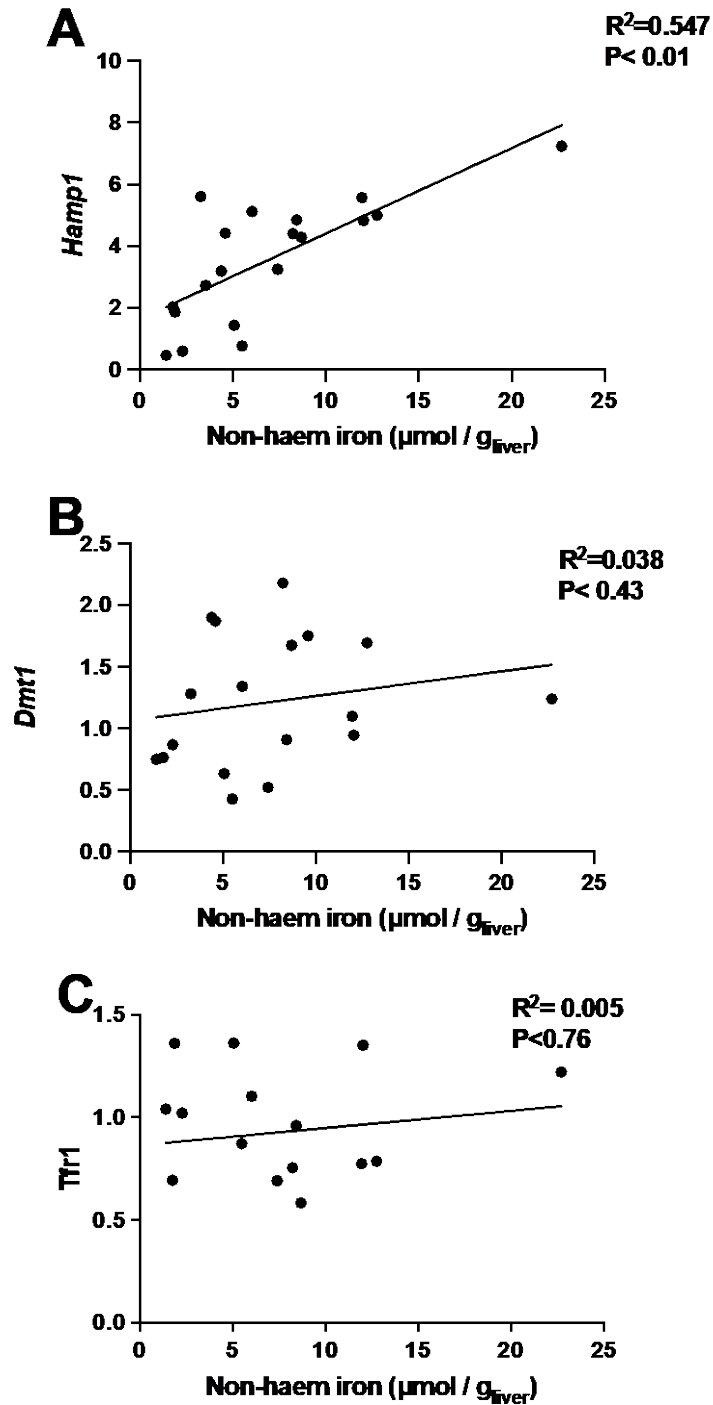


Figure 4.5. **Influence of Iron Loading on Hepatic Iron homeostasis genes.** Relationship between hepatic non-haem iron and hepatic gene expression of (A) *Hamp1*, (B) *Dmt1* and (C) *Tfrr1* in mice fed diets containing 0.02 to 2 % carbonyl iron (n = 18-19). Non-haem iron was measured as stated in section 2.3.8 and gene expression by RT-PCR as described in section 2.3.7.

4.3.5. Genes involved in mitochondrial and peroxisomal fatty acid oxidation

Hepatic expression of mitochondrial fatty acid oxidation genes, Acyl-CoA dehydrogenase short chain (*Acads*) and peroxisomal, Acetyl-Coenzyme A acyltransferase 1a (*Acaal1a*) was examined (**Figure 4.6**). No significant relationship was observed between hepatic iron concentration and *Acaal1a* ($R^2= 0.005$, $P<0.76$) or *Acads* ($R^2= 0.029$, $P= 0.481$). This observation is interesting given that NHI in the mitochondria increased with increasing hepatic iron concentration (**Figure 4.1 B**) and a recent study showed that dietary iron loading negatively affects liver mitochondrial function by impairment of mitochondrial oxidative phosphorylation [243]. However, only a few genes involved in mitochondrial β -oxidation were investigated for this part of the study. This has been addressed in the next chapter where a larger number of genes have been investigated using a single dietary iron concentration.

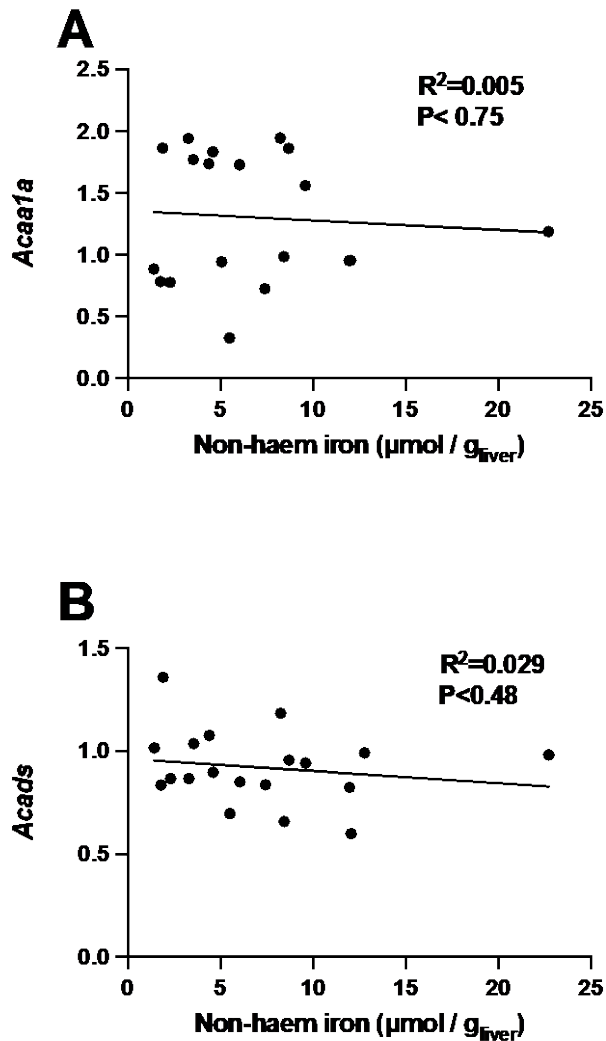


Figure 4.6. **Influence of Iron Loading on Mitochondrial and Peroxisomal Fatty Acid Oxidation Genes.** Relationship between hepatic non-haem iron and hepatic gene expression of (A) *Acaa1a* and (B) *Acads* in mice fed diets containing 0.02 to 2 % carbonyl iron (n = 18-19). Non-haem iron was measured as stated in section 2.3.8 and gene expression by RT-PCR as described in section 2.3.7.

4.4. Discussion

The study discussed in this chapter was aimed at finding a favourable iron concentration that could be used to induce dietary iron overload in mice. This was important because the project investigated the role of iron loading in NAFLD development instead of the more severe stages of the disease which include NASH and fibrosis. Most of the published literature focusses on NASH and fibrosis and uses a concentration of 2% or above to induce secondary iron overload [213, 244]. It is very clear from the current results that increased dietary iron led to an increase in hepatic iron content in a dose dependent manner and it also strongly correlated with mitochondrial iron content. Mice accumulated iron in the liver localised to the peri-portal region. It is important to note that similar stainable liver iron is present in about 34% of patients diagnosed with NAFLD [112]. The pattern of iron distribution observed here is in line with observations made elsewhere in mice and other organisms including humans [238].

In order to test the hypothesis that iron can be targeted towards the mitochondria, NHI was measured in mitochondria isolated from mice fed varying dietary iron concentrations. Mitochondrial NHI increased with increasing dietary iron concentration. This is interesting because the iron transporter Dmt1 was shown to be associated with mitochondrial iron uptake [185] and is present in the OMM [186] and the induction of mitochondrial Dmt1 expression correlated with increased NHI. This observation becomes important as a strong positive correlation was found between hepatic and mitochondrial NHI content in the present study. Excess iron in the mitochondria can be detrimental to mitochondrial function [243] since, apart from inducing ROS production, it can modulate the genes involved in mitochondrial fatty acid oxidation and also alter the electron transport chain [245] by decreasing the activity of complex II/III activity. Impairment of the electron transport chain can lead to mitochondrial dysfunction.

Previously, our group has shown that hepatic iron overload leads to up-regulation of cholesterol biosynthesis genes [46] and increased liver cholesterol. Increased mitochondrial cholesterol has been linked to NAFLD [246] where it is linked to the impairment of specific solute carriers due to the change in physical property of the membrane. Therefore, I measured mitochondrial cholesterol in mice fed varying iron concentration. No difference was observed in the cholesterol content of isolated mitochondria at any iron concentration. This indicates that any cholesterol produced due to iron loading was not targeted to the mitochondria. However, it is NASH that is linked to excess mitochondrial cholesterol, not simple steatosis, so not seeing increased mitochondrial cholesterol in the present study may not be surprising. The present

study suggests that mitochondrial cholesterol loading may begin in the later stages of development from steatosis to NASH.

In several studies involving mice and dietary iron overload, body weight has been found to decrease with increasing iron concentration [238]. Interestingly, in the present study, there was no significant decrease in mouse body weight in any group compared to controls. It has been argued that increased iron concentration makes the diet less palatable resulting in the mice eating less or that the diet is somehow detrimental to the health of the animals [238]. However, in the present study the mice remained healthy throughout the study and did not show any sign of discomfort. One of the reasons for reports of weight loss may be the form in which diet is presented to the animals. In the present study it was noted that mice consume more when the diet is softer than diets presented in pellet form (data not shown). In another study in our group, we have found that grinding the dietary pellets and then making dough from these leads to more rapid consumption by the mice. It is likely to be due to these reasons that the iron diet in the present study did not lead to reduced body weight.

In order to assess the role of varying dietary iron concentration on hepatic expression of genes involved in iron metabolism, mRNA expression of *Hamp1*, *Dmt1* and *Tfr1* was measured and plotted against hepatic NHI. *Hamp1*, the gene that encodes hepcidin, which is a regulator of iron homeostasis, increased with increasing iron concentration in line with previous observations by us [46] and others [238]. In the present study, 1% carbonyl iron showed strong correlation with hepatic NHI as seen by increase in *Hamp1* expression when compared to different concentrations used in the study (data not shown). Interestingly, a previous study [238] reported that *Hamp1* expression plateaued at 0.25% carbonyl iron and no further increase was observed even in mice fed higher carbonyl iron concentration. The current results indicate that *Hamp1* expression does not plateau at 0.25% but increases further in mice fed higher iron concentration up to 2% (**Figure 4.5 A**). There are several reasons which may help explain the differences, including the sex, feeding duration and age of the animals. Sex and strain have been shown to influence the expression of *Hamp1* [151]. The study discussed above [238] made use of male mice and those were fed for two weeks and were younger (6 weeks) than the mice in the present study which were female, iron loaded for three weeks and were sacrificed when 11 weeks old. Oestrogen response elements [86] have been shown to regulate expression of iron genes by modulating *Hamp1* expression [247] and could play a role in controlling the gene expression; however, they were not investigated as the focus of the present study was elsewhere.

Genes involved in iron transport including *Tfr1* and *Dmt1* were also measured, but their expression did not show any correlation with hepatic NHI. *Tfr1* expression is controlled by several factors including iron and oxygen status [248] and *Tfr1* mRNA contains five IREs which are responsible for its post-transcriptional regulation depending on cellular iron concentration [249]. The lack of correlation here does not mean iron status did not have an effect on *Tfr1* expression. It is possible that the system was sufficiently iron loaded that any further iron had no regulatory impact on *Tfr1* expression.

The carbohydrate content of the control diet used here was high and this may have had an impact on the gene expression, as in another study conducted in this project (discussed in chapter 6), high fat diet significantly decreased hepatic iron content and altered hepatic iron metabolism. The same alterations may have occurred here even though the source of fat was different.

Mitochondrial dysfunction has been linked with NAFLD [250] and iron has been found to be targeted towards the mitochondria. Mitochondria are an important site for fatty acid metabolism which may alter fatty acid oxidation and the ETC. In addition, *Dmt1* can facilitate mitochondrial iron uptake [185]. The impacts of iron loading on mitochondrial and peroxisomal fatty acid β -oxidation pathways were investigated in this study. None of the genes investigated showed any correlation with hepatic iron concentration. This may be surprising given that there is an increase in mitochondrial NHI with increasing iron concentration. However, only a few genes involved in fatty acid β -oxidation were investigated as markers of these pathways and, as a result, other genes which may have been impacted may have been missed. This was addressed in the study described in the next chapter where a larger number of genes involved in both mitochondrial and peroxisomal β -oxidation were studied. It is also likely that the hepatic steatosis caused by the high carbohydrate content of the control diet may impact the gene expression by having a regulatory effect on fat and iron metabolism.

In conclusion, 1% carbonyl iron was selected as a favourable concentration to be used in further studies (Chapters 5 and 6). Increase in hepatic iron concentration correlated with increased dietary iron. A similar trend was observed within the mitochondria and a strong correlation was observed between hepatic and mitochondrial iron. Dietary iron loading did not lead to any significant body weight difference in any of the groups. Despite the increase in mitochondrial iron, no significant increase in mitochondrial cholesterol was evident. Increasing iron concentration in the diet led to visible hepatic iron accumulation in the peri-portal region as evidenced by Perls' staining. The increase in hepatic iron also showed a strong correlation with

hepcidin expression but did not affect expression of *Tfr1* or *Dmt1* which are involved in iron transport. A similar observation was made for mitochondrial and peroxisomal fatty acid genes.

Chapter 5 Hepatic Gene Expression in Dietary Iron Loading

5.1. Background

Iron overload has been associated with many pathological conditions including diabetes, cardiovascular complications, and liver-related diseases [251-253]. Among liver-related diseases, NAFLD has been associated with iron overload, and about one-third of patients diagnosed with NAFLD exhibit altered iron homeostasis [218]. The consensus concerning the role of iron overload in NAFLD is that progression is triggered by iron-catalysed oxidative stress [11, 254]. As discussed in section 1.4, iron may not only contribute to the progression of NAFLD but also to the initial lipid accumulation. It has been shown that dietary iron overload in mice leads to upregulation of genes associated with cholesterol biosynthesis pathways and a subsequent increase in hepatic cholesterol [46].

In the previous chapter (4), I showed that there is an increase in hepatic as well as mitochondrial non-haem iron with increasing dietary iron concentration which supports the initial hypothesis that iron is being transported to the mitochondria. It has also been shown that iron loading negatively affects mitochondrial functions by causing a decrease in oxidative phosphorylation [243]. Evidence from this laboratory suggests that iron loading in mice may affect the genes involved in mitochondrial fatty acid oxidation which, in turn, may lead to hepatic fat accumulation along with reduced ATP production, which may explain lethargy seen in patients with haemochromatosis [255, 256]. It is important to note that patients suffering from NAFLD also experience fatigue [257, 258] and this may also have a component attributable to hepatic iron loading [259]. This becomes more meaningful because, as discussed previously, iron loading in mice negatively affects mitochondrial function possibly leading to reduced ATP turnover leading to fatigue [243].

Apart from negatively affecting mitochondrial function, iron overload may also lead to increased cholesterol biosynthesis. It has been shown that in NAFLD, altered cholesterol homeostasis and transport may lead to the accumulation of free cholesterol in the liver [260] which can lead to the formation of hepatic cholesterol crystals. In this study, I investigated the presence of cholesterol crystals during simple steatosis and the effect of dietary iron on cholesterol crystal formation. It has been suggested that cholesterol crystals may be involved in activation of inflammatory pathways, thereby contributing to progression to NASH [135] [261].

The studies presented in this chapter used female C57BL/6J mice to investigate the effect of dietary iron loading on liver, spleen, and duodenal gene expression of iron-related genes along with genes associated with fatty acid oxidation. The role of iron in relation to the formation of hepatic cholesterol crystals, along with its role in activation of hepatic cells (inflammatory, stellate and progenitor), which are markers of liver injury and NAFLD progression, was also investigated.

5.2. Methods

Diets were prepared as described in section 2.3.2. The mice were divided into 2 groups, control (n=10) and 1% iron (n=10). Mice were fed the diets for 3 weeks from 8 weeks of age after which they were fasted overnight before sacrifice. Liver, spleen, and duodenum were collected, and samples taken for RNA isolation and NHI determination. A separate liver sample was embedded in OCT for histology.

RNA was isolated from liver as described in section 2.3.4 followed by cDNA synthesis using the SensiFast™ cDNA kit (Bioline) as described in section 2.3.6. Real-time, quantitative PCR was performed using SensiFAST™ SYBR Lo-Rox (Bioline) chemistry as described in section 2.3.7. Results were quantified as previously described by Graham et al [46] using β -actin as the house-keeping gene. Primer details are provided in Table 2.1. Histology was performed on OCT-embedded tissues which were 5 μ m in thickness as described under section 2.3.9. NHI was determined in liver as described in section 2.3.8.

ORO staining was performed as described in section 2.4.2. Stained liver slides were examined under a Nikon Eclipse microscope with and without polarizing filter for the presence of cholesterol crystals under the guidance of expert blinded histopathologist A/Professor Vincent Williams in the School of Pharmacy and Biomedical Sciences, Curtin University. A quantitative analysis was performed for cholesterol crystallization by counting the number of crystals per 10 randomly selected regions per sample, as described [10]. Sample area per field was calculated using Nikon software.

To determine whether the iron diet caused any hepatic injury, a preliminary investigation using immunohistochemistry (described in section 2.4.4) was performed on the sample from each group that contained the highest number of cholesterol crystals. The details of the primary and the secondary antibodies are listed in Table 5.1.

Epitope	Host Species	Reactivity	Dilution
Primary Antibody			
CD45	rat	murine	1/400
α SMA	murine	murine, human	1/2000
panCK	rabbit	cow, murine	1/400
Secondary Antibody			
IgG	goat	rat	1/400
IgG	goat	murine	1/400
IgG	goat	rabbit	1/400

Table 5.1. List of primary and secondary antibodies.

5.3. Results

5.3.1. Mouse body weight and hepatic iron concentration

All the animals remained healthy through the course of the experiment, not showing any signs or symptoms of physical stress and no observable changes in coat condition or activity. This was reflected in the body weight (**Figure 5.1**) where there was no significant difference between mice fed control (20.5 ± 0.5 g) or iron loaded (19.7 ± 0.5 g) diets. Iron loading in mice led to an increase in hepatic non-haem iron (12 ± 1 $\mu\text{mol} / \text{g}_{\text{liver}}$) compared to the control group (2.3 ± 0.2 $\mu\text{mol} / \text{g}_{\text{liver}}$) ($P < 0.0001$; **Figure 5.2**).

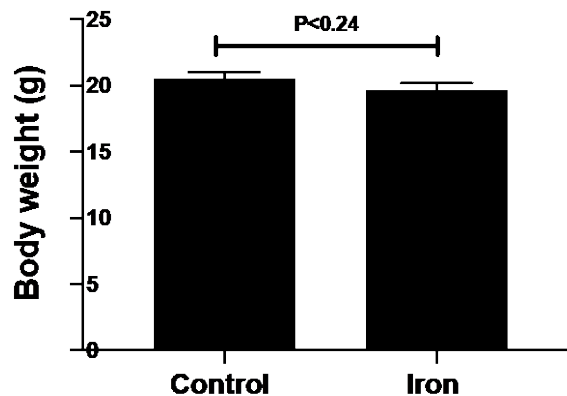


Figure 5.1. **Mouse body weight.** Body weight of control (n = 10) and 1% carbonyl iron- (n = 10) fed mice was measured immediately prior to sacrifice. Data presented as mean \pm SEM.

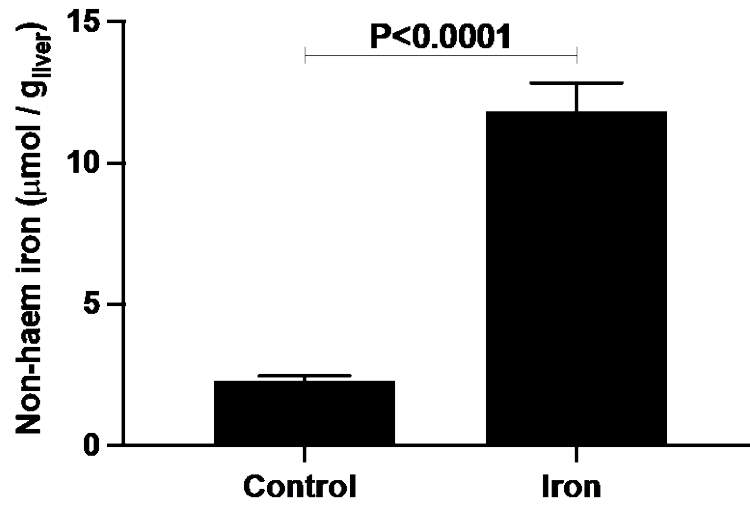


Figure 5.2 **Hepatic non-haem iron concentration.** Hepatic NHI was measured in mice fed control diet (control; $n = 10$) or 1% iron diet ($n = 10$). NHI was measured as described in section 2.3.8. Data presented are mean \pm SEM

5.3.2. Expression of hepatic iron homeostasis genes

Hepatic expression of genes involved in maintaining iron homeostasis was examined in mice fed control or iron loaded diets (**Figure 5.3**). Gene expression showed a significant change in *Hamp1* expression with increasing hepatic iron ($R^2= 0.197$, $P< 0.05$). *Fpn* expression did not exhibit any measurable change with respect to hepatic iron and was not significant ($R^2= 0.006$, $P< 0.74$). *Tfr1* expression exhibited a decrease with iron loading and was very close to statistical significance ($R^2= 0.183$, $P< 0.06$). *Dmt1* expression did not show a significant relationship with hepatic iron ($R^2= 0.106$, $P< 0.18$).

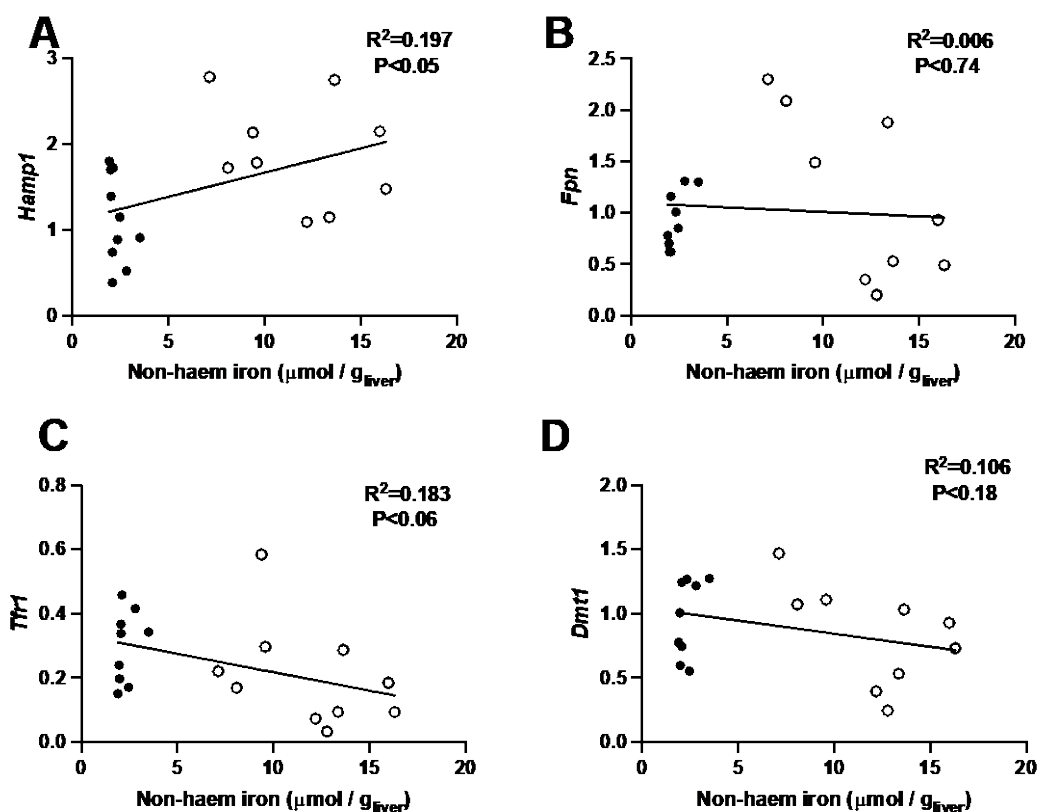


Figure 5.3 **Hepatic expression of iron homeostasis genes.** Relationship between hepatic non-haem iron and hepatic expression of (A) *Hamp1*, (B) *Fpn*, (C) *Tfr1* and (D) *Dmt1* in control (●) (n = 5-10) and 1% iron (○) (n = 8-10) fed mice. Non-haem iron was measured as stated in section 2.3.8 and gene expression by RT-PCR as described in section 2.3.7.

5.3.3. Expression of mitochondrial and peroxisomal fatty acid metabolism genes

Linear regression analysis indicated non-significant relationships between the gene expression of *Acadvl* ($R^2= 0.009$, $P< 0.697$) and *Acads* ($R^2= 0.046$, $P< 0.458$) compared to hepatic NHI content (Figure 5.4A & C). In contrast, *Acadm* exhibited a significant decrease with hepatic NHI ($R^2= 0.267$, $P< 0.03$; Figure 5.4B) and *Hadha* ($R^2= 0.393$, $P< 0.01$; Figure 5.4D) exhibited a statistically significant decrease. The results suggest that hepatic iron loading may cause selective oxidation of fatty acids.

In contrast to mitochondrial fatty acid genes, no changes in expression were evident in genes involved in peroxisomal fatty acid metabolism: *Acaa1a* ($R^2= 0.003$, $P< 0.83$) (Figure 5.5 A), *Ech1* ($R^2= 0.025$, $P< 0.56$) (Figure 5.5 B) and *Slc27a2* ($R^2= 0.001$, $P< 0.68$) (Figure 5.5 C).

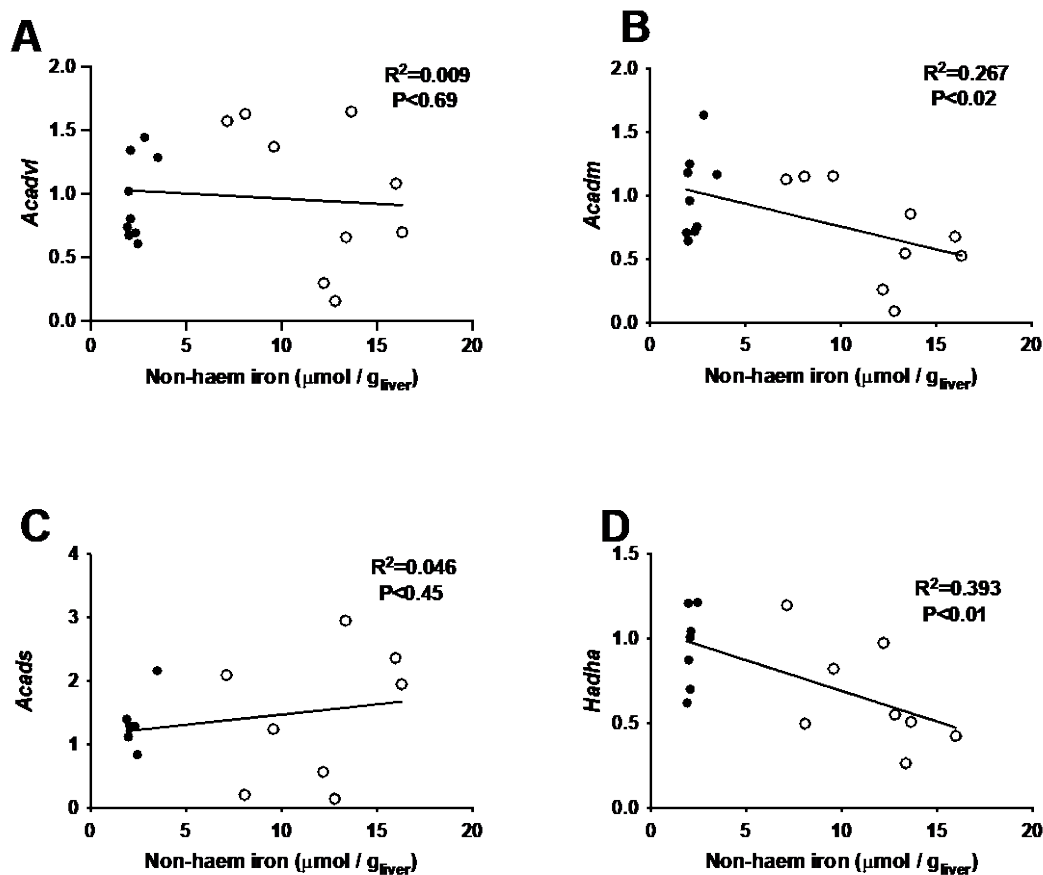


Figure 5.4 Hepatic expression of mitochondrial fatty acid oxidation genes. Relationship between hepatic non-haem iron and hepatic expression of (A) *Acadvl*, (B) *Acadm*, (C) *Acads* and (D) *Hadha* in control ($n = 5-10$) and 1% carbonyl iron ($n = 8-10$) fed mice. Non-haem iron was measured as stated in section 2.3.8 and gene expression by RT-PCR as described in section 2.3.7.

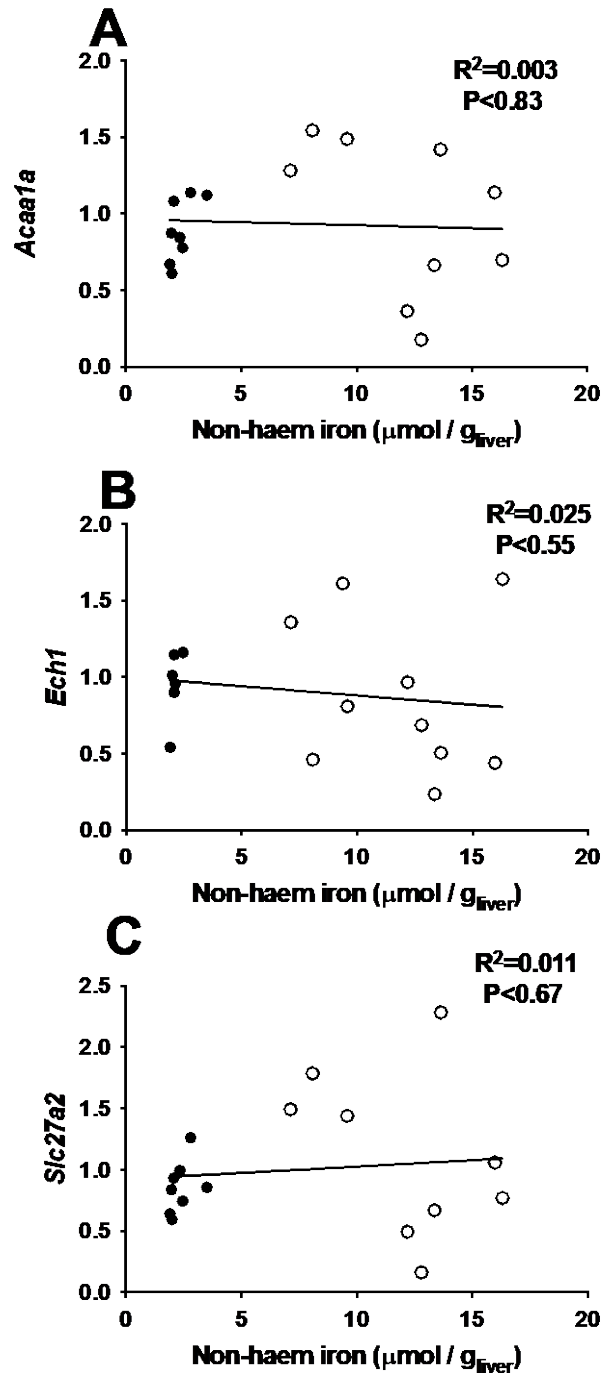


Figure 5.5 **Hepatic expression of peroxisomal lipid metabolism genes.** Relationship between hepatic non-haem iron and hepatic expression of (A) *Acaa1a* (B) *Ech1* and (C) *Slc27a2* in control (n = 5-10) and 1% carbonyl iron (n = 8-10) fed mice. Non-haem iron was measured as stated in section 2.3.8 and gene expression by RT-PCR as described in section 2.3.7.

5.3.4. Effect of iron loading on iron homeostasis genes in the spleen

In order to investigate whether iron loading affects genes involved in iron homeostasis in spleen, expression of *Hamp1*, *Dmt1*, *Fpn* and *Tfr1* was measured (Figure 5.6). *Hamp1* was significantly decreased in the iron loaded group (0.6 ± 0.1 ; $P < 0.05$) compared to control (1.1 ± 0.2). The other genes did not show any statistically significant differences between the two groups of mice.

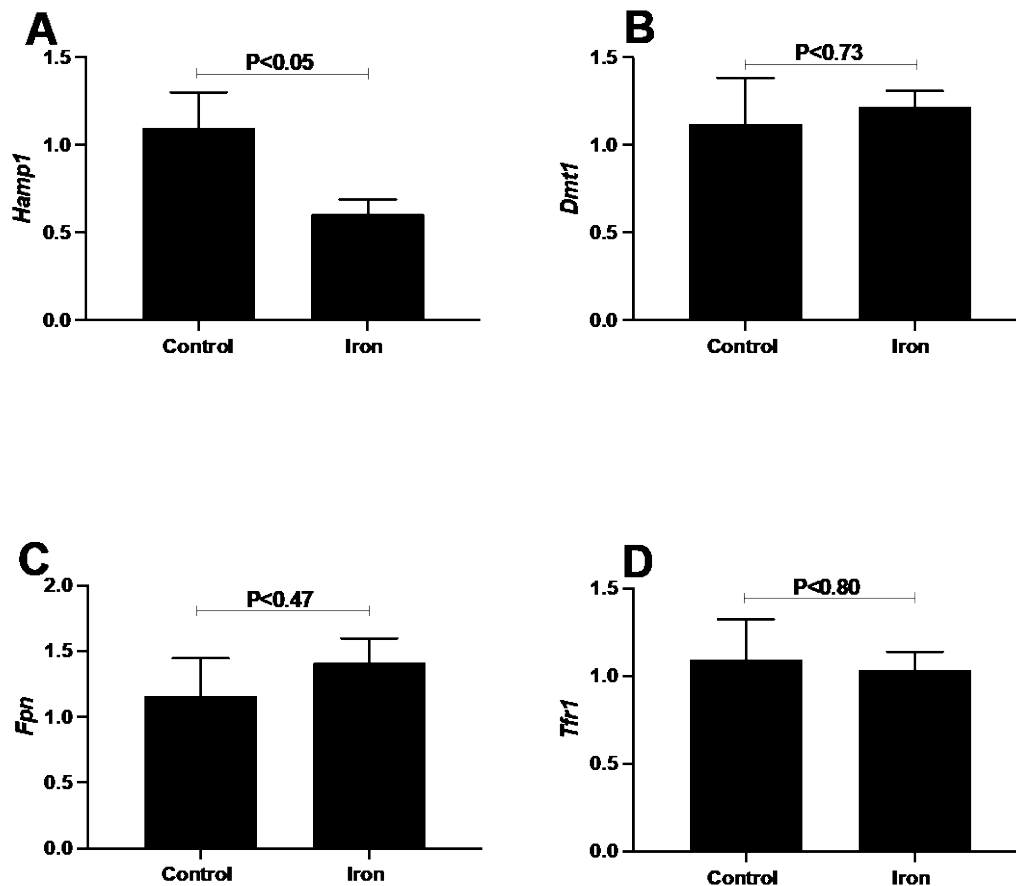


Figure 5.6 Splenic expression of iron homeostasis genes. Gene expression of (A) *Hamp1* (B) *Dmt1* (C) *Fpn* and (D) *Tfr1* in control (n = 6) and 1% carbonyl iron (n = 6) fed mice. Gene expression was performed by RT-PCR as described in section 2.3.7 and was normalised to β -actin. Data presented are mean \pm SEM.

5.3.5. Effect of iron loading on iron homeostasis genes in the duodenum

In order to investigate if iron loading had any effect on duodenal expression of genes involved in iron homeostasis, expression of *Dmt1*, *Fpn* and *Tfr1* was measured and compared to mice fed a control diet (**Figure 5.7**). Interestingly, the expression of *Dmt1* (A) was significantly reduced in mice fed iron loaded (0.3 ± 0.1) diet compared to control (1.3 ± 0.6 ; $P < 0.05$). A similar trend was seen for *Fpn* between control (1.0 ± 0.2) and iron-loaded (0.6 ± 0.1) mice. Although the difference was not statistically significant, it was close to the significance threshold ($P < 0.08$) and is likely to be biologically relevant. *Tfr1* expression did not exhibit any significant differences between the groups ($P < 0.22$).

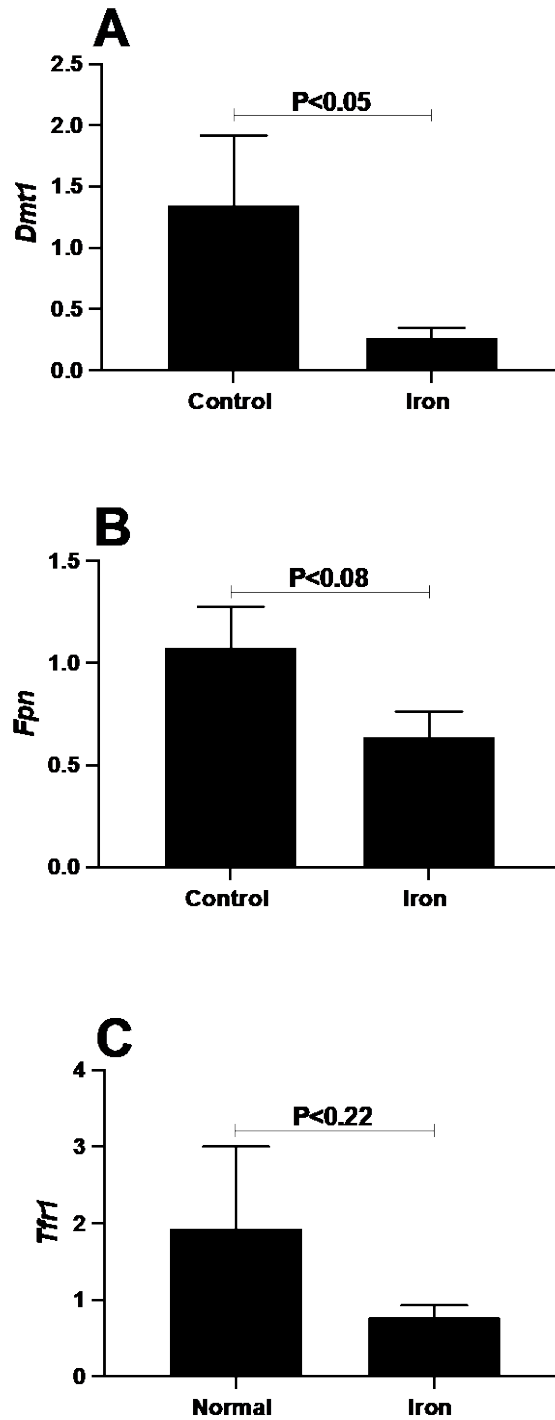


Figure 5.7 **Duodenal expression of iron homeostasis genes.** Gene expression of (A) *Dmt1*, (B) *Fpn* and (C) *Tfr1* in control (n = 5) and 1% carbonyl iron (n = 7) fed mice. Gene expression was performed by RT-PCR as described in section 2.3.7 and was normalised to β -actin. Data presented are mean \pm SEM.

5.3.6. Liver morphology

Liver morphology was studied using H&E staining and the presence of iron was detected using Perls' Prussian blue staining. The control and the iron diet fed mice showed hepatic micro-vesicular fat deposition (**Figure 5.8A & B**) and this is likely to be attributable to the carbohydrate content in the diet. In contrast, mice fed normal chow and iron loaded chow did not exhibit micro-vesicular fat deposition but, interestingly, the iron diet fed mice showed the presence of macrophages (**Figure 5.8 C & D**), suggesting inflammatory necrosis around the portal area. The presence of iron was detected using Perls' staining and can be seen deposited mainly in the peri-portal region (**Figure 5.8 F**). In contrast, no staining was detected in mice fed control diet (**Figure 5.8 E**).

Morphology & Iron Deposition

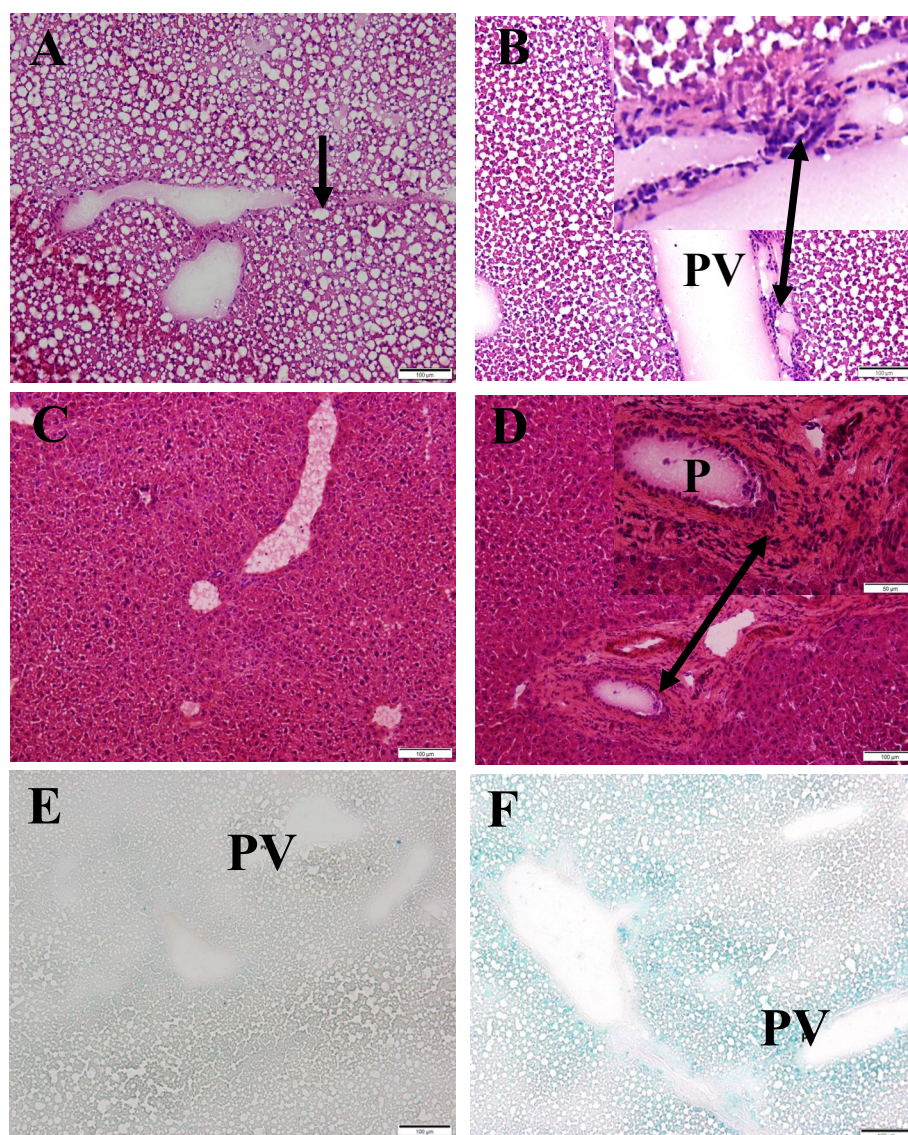


Figure 5.8 **Liver histology.** Representative images of H&E stained livers from (A) control and (B) 1% carbonyl iron fed mice. The arrow on image (A) represents lipid deposition and the double arrow (B & D) inflammatory cells. Images (C) and (D) are H&E-stained sections from mice fed a normal chow diet and 1% carbonyl iron mixed with chow diet. Perls' staining for the presence of iron in livers from (E) control and (F) 1% carbonyl iron fed mice. Blue colour indicates the presence of iron. PV- portal vein. Staining was performed as described in sections 2.4.0 and 2.4.1. Scale bar 100 μm .

5.3.7. Iron loading and hepatic cholesterol crystals

Oil Red O stained liver slides of both control and iron loaded livers were visualised under polarised light (**Figure 5.9**) to evaluate the presence of cholesterol crystals. The crystals were quantified by an accredited histopathologist, counting the crystals in ten random fields per animal (0.26 mm² per field; **Figure 5.9C**). These crystals are rhomboid or needle-like structures and appear birefringent under polarised light. Iron-loaded mice displayed an average of 1.8 ± 0.9 cholesterol crystals / 0.26 mm² compared to control (0.4 ± 0.2 / 0.26 mm²), but the difference was not statistically significant (Figure 5.9C; $P < 0.28$).

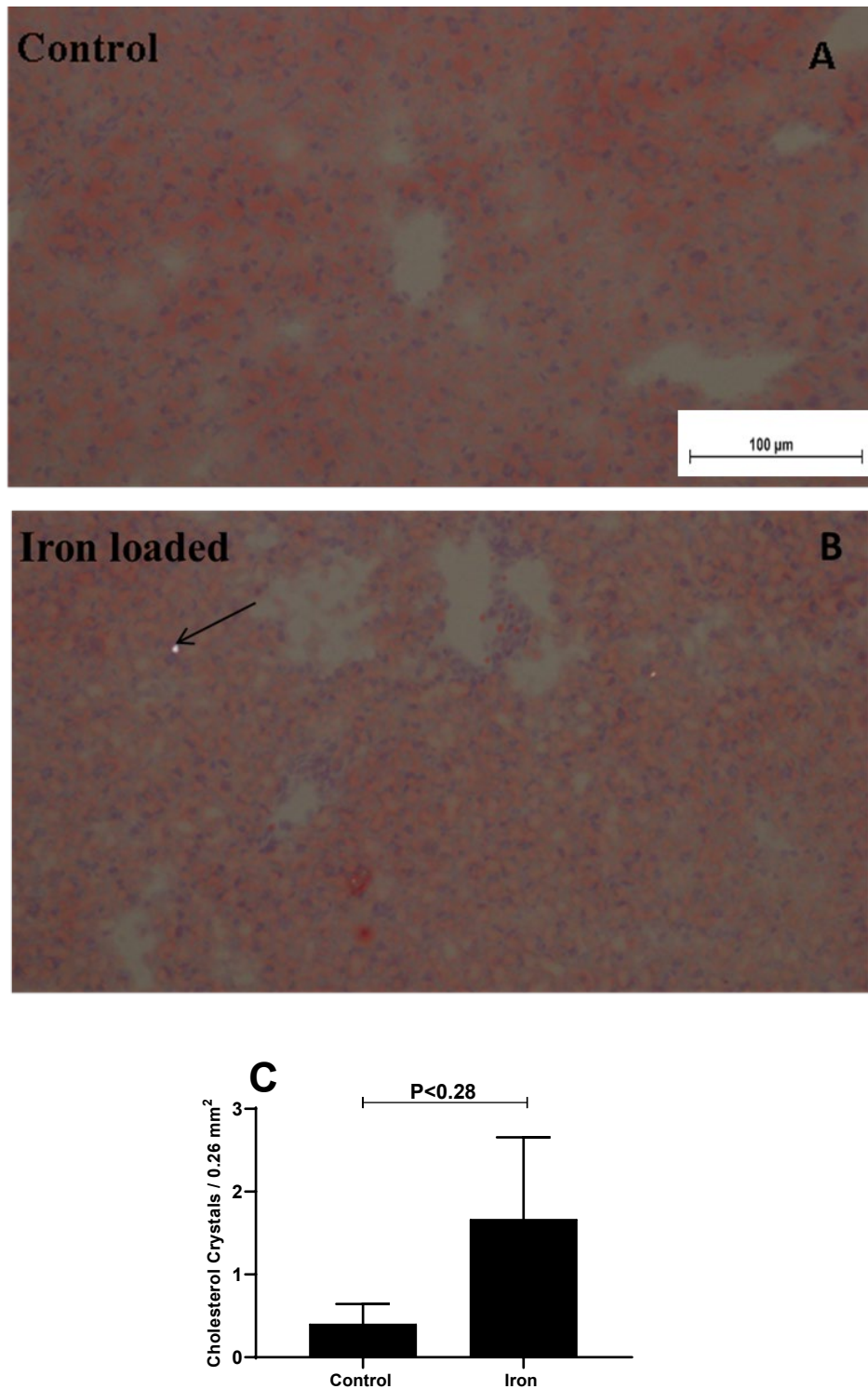


Figure 5.9 **Hepatic cholesterol crystals.** ORO stained slides were visualised under polarised light to detect the presence of cholesterol crystals. Representative images from (A) control (n=5) and (B) iron-loaded (n=6) mice. Arrow indicates the presence of cholesterol crystals. (C) Crystals were quantified as described in section 5.2. Data presented in (C) are mean \pm SEM.

5.3.8. Hepatic injury markers

Given the apparent infiltration of macrophages seen with H&E staining, a preliminary experiment was conducted to confirm whether hepatic injury was, indeed, present by examining one mouse from each dietary group. Livers were examined for the presence of an inflammatory marker (CD45), an activated stellate cell marker (α -SMA) and a liver progenitor cell (LPC) marker (panCK) (**Figure 5.10**). CD45 is a general marker for inflammatory cells whereas stellate cells are known to be present when liver tissue progresses to fibrosis. Liver progenitor cells are often associated with the presence of liver disease, including hepatocellular carcinoma [209].

CD45 (inflammatory cell marker in white) expression was seen in both control and iron loaded mice but a statistical comparison could not be made due to the sample size. Similarly, no conclusion could be drawn for the other markers PanCK (liver progenitor cells in green) and α -SMA (activated stellate cells in red). This was a preliminary experiment designed to investigate a future direction for the project.

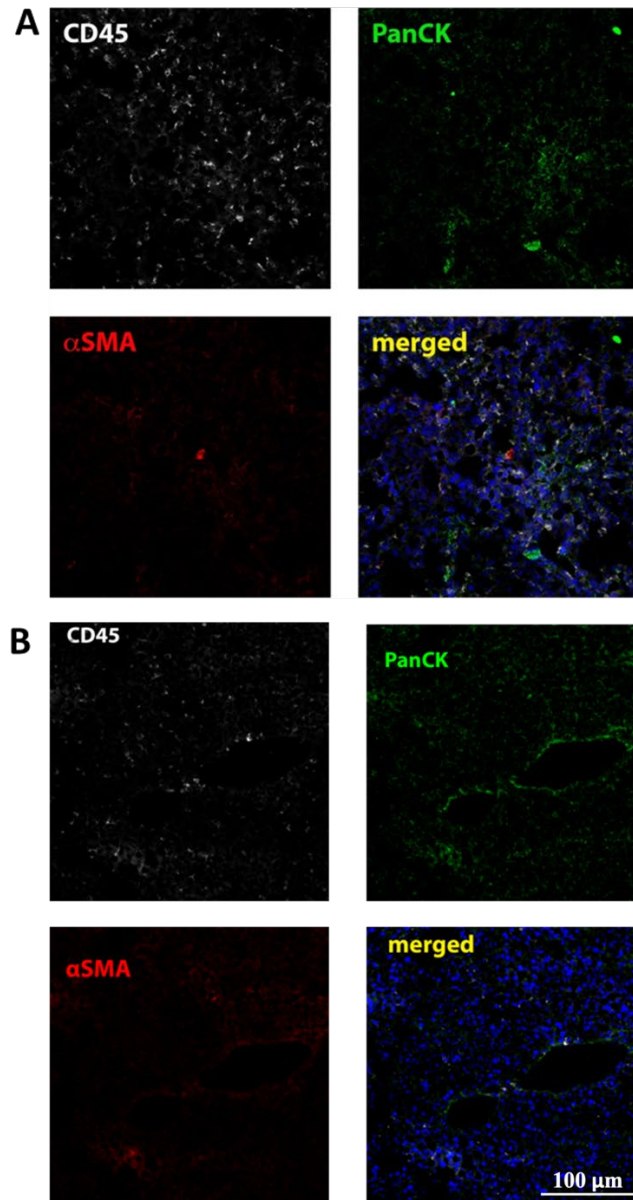


Figure 5.10 **Markers of hepatic inflammation.** Immunohistochemistry of liver from mice fed (A) control or (B) 1% carbonyl iron. One sample from each group was stained for CD45 (inflammatory cell marker), PanCK (activated stellate cell marker) and αSMA (liver progenitor cell marker). DAPI was used to stain the nucleus (blue). Images were taken using a 20X objective lens. The procedure was performed as described in section 2.4.4.

5.4. Discussion

The role of iron overload in the pathogenesis and progression of NAFLD is still not very clear, although increased iron stores in patients diagnosed with NAFLD and NASH has been reported [10]. The results described in this chapter give an insight into the role of iron in the initial stages of NAFLD pathogenesis and progression. There have been reports of hepatic iron accumulation and its role in NASH and fibrosis [244, 262-264] but some of these studies have fed iron diet for a longer period of time and have focussed on chronic iron overload. It is interesting to note here that iron loading (1%) for three weeks in the present study led to the presence of inflammatory and necrotic cells in the liver tissue despite the absence of fibrosis.

The presence of inflammatory cells in mouse liver can be linked to two different responses, the first being the capacity of the liver to maintain organ and systemic homeostasis [265] and the second being activation of inflammatory cytokines which is seen in NASH [266]. It is possible that the mere presence of inflammatory cells in the liver may not lead to NASH or fibrosis as they may work in tandem with, or be a response to, other insults. The cholesterol crystals observed in this project indicate that the insults caused due to iron may very well serve to be a starting point for the progression of NAFLD. The role of cholesterol crystals in NAFLD progression is discussed in detail in Chapter 6.

It is important to note here that changes observed in the gene expression can be attributed to the iron overload induced in the mice through diet. All the animals consumed adequate food in both control and iron loaded group and remained healthy throughout the study. There was no difference in the weights of either group at sacrifice. In some studies, mice on high iron diets have been shown to weigh less than mice fed control diet [238]. Based on the observations made in the present study, the form in which the diet is presented is important. I have noted that mice tend to eat less when the diet is in a hard, pelleted form and addition of carbonyl iron without any palatable additive may lead to mice consuming even less, possibly accounting for the differences observed in the weights in other studies. In the present study, dough was made from the powdered form of the diet and was considerably softer than diets in pellet form.

The Perls' staining and the NHI in the mice liver confirmed iron loading in the peri-portal area and this was also reflected by the increased *Hamp1* expression. *Hamp1* controls hepcidin production which increases in conditions of iron overload, and this has been previously reported by us and others [46, 238, 267] and limits iron absorption under iron loading conditions. The 1% carbonyl iron used in the present study was sufficient to induce iron loading and increase *Hamp1* expression. It has been previously reported that hepcidin expression

plateaus after loading with 0.25% carbonyl iron [238]; however, a plateau was not observed in this study. One of the reasons may be the sex difference between this and the other study as in the present study female mice were used compared to male mice in the other study. Female mice have been shown to have higher hepcidin levels compared to male mice [151].

Fpn and *Dmt1* did not show any significant correlation with NHI. This result is in line with a recently published study which has shown that wild-type and *Hjv*^{-/-} mice can differentially regulate *Fpn* expression in tissues linked with iron export [268] upon iron loading. One of the reasons for not observing any significant correlation may be due to post-transcriptional regulation of *Fpn* in the liver as another study discussed above found no change in *Fpn* mRNA expression upon iron loading [268]. *Tfr1* expression exhibited a decrease with iron loading and was very close to statistical significance, although another study did not report any change in *Tfr1* expression [238]. The reason for seeing a decrease in the present study can be linked to the high hepatic iron as iron exerts a control on *Tfr1* expression as decreased IRP binding leads to degradation of *Tfr1* mRNA under conditions of iron loading.

There are other factors which may play a role in regulation of hepatic gene expression, including age, sex and strain [151], dietary feeding pattern and duration of iron loading. In general, female mice have higher hepcidin levels compared to males; however, findings related to sex differences in iron metabolism are sparse in C57BL/6J mice [103, 151]. In bilaterally ovariectomized and sham-operated C57BL/6J mice, oestrogen has been shown to play an important role in the regulation of iron homeostasis through oestrogen response element (ERE) in *Fpn* promoter region and its effect on hepcidin and ferroportin signalling [86, 247]. Hepatic expression of ferroportin was induced in mice which were ovariectomized as compared to sham-operated mice [86] which highlights the role played by oestrogen in iron metabolism.

Mitochondria play an important role in cellular energy supply by oxidizing fats and sugars to generate ATP [269]. Mitochondrial dysfunction has been linked to NAFLD and its progression to NASH [158] and iron overload has been found to negatively affect mitochondrial function [243]. In the present study, I investigated the role of iron loading and its effect on mitochondrial fatty acid oxidation genes. The results indicate that increased iron in the mitochondria is associated with reduced expression of selected fatty acid oxidation genes. The reduced gene expression is consistent with increased fatty deposition in the liver and is characterised as simple steatosis. The expression of *Acadm*, the gene which encodes the enzyme acyl CoA dehydrogenase for medium chain fatty acids, decreased with iron overload along with *Hadha*, the gene which encodes the alpha subunit of the trifunctional enzyme and catalyses the last

three reactions of mitochondrial β -oxidation [270, 271]. The decreased gene expression upon iron loading as reflected by *Acadm* may be due to several factors including impaired mitochondrial function due to oxidative stress or inflammasome activation. Although oxidative stress and inflammasome activation was not measured in the present study, a previous study in a mouse model of dietary iron overload has shown similar results [244]. In that study, mice on an iron diet showed increased inflammatory immune cell activation along with reduced mitochondrial fatty acid β -oxidation [244]. The finding in the present study suggests that iron overload leads to increased fat accumulation in the liver by decreasing fatty acid β -oxidation. A recent publication from our laboratory has shown that iron loading in AML12 cells leads to *de novo* lipid synthesis [205] which further validates the role of iron in initial fat accumulation. It is important to note that the cellular metabolism of short and medium chain FAs have lesser dependence on fatty acid-binding proteins compared to longer chain FAs [272]. The diet containing 1% carbonyl iron also had an enriched carbohydrate composition which may have a role in gene expression as medium chain FAs which can be transported from the enterocytes through the portal vein to the liver can modulate tissue carbohydrate and lipid metabolism by inhibiting glycolysis and enhancing lipogenesis [272]. In summary, the reduction in gene expression hints at fatty acid accumulation in the liver upon dietary iron loading which strengthens the hypothesis that iron overload plays an important role in fatty accumulation seen in NAFLD.

Dietary non-haem iron, which is in ferric form, gets converted into the transportable form (Fe^{++}) by duodenal cytochrome b (*Dyctb*), a ferric reductase [273]. The reduced iron is then transported by *Dmt1* into the intestinal enterocytes and then further exported through basolateral membrane by *Fpn*. The duodenal gene expression of *Dmt1*, *Fpn* and *Tfr1* was measured in control and iron loaded mice. The expression of *Dmt1* was increased in control mice compared to iron loaded mice which is in line with similar observations made by another group [274]. The expression of *Fpn* too showed a similar trend and was very close to being statistically significant, and no change was observed in the expression of *Tfr1*. These results make biological sense as iron loading in mice led to increased hepatic iron and *Hamp1* expression. This is consistent with decreased uptake of iron into the duodenum, highlighted by a decrease in *Dmt1* expression in iron loaded mice and also a decreased export from enterocytes into the circulation. A similar observation was made in a study conducted on patient samples where decreased gene expression of *Dmt1* & *Fpn* also led to a decrease in protein expression. The results suggest that there is a tight linkage between body iron stores and dietary iron

absorption and confirms the presence of adaptive regulation of *Dmt1* and *Fpn* under condition of secondary iron overload.

In order to investigate if dietary iron loading led to changes in iron gene expression in the spleen, the expression of *Hamp1*, *Fpn*, *Dmt1* and *Tfr1* was measured in the spleens of mice fed control or high iron diet. Although spleen iron content was not evaluated in the present study, *Hamp1* expression in the spleen was found to be decreased compared to control mice. None of the other genes showed any significant differences. In another study, the NHI content of the spleen was found to increase with dietary iron overload [238] whereas another study in mice which used 3% carbonyl iron did not find any statistical difference in *Hamp1* mRNA in the spleen [275]. It is not very clear why *Hamp1* expression decreased in iron loaded mice. One possible reason may be that the C57BL strains have much lower spleen iron content compared to some other strains [276]. *Hamp1* is very tightly regulated by iron stores and a low iron store in the spleen may lead to reduced expression. Genetic modifiers may also play a role in high or low iron phenotype as a genetic variation in *Mon1a*, a protein involved in the vesicular trafficking of FPN to the cell membrane, has been found to modify iron loading in macrophages [276].

H&E staining was performed to investigate the effect of iron loading on liver morphology. Both control and iron loaded mice showed steatosis, characterised by micro-vesicular fat deposition. These observations have been made in another study where high carbohydrate and high fat diet led to high fatty acid accumulation which was more noticeable in high carbohydrate diet as compared to HFD [277]. The present control diet had a high concentration of digestible carbohydrate which would have contributed to steatosis, which may explain the higher number of the fat vacuoles compared to the high fat diet, which will be discussed in chapter 6.

Excessive iron in the liver has been shown to induce inflammation by activating nuclear factor κ B (NF- κ B) which in turn activates transcription of proinflammatory cytokines including tumour necrosis factor α (TNF α) and interleukin-6 (IL-6) [278]. In rodents, iron loading led to an increase in mRNA of TNF α along with that of several other proinflammatory cytokines such as IL-6 and IL-1 β [279, 280]. Despite such evidence, any histological proof of the presence of inflammatory cells in human or rodent liver is lacking in the current literature [262]. The present study appears to be the first to report that short term iron loading leads to the presence of inflammatory cells around the blood vessels and bile ducts which may or may not be activated and this will need further investigation. The possibility of this being due to

carbohydrate content of the diet can be eliminated as this observation was also made in mice fed an iron loaded standard chow diet which did not lead to the manifestation of steatosis. In short, dietary iron overload is associated with the presence of inflammatory cells in the liver which induce inflammatory response.

Hepatic cholesterol crystals have been reported to distinguish between simple steatosis and NASH [135]. There have been reports where dietary cholesterol has been linked to the progression of NAFLD in animal models [134, 281]. In order to determine if iron has any link to cholesterol crystal formation in NAFLD, liver samples from both control and iron diet were stained for the presence of neutral lipids and the slides visualised under polarised light, as cholesterol crystals are birefringent. Cholesterol crystals have been shown to be present inside lipid droplets [281]. Interestingly, when the crystals were quantified, no significant difference was found between the two groups. In other words, the control group had negligible cholesterol crystals and few crystals were seen in the iron loaded group. The most likely reason for this is that the iron diet did not increase the production of cholesterol sufficiently to allow it to consistently precipitate and form crystals.

Iron overload and its effect on hepatic fibrosis and cirrhosis has been extensively investigated in several animal models of hepatic iron overload but has failed to generate a general consensus on iron's role in the development of either fibrosis or cirrhosis [150, 282, 283]. It has to be noted here that the form of iron administration in the animals may lead to a different distribution pattern in the body. For example, dietary iron loading using carbonyl iron or ferrocene leads to peri-portal iron accumulation in the liver which mimics hereditary haemochromatosis [284, 285]. In parenteral methods of iron loading, including intravenously, intramuscularly, or intraperitoneally administered ferric nitrilotriacetate, iron dextran or iron sorbitol, iron accumulates in the hepatocytes without any zonal pattern, which is similar to that seen during secondary iron loading in thalassaemia [262]. Iron accumulation in these models can be increased up to 75-fold without having overt toxicity [262]. It is noteworthy that despite using a very high iron concentration in whatever form for a prolonged period of time, neither mice nor rat models show any sign of hepatic fibrosis [150, 286, 287]. Even though hepatic inflammatory cells were seen in mice fed the iron diet in the present study, it did not progress to fibrosis. The second reason may be due the influence of strain as C57/BL6 mice are relatively resistant to liver fibrosis due to altered T-cell responses [288]. Therefore, iron on its own may not be able to cause fibrosis but other external or internal factors including signalling pathways

and strong inflammatory response may be needed to cause any degree of noticeable hepatic fibrosis.

In order to find if iron loading had any effect on hepatic injury, I looked at inflammatory, fibrotic and cancer cell markers on mouse liver from the control and iron loaded group. In both groups, expression of CD45 (inflammatory marker) was prominent. This can be explained by the presence of inflammatory cells which were detected in both control and iron loaded groups. A previous study has shown that mice fed a high carbohydrate diet exhibit increased hepatic inflammation [277]. The carbohydrate content is able to increase the production of pro-inflammatory cytokines such as IL-1 β and TNF- α which in turn increase nitric oxide production which ultimately leads to increased inflammation [277]. The high carbohydrate content of the diet also led to prominent visible steatosis in the liver sections stained with H&E which is in line with a similar observation made by another group [289]. Although it was a preliminary experiment, the inflammatory cell marker (CD45) in the iron loaded group was seen to be localised towards the portal area in comparison to the control diet where it was far more spread throughout the tissue. This pattern could be due to the peri-portal distribution of iron, adding weight to the suggestion that it is iron that causes the infiltration of inflammatory cells. The other markers, α SMA for activated HSC, and PanCK for LPC, did not show any conclusive differences. This experiment was carried out on selected samples only and a higher sample size should provide more conclusive evidence of any role for inflammatory cells, hepatic stellate cells and liver progenitor cells in iron loaded liver.

In summary, the present study has shed some light on the role of iron loading in NAFLD. The hepatic distribution of iron was found to be around the portal area as has long been observed. The results discussed in this chapter indicate that dietary iron loading may lead to hepatic fat accumulation in the liver by reducing mitochondrial β -oxidation of fatty acids. Dietary iron loading also led to an increase in liver NHI which in turn appeared to lead to the presence of inflammatory cells in the liver, indicating that iron may be a driver of hepatic insults that initiate or facilitate the progression of NAFLD. The increase in hepatic iron and decreased expression of *Dmt1* and *Fpn* expression being very close to the statistical significance threshold in the duodenum suggests decreased iron absorption by the duodenum and decreased export from the enterocytes. Previous research in the laboratory has shown that iron loading led to increased cholesterol biosynthesis, but such an observation was not made in the present study. One of the reasons for this may be the lower dietary iron concentration used in this study compared to the previous study [46] which may not have been enough to induce observable cholesterol

biosynthesis over the timeframe of the experiment. Additionally, gender and strain differences may have played a role. In the present study, very few cholesterol crystals were observed in the liver of either control or iron fed mice although both iron loaded, and control mice showed some hepatic inflammatory cell markers (CD45). Overall results point to a role for iron in initial fat accumulation in NAFLD as well possibly driving hepatic inflammation which can lead to NAFLD progression on prolonged dietary iron loading.

Chapter 6 Hepatic Changes Associated with High fat and High Iron diet

6.1. Background

The interaction between iron and lipid metabolism has been a focus area for understanding the pathogenesis and progression of NAFLD. The liver occupies centre stage of iron and lipid metabolism because it is the major site of lipid metabolism and iron storage [14]. Many studies in this area have linked iron to the progression of NAFLD due to its ability to induce oxidative stress and inflammation [10, 218], affecting hepatic mitochondrial function, thereby leading to reduced ATP production [243]. However, little information is available concerning how iron accumulation contributes to the initial fatty deposition in the liver. Previous data from the laboratory suggests that hepatic iron loading leads to increased lipid deposition in the liver caused by increased expression of cholesterol biosynthesis genes [46]. Therefore, along with causing oxidative stress, iron overload may also play an important role in hepatic lipid deposition and reduced mitochondrial function, and hence is an important contributing factor in NAFLD pathogenesis and progression.

Many studies have investigated the role of iron and high fat alone, but I am unaware of any studies that have investigated the role of dietary iron and lipid interaction together. The review by Ahmed et al [14] discussed conflicting results in a study conducted on rats. Another study [147] reported no changes associated with cholesterol synthesis and excretory pathways, but an upregulation of the cholesterol secretory pathways. A study from our laboratory [46] reported an increase in hepatic cholesterol synthesis upon iron loading in mice. The conflicting results may be due to different experimental models, dietary feeding pattern as well as sex, strain and age of the animals used [15, 151]. Additionally, most studies looked at the latter stages of NAFLD - NASH and fibrosis [290]. It is important to note here that the studies discussed above were carried out by inducing dietary iron overload in the absence of HFD as they investigated the effect of iron on lipid metabolism and not the interaction. In the study discussed in this chapter, mice were fed HFD along with dietary iron to understand the effect of both nutrients fed together on hepatic changes in NAFLD.

An excess of cholesterol which may be present in the liver either due to iron overload, as discussed earlier, or accumulated as a result of high fat diet with added cholesterol, can be detrimental to health. High cholesterol has been shown to enhance endoplasmic reticulum stress which is linked to NAFLD and NASH [291]. Cholesterol crystals are formed due to unesterified cholesterol supersaturation leading to crystal precipitation in the cell [292]. In a study which looked at cholesterol crystal mediated inflammation, it was shown that the

cholesterol crystals interact with cellular membrane. The crystals, once bound to the cell membrane, extract cholesterol from the cell surface leading to the rupture of the membrane. Interestingly, some authors have argued that the presence of hepatic cholesterol acts as a marker of NASH [135, 290]. Cholesterol crystals have also been linked to fibrosing NASH in NAFLD patients [137]. It is important to note that the process of cholesterol crystal formation in the lipid droplet in mice exhibits phase transition capabilities [293] starting with isotropic droplet transitioning to liquid crystal and then to complete crystals. The study which indicated cholesterol crystals to be a marker of NASH may have concentrated on NASH patients as majority of them (15/16) presented with cholesterol crystals as compared to patients with simple steatosis (3/14). It should be noted that patients with iron overload were excluded from the study [137] whereas, in the current study, mice fed with high iron along with HFD were used to investigate the interaction of the two nutrients and their role in hepatic cholesterol crystal formation.

The study discussed in this chapter investigated the effects of high iron combined with high fat and presents important insights into their interaction and subsequent impact on NAFLD. The major observations are a reduction in hepatic iron concentration in the presence of HFD, and a reduction in cholesterol crystals in the presence of iron and high fat compared to high fat alone. The HFD increased the gene expression of genes involved in peroxisomal fatty acid oxidation, suggesting increased import, possibly leading to enhanced fat accumulation in the liver.

6.2. Methods

Diets were prepared as described in section 2.3.2. The mice were divided into two groups, HFD (n=10) and HF + 1% iron (n=10). All mice were fed HFD diet for 8 weeks, following which one group continued with the HFD for 3 weeks and the other group were fed HF + iron for 3 weeks. Mice were fasted overnight before sacrifice. Liver, spleen, and duodenum were collected, and samples taken for RNA isolation and NHI determination. A separate liver sample was embedded in OCT for histology. All tissues were snap-frozen in liquid nitrogen.

All the other procedures including RNA isolation, qPCR, NHI assay, and histological studies were performed as described in the previous chapter (**Section 5.2**). Data analysis was performed using GraphPad Prism 8 software.

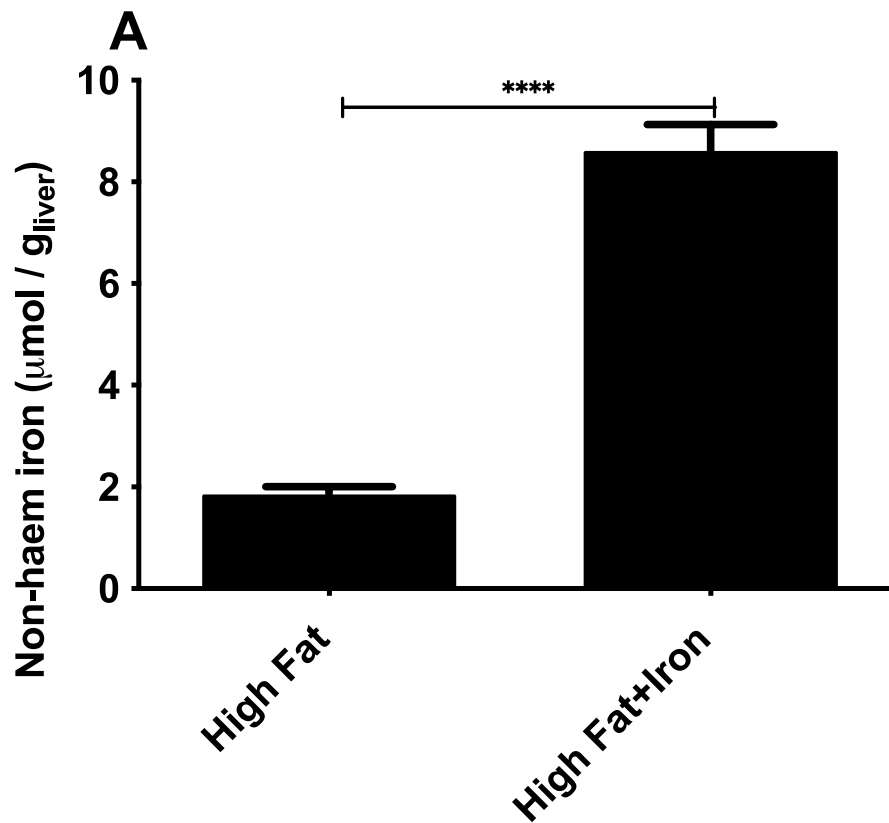
6.3. Results

6.3.1. Mouse hepatic iron concentration and liver histology

Mice fed HFD had lower hepatic NHI content ($1.8 \pm 0.1 \mu\text{mol} / \text{g}_{\text{liver}}$) compared to the group fed HFD + iron ($8.6 \pm 0.5 \mu\text{mol} / \text{g}_{\text{liver}}$; **Figure 6.1 A**; $P < 0.0001$). Interestingly, the HFD ($1.8 \pm 0.1 \mu\text{mol} / \text{g}_{\text{liver}}$) led to a small decrease ($P < 0.05$) in hepatic NHI content compared to mice fed the control diet ($2.3 \pm 0.2 \mu\text{mol} / \text{g}_{\text{liver}}$) as shown in **Figure 5.1A**.

The difference in the NHI content between the HFD and HFD + iron group was further validated by staining the liver tissue for the presence of iron (**Figure 6.1 B&C**). The HFD fed group exhibited minimal Prussian blue staining (**Figure 6.1B**) compared to the HFD + iron (**Figure 6.1C**) group. Importantly, the high-fat diet did not appear to change the distribution of iron, which was peri-portal, similar to the distribution in control mice (see **Figure 5.8 E&F**).

Morphological changes associated with feeding mice HFD or HF + iron were studied using H&E staining (**Figure 6.2**). The nucleus is stained blue and the cytoplasm pink. Both diets led to fat deposition in the liver indicating the presence of steatosis. Microvesicular fat deposits (arrows) were seen in both HFD (**Figure 6.2A**) and HF + iron (**Figure 6.2B**) fed mice. The fat droplets were found near the portal vein which was confirmed by Oil Red O staining (**Figure 6.2 C & D**). The fat droplets showed different colour intensity when stained with Oil Red O. It is possible that this may be due the presence of different lipid classes in the liver with varying concentration.



Perls' Prussian blue Staining

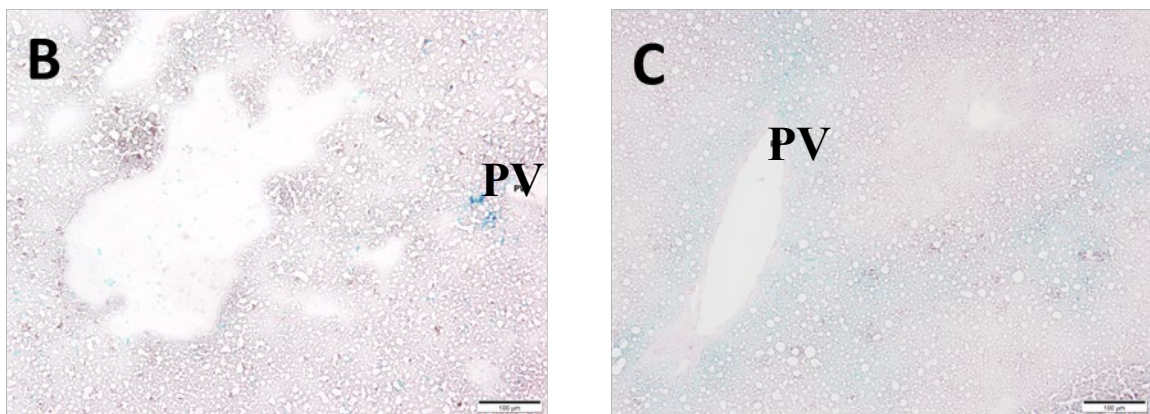


Figure 6.1 **Hepatic non-haem iron concentration.** (A) Hepatic NHI was measured in mice fed high fat diet (HFD; n = 10) and high fat + iron diet (n = 10). NHI was measured as described in section 2.3.8. All data presented are mean \pm SEM. Perls' staining for the presence of iron in livers from (B) HFD and (C) HFD + iron fed mice. Blue colour indicates the presence of iron. PV- portal vein. Images were taken using a 10X objective lens. Staining was performed as described in section 2.4.0. Scale bar is 100 μ m

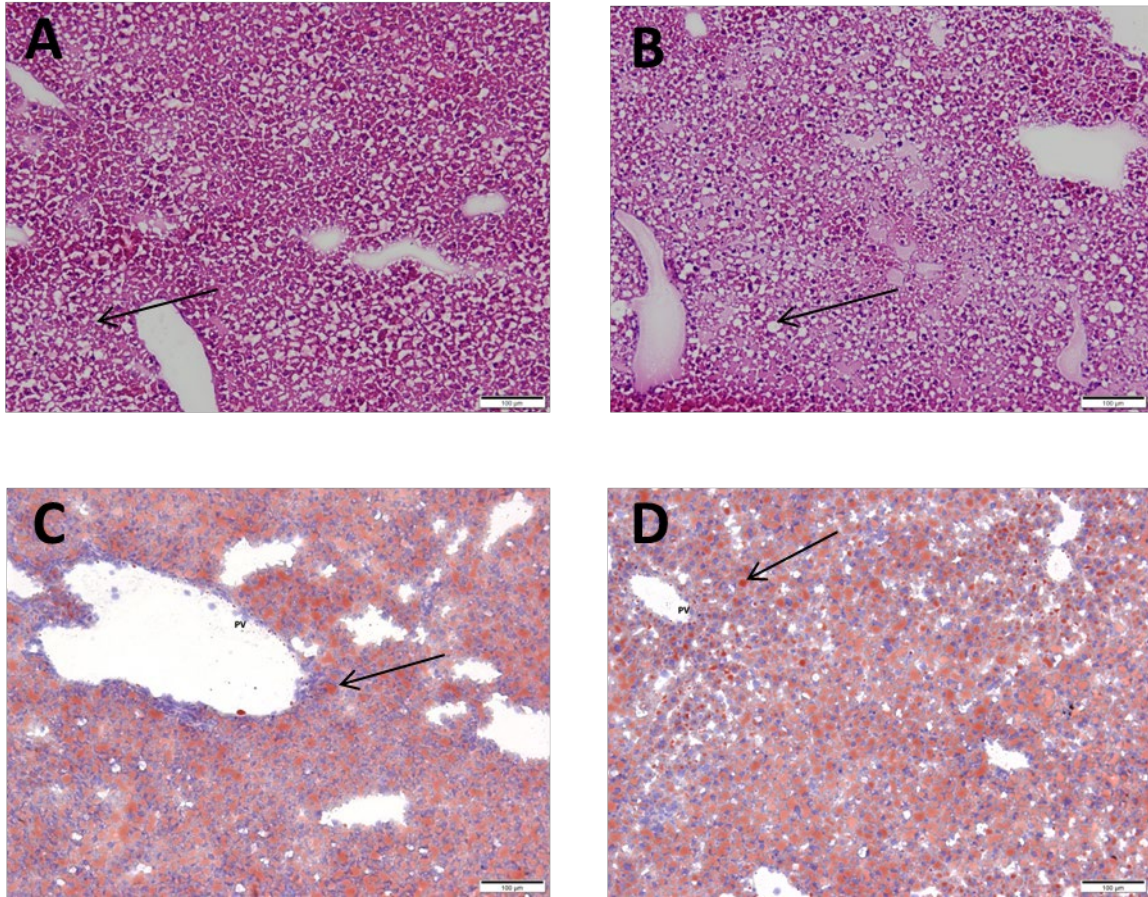


Figure 6.2 **Liver histology & neutral lipid staining.** Representative images of H&E staining of livers from (A) HFD and (B) HFD + iron fed mice. The arrows indicate representative fat deposition. Oil Red O counterstained with hematoxylin for the presence of neutral lipids in livers from (C) HFD and (D) HFD + iron fed mice. Red colour indicates the presence of lipid highlighted by the arrows. PV- portal vein. Images were taken using a 10X objective lens. Staining was performed as described in section 2.4.1 and 2.4.2. Scale bar = 100 μm

6.3.2. Mouse body and liver weight

Body weight of the mice fed HFD or HFD + iron was measured just before sacrifice (**Figure 6.3 A**). The difference in body weight between mice fed HFD (21.0 ± 0.8 g) and mice fed HFD + iron (19.0 ± 0.3 g) did not reach statistical significance ($P < 0.06$) indicating that addition of iron in HFD did not have any effect on the body condition. The whole liver weight of the animals was measured (**Figure 6.3 B**), and no significant difference was observed between the two groups ($P < 0.72$).

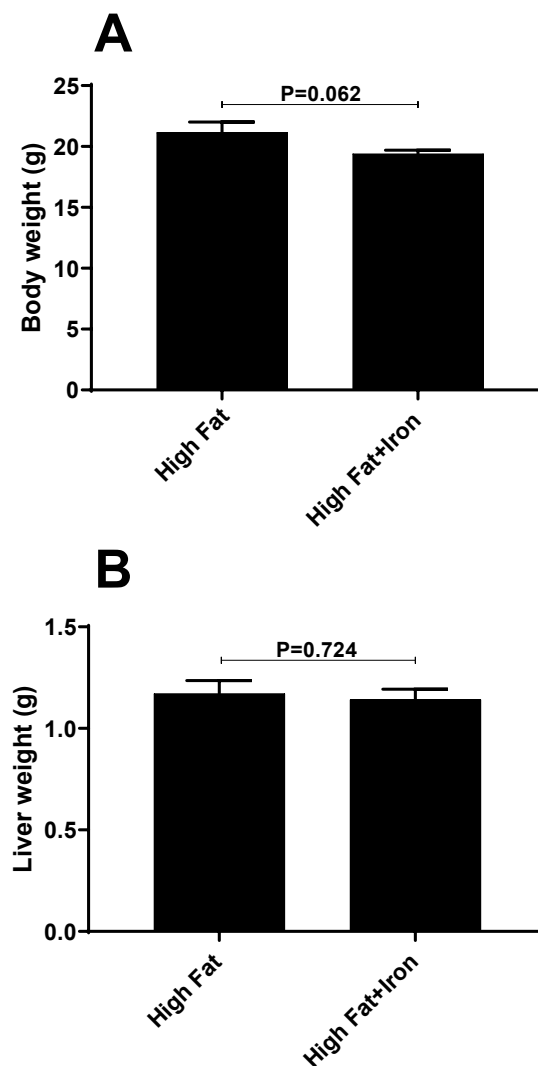


Figure 6.3 **Mouse body and liver weight**. (A) Body weight of HFD (n = 10) and HFD + iron (n = 10) fed mice was measured immediately prior to sacrifice. (B) Wet liver weight measured immediately after removal. Data presented as mean \pm SEM.

6.3.3. Expression of hepatic iron homeostasis genes

Hepatic expression of iron homeostasis genes was examined in mice fed HFD and HFD + iron (Figure 6.4). There was a statistically significant linear increase in *Hamp1* expression in mice fed HF + iron compared to HFD fed mice ($R^2=0.532$, $P<0.0001$). A similar significant increase was seen for *Fpn* ($R^2=0.258$, $P<0.05$). Of the other two genes, *Dmt1* increased significantly with hepatic iron ($R^2=0.206$, $P<0.05$) and *Tfr1* showed no significant correlation ($R^2=0.129$, $P<0.17$).

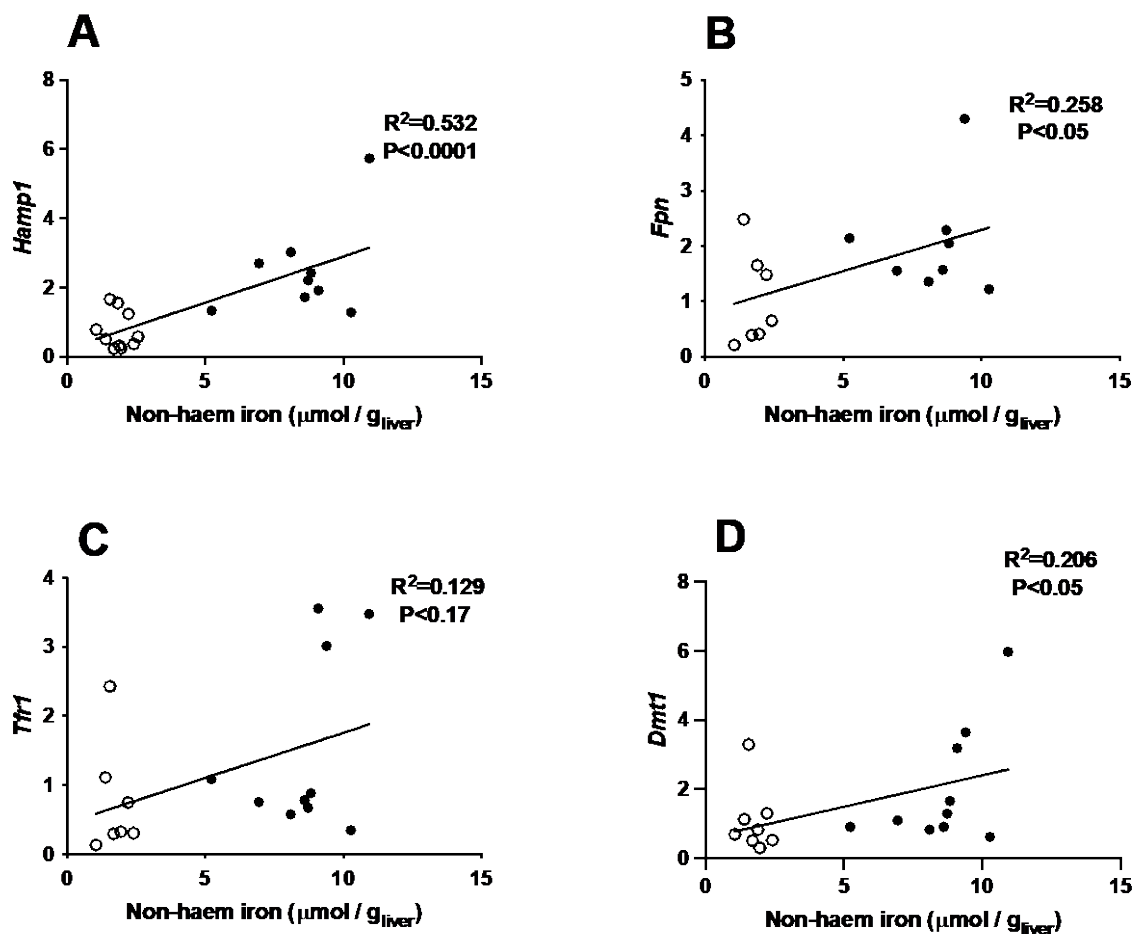


Figure 6.4 **Hepatic expression of iron homeostasis genes.** Relationship between hepatic non-haem iron and hepatic expression of (A) *Hamp1* (B) *Fpn* (C) *Tfr1* and (D) *Dmt1* in HFD (○)(n = 7-9) and HFD + iron (●) (n = 7-9) fed mice. Non-haem iron was measured as stated in section 2.3.8 and gene expression by RT-PCR as described in section 2.3.7.

6.3.4. Expression of mitochondrial and peroxisomal fatty acid metabolism genes

The effect of HFD on mitochondrial fatty acid oxidation genes was investigated in mice fed HFD or HF + iron. (**Figure 6.5**). The expression of genes involved in the first step of mitochondrial beta oxidation of very long (*Acadvl*), medium (*Acadm*) and short chain (*Acads*) fatty acids, as well as the alpha subunit of the trifunctional enzyme (*Hadha*) that catalyses the remaining three reactions, was investigated. Linear regression analysis revealed no significant relationships between hepatic NHI content and the gene expression of *Acadvl* ($R^2= 0.012$, $P<0.68$), *Acadm* ($R^2= 0.137$, $P<0.12$), *Acads* ($R^2= 0.084$, $P<0.24$) or *Hadha* ($R^2= 0.030$, $P<0.51$). The results suggest that the effect of hepatic iron on fatty acid oxidation is lessened in the presence of high fat compared to the results from mice fed the control diet, with or without iron (Chapter 5).

The expression of peroxisomal fatty acid oxidation genes in mice fed HFD and HF + iron was also investigated (**Figure 6.6**). Expression of the acyl transferase (*Acaal1a*) and hydratase/isomerase (*Ech1*), genes involved in peroxisomal fatty acid β -oxidation, and fatty acid transporter and synthetase (*Slc27a2*), were plotted against hepatic NHI. Linear regression analysis showed a positive correlation with *Acaal1a* ($R^2= 0.255$, $P<0.04$) and *Slc27a2* ($R^2= 0.300$, $P<0.02$) whereas *Ech1* ($R^2= 0.085$, $P<0.27$) did not show significant correlation.

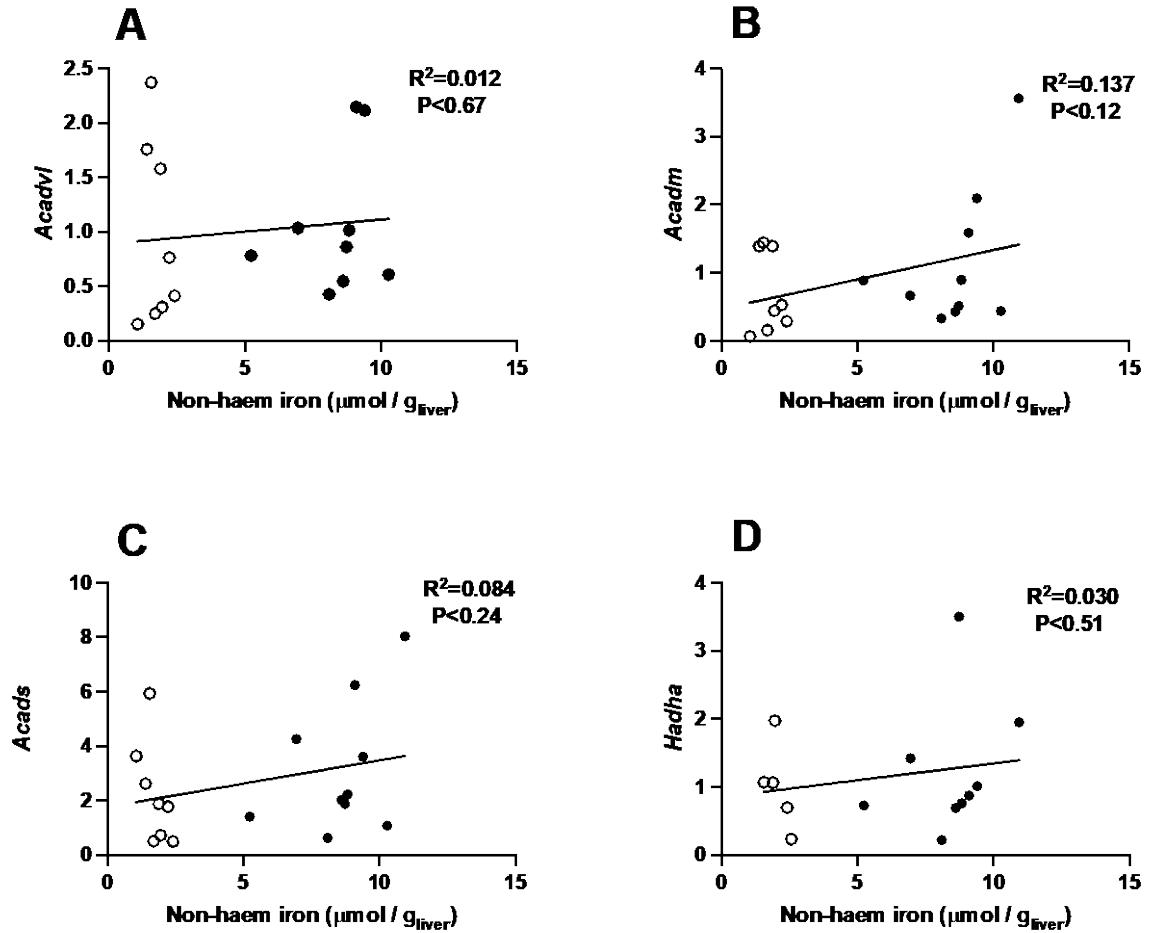


Figure 6.5 **Hepatic expression of mitochondrial fatty acid oxidation genes.** Relationship between hepatic non-haem iron and hepatic expression of (A) *Acadvl* (B) *Acadm*, (C) *Acads* and (D) *Hadha* in HFD (n = 6-9) and HFD + iron (n = 8-10) fed mice. Non-haem iron was measured as stated in section 2.3.8 and gene expression by RT-PCR as described in section 2.3.7.

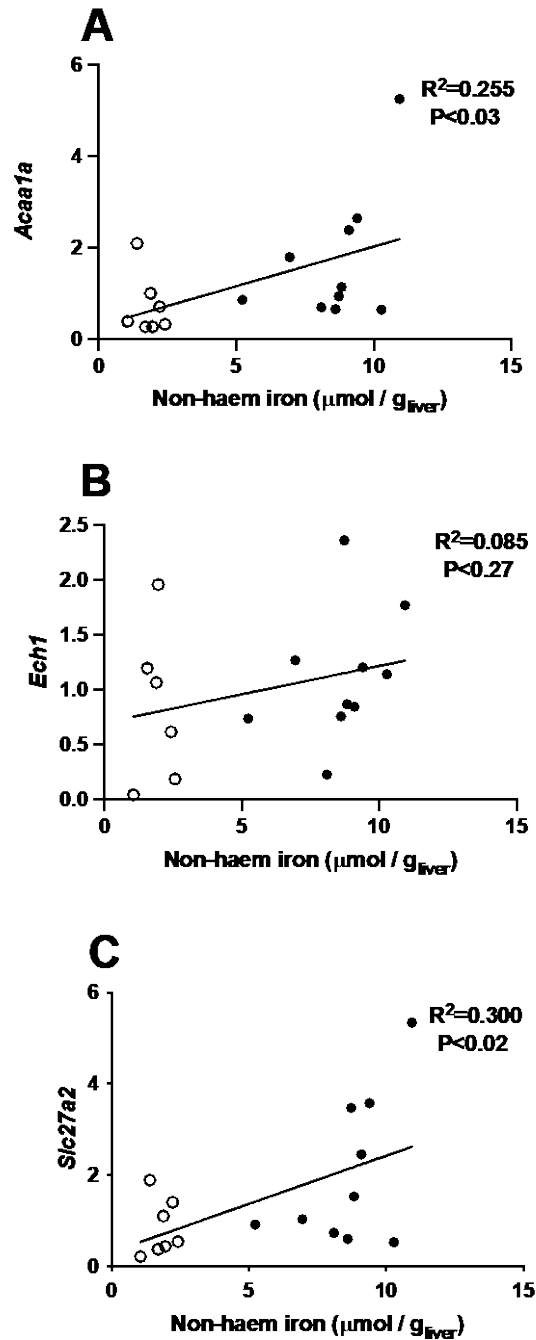


Figure 6.6 **Hepatic expression of peroxisomal lipid metabolism genes.** Relationship between hepatic non-haem iron and hepatic expression of (A) *Acaa1a* (B) *Ech1* and (C) *Slc27a2* in HFD (n = 6-7) and HFD + iron (n = 9-10) fed mice. Non-haem iron was measured as stated in section 2.3.8 and gene expression by RT-PCR as described in section 2.3.7.

6.3.5. Effect of high fat and high fat plus iron on iron homeostasis genes in the spleen

In order to investigate if the reduction in hepatic NHI due to HFD had any effect on genes involved in iron homeostasis in the spleen, expression of *Hamp1*, *Dmt1*, *Fpn* and *Tfr1* was measured (Figure 6.7). The results are plotted differently from those in figures showing hepatic data as tissue iron content was not measured. Splenic gene expression was investigated with the hypothesis that the excess hepatic iron, which was decreased following feeding of HFD, may be targeted to the spleen. The increased iron in turn may regulate the expression of iron genes. However, no significant association was found between any of the measured genes when HFD and HFD + iron groups were compared: *Hamp1* ($P < 0.17$), *Dmt1* ($P < 0.64$), *Fpn* ($P < 0.35$) and *Tfr1* ($P < 0.12$).

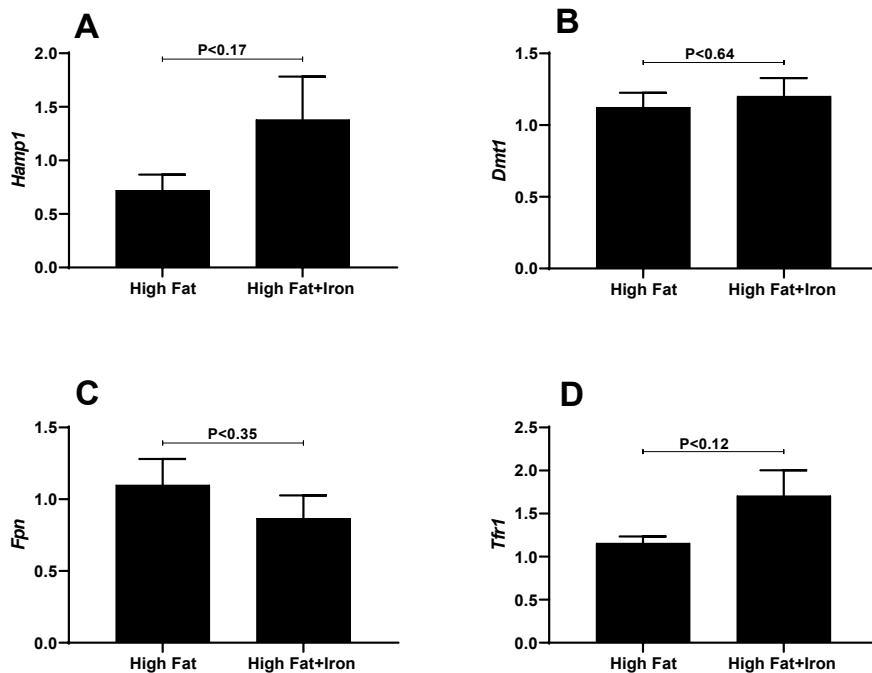


Figure 6. 7 **Splenic expression of iron homeostasis genes.** Gene expression of (A) *Hamp1*, (B) *Dmt1*, (C) *Fpn* and (D) *Tfr1* in HFD (n = 8) and HFD + iron (n = 9-10) fed mice. Gene expression was performed by RT-PCR as described in section 2.3.7. All data presented are mean \pm SEM.

6.3.6. Effect of high fat and high fat plus iron on iron homeostasis genes in the duodenum

Expression changes associated with iron genes in the duodenum of mice fed HFD and HF + iron diet was investigated (**Figure 6.8**). *Dmt1* expression was significantly increased in HF + iron fed mice (0.62 ± 0.07 relative units) compared to HFD (0.35 ± 0.08 ; $P < 0.05$). Similarly, *Tfr1* expression was significantly higher in HF + iron fed mice (20 ± 6 relative units) compared to HFD (4.1 ± 1.4 ; $P < 0.05$). Irrespective of the observed differences in *Dmt1* and *Tfr1*, *Fpn* expression did not show any significant difference between the two groups ($P < 0.15$).

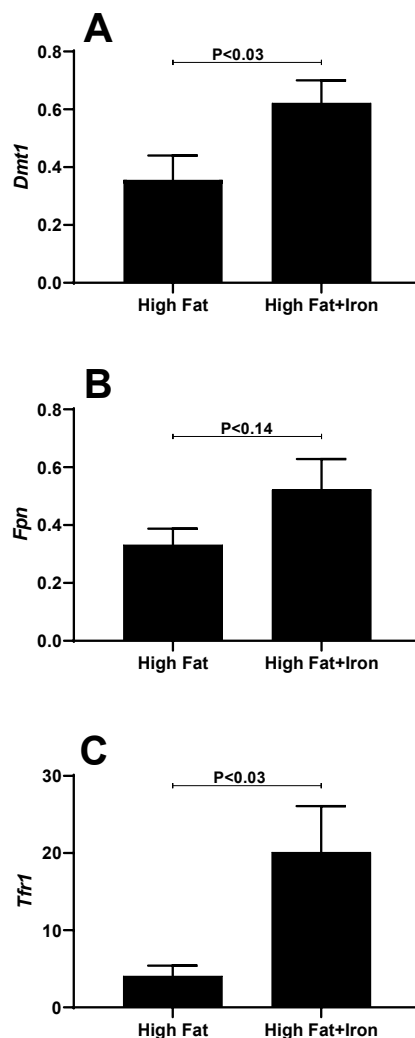


Figure 6. 8 **Duodenal expression of iron homeostasis genes.** Gene expression of (A) *Dmt1*, (B) *Fpn* and (C) *Tfr1* in HFD (n = 6-7) and HFD + iron (n = 7-10) fed mice. Gene expression was performed by RT-PCR as described in section 2.

6.3.7. Differences in hepatic cholesterol crystals associated with high fat and high fat plus iron

Cholesterol crystals of different shapes and sizes were detected in mice fed HFD and HF + iron (**Figure 6.9**). The crystals are rhomboid or needle-like structures and appear birefringent under polarised light. The crystals were quantified by an accredited histopathologist, counting the crystals in ten random fields per animal (0.26 mm² per field; **Figure 6.9 C**). There were significantly more crystals ($P < 0.0001$) observed in HFD (6.7 ± 0.8 crystals / 0.26 mm²) compared to HF + iron-fed mice (1.5 ± 0.3 crystals / 0.26 mm²). It is interesting to note that there was a strong negative correlation ($R^2 = 0.648$, $P < 0.01$) between cholesterol crystals and NHI (**Figure 6.9 D**), suggesting that the decrease in hepatic cholesterol crystals was mainly due to the presence of iron in the mouse livers.

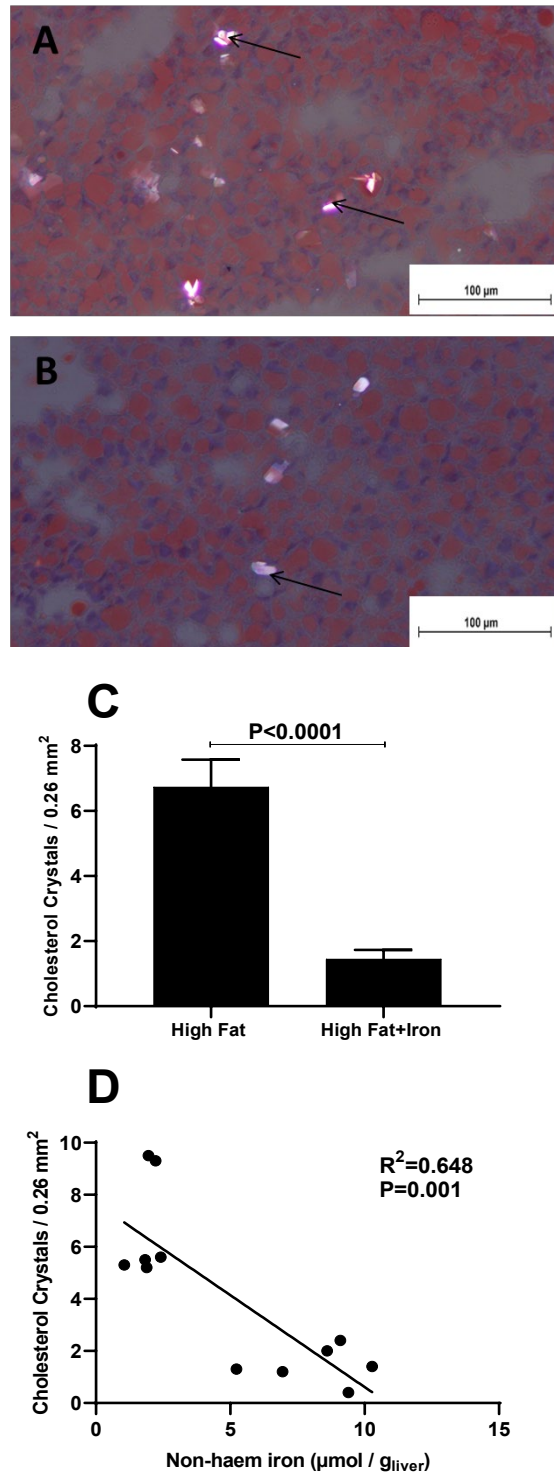


Figure 6.9 **Hepatic cholesterol crystals.** ORO stained slides were visualised under polarised light to detect the presence of cholesterol crystals. Representative image from (A) HFD (n=6) and (B) HFD + iron (n=6) fed mice. Arrows indicate the presence of cholesterol crystals. Images were taken using a 20X objective lens. (C) Quantification of hepatic cholesterol crystals. Crystals were quantified as described in section 5.2. Data presented are mean ± SEM. (D) Relationship between hepatic NHI and cholesterol crystals.

6.3.8 Markers of hepatic injury

In order to investigate whether HFD or HF + iron fed mice developed any hepatic injury, a liver from one mouse from each dietary group was examined using immunohistochemistry (triple staining) for the presence of an inflammatory marker (CD45), a hepatic stellate cell marker (α -SMA) and a liver progenitor cell (LPC) marker (PanCK) (**Figure 6.10**). These have been discussed previously in section 5.3.8.

In the HFD fed animal (**Figure 6.10A**), there was an observable presence of inflammatory cells (white) in liver tissue with minimal expression of LPC (green) and no hepatic stellate cell expression (red). However, in the animal fed HF + iron (**Figure 6.10B**), there was increased presence of both inflammatory cells and LPC. The expression of stellate cells was the same in both animals. Although this observation is preliminary, being made from only a single animal from each condition, it is possible that the presence of iron in HFD further adds to hepatic injury by increasing inflammatory cells as well as LPCs and will be investigated in depth in future studies.

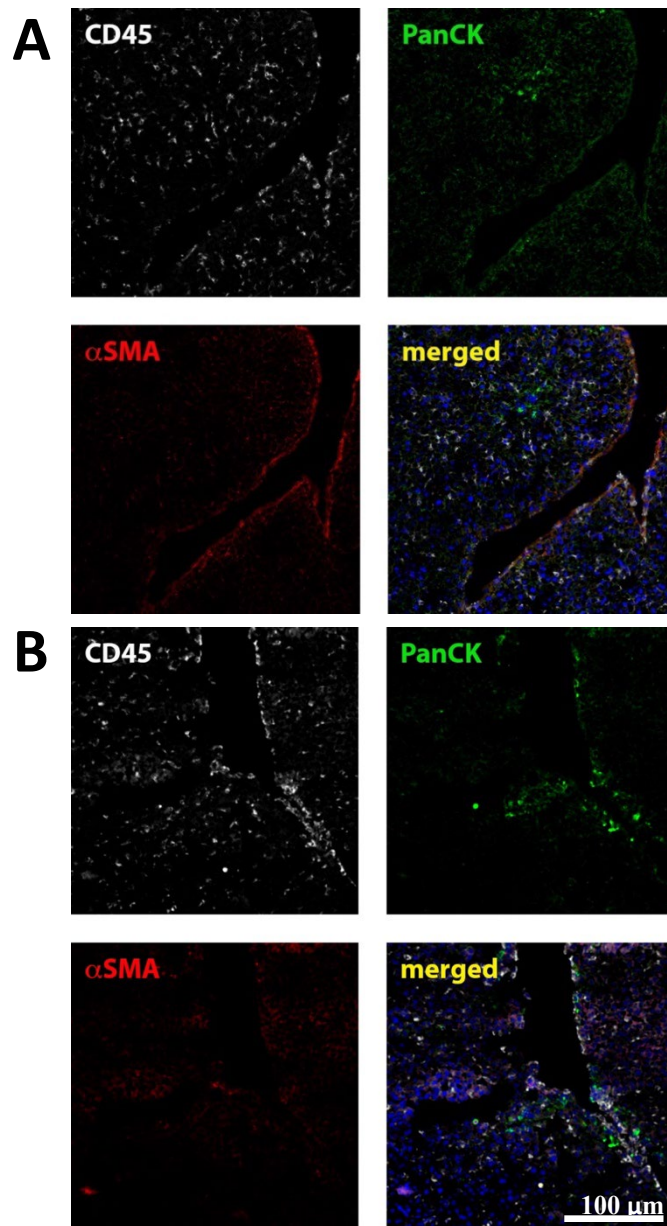


Figure 6.10. **Immunohistochemistry of mouse liver.** Mice were fed (A) HFD or (B) HFD + iron diet. One sample from each group was stained for CD45 (inflammatory cell marker) PanCK (activated stellate cell marker) and α SMA (liver progenitor cell marker). DAPI was used to stain the nucleus (blue). Images were taken using a 20X objective lens. The procedure was performed as described in section 5.2.

6.4. Discussion

In the study described in this chapter, the effect of high fat and high fat + iron diet on iron genes, cholesterol crystal formation and hepatic injury was investigated. Unsurprisingly, the mice fed HFD had significantly less hepatic NHI compared to mice which were fed HFD+iron. The liver iron concentration was further validated by Perls' stain. The blue colour which represented iron deposition was clearly visible in livers of mice supplemented with iron and was not detectable in mice fed only high fat diet, visually confirming the colorimetric hepatic iron measurements. It is interesting to note here that despite the differences in hepatic iron concentration, there was no significant difference observed between the body or liver weights of mice fed HFD or HFD + iron. The increase in body and liver weight reported elsewhere [294] is likely due to age and longer feeding pattern as these mice were fed HFD for 80 weeks which is very long compared to the 8 weeks in the present study.

The mRNA expression of hepcidin (*Hamp1*) increased with increasing hepatic NHI. It can be argued that the presence of high fat exerts some sort of control over hepcidin expression as the regression analysis showed that correlation between *Hamp1* and iron appears to be tighter in the presence of high fat than in its absence as discussed in chapter 5. It is important to note that hepatic iron levels are an important regulator of hepcidin, the HFD + iron mice had higher liver *Hamp1* expression than HFD alone and can be linked to the higher liver iron observed in the former.

In the present study, expression of iron related genes was measured in spleen. The expression of *Hamp1* in the spleen was not significantly different between the two groups. Similarly, the other genes, *Dmt1*, *Tfr1* and *Fpn* did not show any significant difference between mice fed HFD or HFD+iron. In a study conducted on mice, iron loading led to increased *Fpn* gene expression but reduced *Fpn* protein expression [275] and increased *Tfr1* expression. The authors argued that such an observation may be due to the presence of an undefined mechanism of *Tfr1* mRNA production which may overcome the IRP/IRE based regulation. One of the reasons for not observing any significant gene expression change may be due to the concentration of iron in the spleen which may be lower than other studies which used 3% carbonyl iron [275, 295] compared to 1% in the present study and shorter feeding duration. *Tfr1* is also expressed in low levels in the spleen [295].

The duodenal expression of both *Dmt1* and *Tfr1* was high in HFD + iron loaded mice compared to HFD fed mice. This is surprising because high iron normally leads to decreased *Tfr1* expression. Thus, investigating the duodenal expression of iron genes gives an indication that

iron absorption may be partly regulated by high fat because hepatic iron concentration is lower in mice fed HFD ($1.8 \pm 0.1 \mu\text{mol} / \text{g}_{\text{liver}}$), without added iron, compared to the control ($2.3 \pm 0.2 \mu\text{mol} / \text{g}_{\text{liver}}$; $P < 0.05$) from chapter 5, (discussed further in Chapter 7), and hepcidin, produced mainly in the liver, regulates intestinal iron absorption [296]. As there is no controlled excretion mechanism for iron, its level in the body is regulated by absorption through the duodenum. The first step in this process is iron uptake from the lumen followed by binding of iron to cytosolic components. Iron can also be taken up from the circulation by duodenal cells [296] by processes involving *Dmt1* and *Tfr1*. *Dmt1* is present at the basolateral surface, as shown in a study in rats in which iron supplementation by gavaging led to the relocation of *Dmt1* to the basal domain [296]. Both *Dmt1* and *Tfr1* expression was upregulated in the HFD+iron group. Although the polarity of *Dmt1* expression was not measured in the present study, if it did relocate to the basolateral membrane upon iron supplementation, it suggests that circulating iron was possibly being redirected to the duodenum to be exported. It is therefore possible that there may exist an unrecognised form of controlled excretion for iron which may manifest under high fat/ cholesterol conditions. Duodenal iron content was not measured in this study; however, further studies measuring duodenal iron and absorption kinetics would be useful to determine the extent to which these parameters contribute to changes in iron loading in the presence of a diet rich in fat.

Previous work in our laboratory has shown a relationship between iron loading and cholesterol biosynthesis [46]. When the gene expression of mitochondrial and peroxisomal fatty acid metabolism was studied, no correlation was found in the mitochondrial genes investigated, but two out of three peroxisomal genes showed a strong positive correlation with hepatic NHI content. This points to the possibility of an interaction between iron and long-chain fatty acid metabolism. A high fat diet has previously been shown to alter PPARs and increase expression of iron transport genes [297]. A strong correlation has been shown between hepcidin expression and serum cholesterol, triglycerides, and LDL levels in patients with iron-associated NAFLD [267]. In mice fed an iron-loaded HFD, increases in the hepatic gene expression of fatty acid transporter, *Slc27a2* and the thiolase *Acaa1a* were observed. This suggests an increased metabolism of very long chain FAs; however, the lack of increase in mitochondrial FA-associated genes suggests that FA metabolism reaches a bottle-neck once the FAs are passed to the mitochondria for final oxidation, further strengthening the hypothesis that iron overload leads to fat build up. Increased expression of *Slc27a2* has been linked to the progression of NAFLD. It is the most expressed fatty acid transporter in liver cells and contributes profoundly

to long chain fatty acid uptake [298]. It is possible that no correlation was seen between mitochondrial gene expression and hepatic iron content because the amount of iron present was not able to induce measurable changes. This contrasts with the results discussed in the previous chapter in which iron loading on its own (in the absence of HFD) was able to induce changes in mitochondrial FA oxidation genes. It is possible that high fat limits the amount of iron that can be targeted to the mitochondria, thus limiting the effect on mitochondrial gene expression. Taken together, these results suggest that iron and fat modulate mitochondrial and peroxisomal lipid metabolism in different ways, resulting in accumulation of fat and contributing to NAFLD progression.

The observation of cholesterol crystals in the livers of HFD fed mice is a novel and important finding. Crystals have been reported to be associated with progression to NASH in the latter stages of NAFLD [137] but not in simple steatosis. The observation of crystals in the present study indicates that their presence begins in the initial stages of steatosis and is not just associated with NASH. This implies that cholesterol crystal formation starts as early as simple steatosis and may cause damage by rupturing plasma membrane and leading to necrosis and also initiate inflammation by activating NLRP3 inflammasome pathway [299, 300]. Additionally, in the present study, hepatic crystals developed in the presence of a lower concentration of dietary cholesterol (8 weeks of a diet containing 0.15% cholesterol) compared to other studies in which mice were fed a higher concentration (6 months of diet containing 0.25 - 1% cholesterol) [290].

Importantly, the HFD + iron group had a significant reduction in the number of cholesterol crystals compared to the HFD group. There does not appear to be any previous reports of this observation. The observation is surprising given that iron overload, in the absence of high fat, has been shown to increase cholesterol biosynthesis. Additionally, iron overload has been found to reduce bile acid synthesis and export in rat liver [301]. On the other hand previous data from our laboratory has shown that cholesterol export genes are upregulated on iron loading [46]. Hence, it may be possible that even though iron increases cholesterol biosynthesis, it may be transported out of the liver, resulting in formation of fewer crystals. It becomes clear from these observations that iron may play an important role in cholesterol crystal metabolism and may depend on the dietary iron concentration used to feed the mice. Against the background of a HFD, there is a negative relationship between hepatic iron concentration and cholesterol crystal formation in the liver which can be seen clearly by plotting hepatic NHI against cholesterol crystals. It is possible that the increased cholesterol,

present as a result of iron loading, is exported into the circulation as reported in a study conducted in rats [301]. In addition, overexpression of *Cyp7a1* in a mouse model of liver injury, decreased hepatic free cholesterol content [302]. Iron has been found to be a regulator of mRNA and protein expression of *Cyp7a1* [303].

In order to investigate whether cholesterol crystals were linked with hepatic injury and NAFLD progression, preliminary immunohistochemistry staining was carried out on samples containing the highest number of cholesterol crystals within each group. However, CD45, a marker of inflammation, was higher in the HFD + iron group. Similarly, PanCK, the marker for liver progenitor cells, which play a major role in driving fibrosis [304], was also higher in the in the HFD + iron group. This was a preliminary study and will form the basis of future work with higher sample size; however, the results suggest a role for iron in causing hepatic injury as seen by comparative increase in the expression of PanCK and CD45 markers in the presence of iron.

In conclusion, both HFD and HFD+iron influenced iron gene expression in the liver and duodenum. In the duodenum, the gene expression results point to a possible mechanism of controlled iron excretion from the duodenum. Genes associated with peroxisomal fatty acid metabolism were upregulated in the presence of HFD+iron, which also suggested the beginnings of hepatic injury. One of the most exciting discoveries, and one that warrants further investigation, was that of reduction of cholesterol crystals in the presence of iron. These crystals are very toxic to cell membranes and have previously been associated with NASH. However, interestingly, the number of crystals observed in the liver indicates that these crystals are not just associated with NASH but can be present even during simple steatosis. Given all these findings, it becomes very clear that iron overload and high fat play an important role in NAFLD development and progression both at the molecular and physiological levels.

Chapter 7 General Discussion

7.1 Background

The present study was undertaken to investigate the role of iron and lipid metabolism in NAFLD. The liver is an important organ as it is the major storage site for iron and it has a central role in lipid metabolism. The interaction between iron and lipids, and the role of iron overload in the initial development of steatosis is not very clear. Many studies have linked iron overload with the progression from NAFLD to NASH and the more severe forms of NAFLD [305, 306]. This study was designed with the hypothesis that iron overload may lead to lipid accumulation in the liver as well as influence fatty acid metabolism in hepatic mitochondria given that fat deposition and mitochondrial dysfunction have been linked to NAFLD pathogenesis and progression [10, 173]. Both *in vitro* and mouse models of dietary iron and fat loading were studied to examine the changes in hepatic, duodenal and spleen associated gene expression, along with changes in liver histology associated with iron and fatty acid loading to understand the differential regulation of gene expression under conditions of iron and fat overload. *In vitro* analysis of mitochondrial respiration revealed how mitochondria respond to excess iron and fatty acid changes. The present work also sheds light on the role of a HFD and its role in reduction of hepatic iron concentration. An exciting observation linked the modulation of hepatic cholesterol crystals to the condition of iron overload. These findings hint at an interaction between iron and fat which leads to steatosis as well as to progression to NASH and end stage liver disease.

7.2 Effect of iron and lipid loading on mitochondrial respiration

The results from the *in vitro* study reported in chapter 3 suggest a role of iron in modulating mitochondrial bioenergetics. Loading cells with iron led to a small but significant decrease in cell viability but it was not as large as for PA. So, it can be speculated that the corresponding changes observed in various parameters associated with mitochondrial bioenergetics were not a result of reduced cell viability at least in the iron loaded groups. Iron is often said to cause oxidative stress, and research from our laboratory has shown that iron loading AML12 cells led to an increase in lipid deposition [205] consistent with the current hypothesis that iron loading may lead to the initial fat accumulation seen in NAFLD. Cells treated with iron and OA+iron exhibited an increase in ATP production. This is in line with similar observations made in other studies [225, 231]. It should be noted that both iron and FA were loaded for 12h and a longer incubation may lead to iron-induced oxidative stress and may contribute to mitochondrial dysfunction by impairing ETC complexes II/III [245]. Iron overload can also

lead to lipid peroxidation, damaging mitochondrial membrane integrity, also leading to uncoupling of electron transport and energy production [307] but in the present study iron loading did not lead to a decrease in mitochondrial bioenergetics and another study has shown that iron supplementation in mice fed HFD led to an increased hepatic ATP compared to mice which were only fed HFD [308]. Iron supplementation was associated with reduced morphological abnormalities in the mitochondria when compared to mice which were not supplemented with iron. The morphological abnormalities included swollen mitochondria and disturbed organisation of sarcomeres [308]. The authors argued that iron supplementation led to increased synthesis of iron prosthetic groups which can improve mitochondrial function. A similar increase in ATP production was observed in cells loaded with iron and/or OA indicating improved mitochondrial function.

Saturated fatty acids are considered to be a major contributor in fatty liver disease [309, 310], but in this study palmitate had few effects on mitochondrial function. This is possibly related to the conditions used. Liu *et al* showed that 48 h treatment with 25 μ M palmitate improved mitochondrial oxygen consumption in AML12 cells, whereas a subsequent challenge with 500 μ M palmitate led to mitochondrial damage [311]. Liu *et al* has shown that a low concentration (25 μ M) of palmitate helps to enhance mitochondrial metabolism by regulating SIRT3, a mitochondrial deacetylase. Low palmitate contributes to SIRT3 phosphorylation which, in turn, causes CPT2 dimerisation and therefore enhances fatty acid import and oxidation [311]. While I used a much higher dose (100 μ M), it was also for a shorter duration (12 h vs 48 h). On the other hand, OA, which is an unsaturated fatty acid, in combination with iron was associated with increased OCR in the majority of parameters associated with mitochondrial bioenergetics in the present study. Such a change was not observed in cells treated with OA alone. In summary, mitochondrial respiration is differentially regulated by saturated and unsaturated fatty acids, and short-term iron loading is associated with improved mitochondrial function but may change depending upon the incubation time as long-term iron loading can alter mitochondrial bioenergetics and lead to NAFLD pathogenesis.

7.3. Effect of varying dietary iron concentration on hepatic gene expression

Dietary iron overload has been used in animal models to study the effect of iron overload on hepatic iron metabolism genes [46, 280]. Published investigations have largely focussed on the role of iron overload in the progression of NAFLD, linking it to NASH and fibrosis [213, 305, 312]. Most of these studies have used 2% carbonyl iron to induce iron overload in animal

models [46, 235]. Previous data from our laboratory also suggests that iron overload in NAFLD may be linked to lipid accumulation and cholesterol biosynthesis [46].

Dietary iron overload in mice has been associated with a decrease in body weight [238] but in this study there was no significant decrease in body weight upon iron loading the mice for 3 weeks. This observation is interesting as reduced body weight is often linked to reduced dietary intake by mice [238], but observations made in the present study suggest that reduced intake may not be due to the presence of iron in the diet but due to the way it is formulated. In the present study, the diet was presented in dough form, which is softer than the pellet form in which diets are often presented. Mice would be expected to consume less of the harder pellet diet, leading to a lower absorption of iron. This factor should be taken into consideration whenever interpreting results based on dietary intake as feeding a higher concentration in pellet form may lead to less iron accumulation in the liver compared to a diet of equal concentration fed in more palatable form.

In the study by Rishi *et al* [238], 0.25% carbonyl iron was found to be sufficient to induce hepcidin response and any further increase in iron concentration did not lead to increased *Hamp1* expression [238]. However, in the present study, it was found that 1% carbonyl iron was associated with stronger correlation with *Hamp1* expression compared to other lower concentrations (Appendix A). This formed the basis for the iron concentrations used for the further studies in chapter 5 and 6.

Hamp expression has been linked to body iron content [313] in NASH patients. It is interesting to note that hepcidin levels did not correlate with degree of steatohepatitis in the patients. Iron appears to play an important role in the initial stage of fat accumulation (steatosis) but it is possible that its effect on further NAFLD progression may diminish as fat builds up in the liver. This claim can partially be attributed to the results discussed in the next section where high fat diet has been shown to decrease hepatic iron concentration. This strengthens our hypothesis that initial iron loading is an important trigger in initial fat accumulation and increased *Hamp1* expression is indicative of hepatic iron loading.

Apart from playing a role in initial fat accumulation, iron loading is also associated with mitochondrial dysfunction in NAFLD [243]. A role for iron is likely as results from the current study indicate a gradual increase in mitochondrial NHI content with increasing dietary iron concentration and correlating strongly with hepatic NHI. Even though there were no changes evident in expression of genes associated with mitochondrial fatty acid oxidation, increased

mitochondrial iron may be a good reason why mitochondrial dysfunction is found to be linked to NAFLD. The fatty acid oxidation genes measured are expressed in the nucleus and the proteins exported to the mitochondria. Therefore, mitochondrial iron loading may affect enzyme activity rather than gene expression.

It is important to note that in the present study a high carbohydrate content was present in the diet which was used as a control for the HFD. Due the presence of high carbohydrate, the livers of the mice fed the control diet exhibited many fat vacuoles which resembled steatosis. This diet was the correct nutritional control for the HFD but not for fatty liver. High carbohydrate diets have been previously used to induce fatty liver in mice [289]. The effect of high carbohydrate on iron gene regulation has not been well explored, but high carbohydrate is well known to decrease the expression of fatty acid oxidation and cholesterol metabolism genes [289].

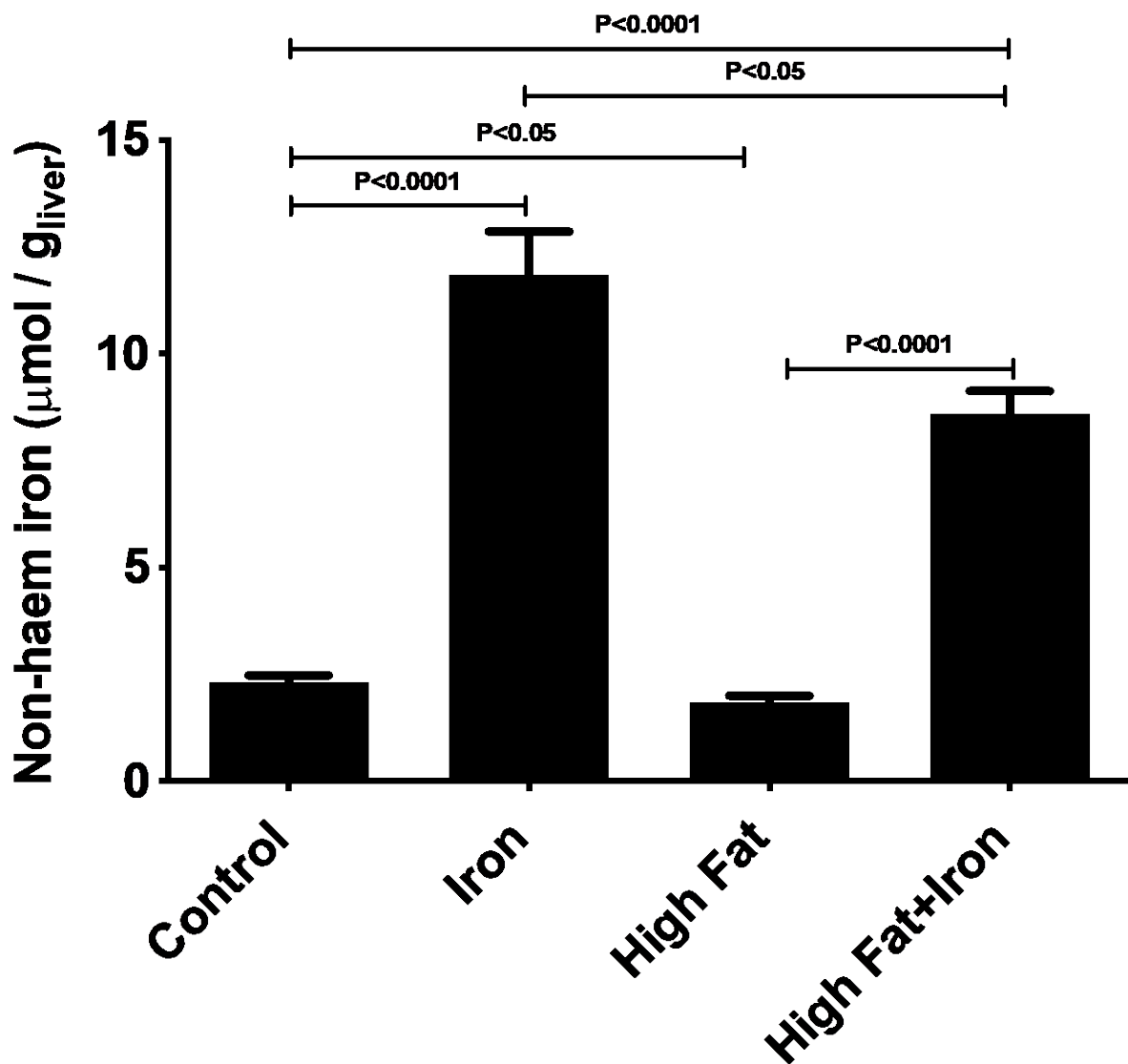


Figure 7.1 **Hepatic non-haem iron concentration.** (A) Hepatic NHI was measured in mice fed control (n=10), iron (n=10), high fat diet (n = 10) and high fat + iron diet (n = 10). NHI was measured as described in section 2.3.8. All data presented are mean \pm SEM. This figure is a comparison of data shown in Figures 5.1 and 6.1A.

7.4. Hepatic changes associated with dietary iron overload and high fat diet

Iron overload has been linked to NAFLD because approximately 30% of patients diagnosed with NAFLD and NASH present with increased iron stores [10]. Most commonly, iron overload has been linked to oxidative stress in NAFLD [254]. There were four different types of diet used in the present study and results have shown that both iron and HF diet can contribute to NAFLD. The iron diet was associated with reduced expression of mitochondrial fatty acid genes which may lead to fat accumulation in the liver leading to steatosis. The control diet used in this project was a nutritional control for the HFD. The control diet was rich in carbohydrate and that led to fatty deposition in the liver of control mice. While investigating the role of carbohydrate and iron in NAFLD is likely to provide important information about the interaction of the two nutrients, to do so was beyond the scope of this project, but it is something which will be included in future studies. The role of iron loading on its own and in combination with high fat was also evaluated and indicated a selective effect on fatty acid oxidation genes in the mitochondria and the peroxisomes. HF on its own led to an increase in peroxisomal fatty acid oxidation genes along with cholesterol crystal formation in the liver whereas iron diet was associated with decreased mitochondrial fatty acid oxidation.

An important observation made in the present study was the decrease of hepatic NHI in the presence of HFD (**Figure 7.1**). It is important to note here that the concentration of dietary iron was same in mice fed iron and HFD+iron diet. It is surprising that HFD on its own was able to decrease hepatic NHI when compared to control (**Figure 7.1**). This observation is interesting because patients suffering from NAFLD have more fat than normal in the liver and one-third of patients present with iron overload [314]. There may be several reasons which contribute to the reduction of hepatic iron in the presence of high fat, including a decrease in iron absorption, iron being absorbed normally but redirected to other organs, or involvement of genetic regulation which may influence hepatic iron concentration. The mice used in the present study were not obese and did not show any significant weight differences and were used to investigate the development of simple steatosis by using the four dietary interventions. The iron loaded diet increased the expression of *Hamp1* in the presence of HF indicating a very strong correlation with hepatic NHI and was very close to the significance threshold in mice fed iron in the presence of control diet. This observation is in line with a previous report despite using a lower concentration of carbonyl iron [46]. It is now proposed that iron loading exerts a negative effect on mitochondrial function [243]. There is evidence that *Dmt1* plays a role in iron transport to the mitochondria [185], which is supported by the results of the present study

where the mitochondrial NHI increased with increasing hepatic iron concentration and strengthens the hypothesis that excess iron is at least in part targeted to the mitochondria. Iron diet led to a decrease in the expression of *Acadm* and *Hadha*. *Acadm* is involved in medium chain fatty acid oxidation and *Hadha* encodes the alpha subunit of the mitochondrial trifunctional protein (MTP) which is involved in fatty acid oxidation in the mitochondria [315]. The downregulation of both these genes by iron suggests that fatty acid breakdown decreases with increased iron, leading to accumulation of fat in the liver and to steatosis. It has been shown that young mice which had a defect in MTP developed steatosis when fed HFD as a result of reduced fatty acid oxidation compared to wild type control [315]. All these results indicate that iron plays an important role in NAFLD through initial fat accumulation leading to steatosis. Mice in the present study were fed HFD for 8 weeks but that did not lead to any changes in the mitochondrial fatty acid oxidation genes investigated; neither were any changes observed when iron and HFD were fed together but instead peroxisomal fatty acid oxidation genes *Acca1a* and *Slc27a2* were upregulated in mice fed HFD+iron compared to HFD alone. HFD has been shown to increase the expression of *Acca1a* [316], consistent with steatosis, and increased expression of *Slc27a2* has been linked to NAFLD progression as it enhances long chain fatty acid transport [298]. One factor which is common in all the significant gene expression changes in both mitochondria and peroxisomes is the presence of iron, and it can be speculated that iron functions by decreasing fatty acid oxidation in mitochondria and increasing fatty acid transport in the peroxisomes. Based on the gene expression results, it can be argued that iron loading can independently play a role in mitochondrial fatty acid oxidation leading to fat deposition in the liver and promote steatosis whereby peroxisomal fatty acid oxidation is affected by both the HF and iron diets.

The presence of iron in HFD has been shown to exacerbate hepatic steatosis and has been linked to proinflammatory mediators and cytokines [317]. Iron has also been linked to the production of tumour necrosis factor- α (TNF- α) which is an important pro-inflammatory cytokine. It was found to be elevated in NAFLD patients with much higher levels detected in NAFLD patients with iron overload [140]. The present project did not investigate the signalling pathways associated with inflammation; however, preliminary immunohistochemistry analysis revealed the presence of inflammatory cells in mouse liver stained for CD45. The inflammatory cells were detected in both mice fed the nutritional control diet and iron loaded mice but were slightly higher in the iron loaded group. No quantitative analysis was performed; however, future work will investigate more samples to test this hypothesis. If found to be reproducible,

this would mean that iron in the diet is able to trigger inflammatory response in the very early stages of NAFLD and could be an important trigger which can lead to hepatic insult ultimately leading to liver dysfunction.

All the four dietary groups exhibited the presence of lipids, clearly visible as fat vacuoles in H&E staining. Another important histological observation was the presence of a small number of inflammatory cells in the iron loaded groups which are not commonly detected in HFD fed mice. This suggests that chronic iron loading may lead to inflammation which is also evidenced by the increase in inflammatory cytokines as discussed in the previous paragraph. The other important observation was the decrease of hepatic iron by HFD compared to control. In order to investigate whether the decrease in liver iron was due to decreased absorption from the gut or whether it was being targeted to other organs after being absorbed, iron genes were measured in duodenum and spleen. *Hamp1*, *Tfr1*, *Dmt1* and *Fpn* expression did not change in high fat + iron loaded mice compared to the high fat only group in the spleen. One possibility may be that spleen iron did not change and thus gene expression did not change. It was interesting to note that *Tfr1* and *Dmt1* expression was higher in the duodenum of mice fed high fat + iron compared to high fat only even though the former had more hepatic iron which suggests increased absorption of iron from the duodenum. Duodenal iron was not measured in this instance therefore further investigation is required before a definitive cause can be elucidated. However, the observed increase in *Tfr1* may indicate that iron is being taken up by the enterocytes from the circulation (see **Figure 6.8 C**), explaining the decrease in hepatic NHI. This means both absorption and reuptake of iron is balanced in the presence of HF. It is possible that this mechanism only manifests in the presence of high fat / cholesterol.

In conclusion, high fat led to a reduction in hepatic iron as evidenced by a decrease in NHI content, and iron and high fat selectively regulated gene expression changes associated with mitochondrial and peroxisomal fatty acid oxidation. Iron appeared to be the central player as it led to decreased expression of mitochondrial fatty acid oxidation genes hinting at increased fat deposition in the liver, and upregulation of peroxisomal fatty acid genes, where the increased fat accumulation can be linked to the increased expression of the fatty acid transporter (*Slc27a2*) and *Acaa1a* which is not consistent with the increased fat accumulation. The apparent contradiction here may be due to the adaptive nature of the liver to balance the insult caused by fatty acid deposition. The presence of iron also indicated an increase in inflammatory cells as seen in the histological examinations, but a larger sample size is needed to validate the results further.

7.5. Effect of Iron Overload on Hepatic Cholesterol Crystal

The liver plays a central role in iron and lipid metabolism [14] along with its role in production and processing of circulating lipoproteins [132]. Excess cholesterol can be excreted directly into the bile, the main pathway for its removal [132]. However, in NAFLD, liver cholesterol homeostasis is dysregulated resulting in cholesterol accumulation [132]. Iron overload has been shown to increase cholesterol biosynthesis in mice by upregulating cholesterol biosynthesis genes [46]. Dysregulated cholesterol homeostasis may lead to unesterified cholesterol supersaturation in cells which may lead to its precipitation in the form of crystals [292]. The present study has led to a novel finding whereby iron overload in the presence of high fat led to a significant decrease in the number of cholesterol crystals when compared to high fat diet without any added iron. To the best of my knowledge this is the first report linking iron overload to decreased cholesterol crystal formation in a mouse model of NAFLD.

An important point worth noting in the context of cholesterol crystal formation is the dual role played by iron. On one hand, iron loading led to increased hepatic cholesterol, and, on the other hand, it reduced cholesterol crystal formation in the liver. The basal diet used in the study by Graham *et al* [46] did not have any added fat or cholesterol whereas, in the present study, the diet was a Western style diet containing high fat along with added cholesterol. It is possible that iron on its own may lead to increased cholesterol biosynthesis but, in the presence of high fat, the regulation of cholesterol biosynthesis by iron may be overwhelmed due to regulation by dietary cholesterol. Higher iron status has also been found to decrease the risk of gallbladder cholesterolosis [318] and it is possible that iron overload may have a protective role by reducing the accumulation of cholesteryl esters. Alternatively, there is a possibility that iron overload may lead to cholesterol being transported out of the liver [46], thus decreasing the amount of free cholesterol which, in turn, may lead to reduced crystal formation.

The present observation related to cholesterol crystal formation also sheds light on the role of these crystals in progression of NAFLD. So far, cholesterol crystals have been linked with NASH [137, 290] but not to initial fat deposition (steatosis). However, the current study presents strong evidence to show that cholesterol crystal formation starts early in steatosis, prior to the liver showing any clinical features of NASH. The study [290] which reported cholesterol crystal formation in murine NASH used older mice (four-month-old), fed HFD with a much higher cholesterol content (up to 1%) for 6 months compared to 3-week-old mice fed a HFD containing 0.15% cholesterol for 8 weeks in the present study. The number of crystals detected in the present study were much higher than seen in the study with higher dietary

cholesterol. This observation is clinically relevant as cholesterol crystals have been shown to activate NOD-, LRP- and pyrin- domain containing protein 3 (NLRP3) inflammasomes in Kupffer cells which subsequently lead to release of pro-inflammatory cytokines [290]. Cholesterol crystals are also believed to disrupt the function of lipid droplets by reducing their fluidity [132] and, in some cases, by disrupting the physical integrity of the surrounding membrane [319]. The present work appears to be the first report of cholesterol crystal formation and its decrease by iron in early hepatic steatosis. Future studies are needed to study the role of iron in the decrease in hepatic cholesterol crystals. The role of iron in the presence of HFD without added cholesterol should be investigated to determine if iron leads to cholesterol transport out of the liver or plays another role in the process of cholesterol crystal formation. Measurement of extrahepatic cholesterol will also help answer some of the questions raised here, as it will be able to confirm or rule out the transport of cholesterol to extra-hepatic tissues. If confirmed, it will be good evidence that decreased crystal formation is linked to decreased cholesterol in the liver. In summary, the cytotoxic effects of excess free cholesterol cannot be overlooked. It has been shown that cholesterol-lowering drugs can reverse hepatic cholesterol crystallization and experimental fibrosis [320]. Therefore, future interventional studies looking at a more diverse sub-group of patients as well as animal models are required to ascertain the role played by either free cholesterol or cholesterol crystals in the pathogenesis of NAFLD.

In conclusion, the present study has shown that excess dietary iron is targeted towards the mitochondria, which may lead to mitochondrial dysfunction by affecting the electron transport chain/complexes as well as oxidative phosphorylation. There appears to be an interaction between fat and iron which leads to selective effects on mitochondrial and peroxisomal fatty acid oxidation, indicating iron overload can contribute to the initial fat accumulation in the liver. The presence of high fat also exhibited a much stronger control on hepcidin expression compared to the control diet without any high fat content. One of the most important findings of the study was the decrease of cholesterol crystals in the presence of high fat by iron, suggesting that cholesterol crystals are present in the early stages of steatosis and not only during NASH. Cholesterol crystals therefore appear not to be a marker of NASH but may be a predictor of NAFLD progression.

7.6. Conclusion

The study discussed in this thesis investigated the relationship between iron and lipid metabolism in NAFLD using *in vitro* and animal studies. The results from the *in vitro* study indicate that saturated and unsaturated fatty acids exert differential effect on mitochondrial respiration where PA is more cytotoxic than OA. Both the fatty acids stimulate mitochondrial bioenergetics but with varying profiles. In the present study, iron has been shown to enhance the effects of OA which has been shown to be protective against cell lipotoxicity. Furthermore, the results also indicate that treatments with iron, OA and PA increased mitochondrial function. The results from the mouse study indicate that high fat led to a decrease in hepatic iron as evidenced by a decrease in NHI content, and iron and high fat selectively regulated gene expression changes associated with mitochondrial and peroxisomal fatty acid oxidation. Iron overload was associated with decreased mitochondrial beta oxidation which can lead to the accumulation of fatty acid in the liver and is consistent with the hypothesis that iron plays an important role in the development of steatosis which is the very first stage of NAFLD. In the presence of iron in HFD there was an upregulation of peroxisomal fatty acid genes which is not consistent with increased fat accumulation and may be a suitable response by the liver to counter the insult due to fatty acid deposition.

An especially important finding from the study was the reduction of hepatic cholesterol crystals in the presence of iron. Cholesterol crystals have been implicated in the progression of steatosis to NASH but in the present study these crystals were visible as early as steatosis. Therefore, these can be considered as a marker of NAFLD progression. Overall, iron has been shown to play an important role in the initial stage of NAFLD and appears to be protective against hepatic cholesterol crystal formation.

7.7. Limitations

The present study has given important insights into the role of iron and lipids in the development and progression of NAFLD. Nevertheless, there are some limitations associated with the study. The study made use of liver tissue, but lipids were not quantified in the blood or plasma which can give an insight into the transport of cholesterol and other lipids out of the liver and may help explain the decrease in cholesterol crystals in the presence of iron. In order to study the effect of iron and lipid loading on mitochondrial bioenergetics a longer incubation of more than 12 h may provide more detail on mitochondrial health. The animal study made

use of HFD with added cholesterol but using a diet with no added cholesterol may help in explaining the role of cholesterol crystal formation and its subsequent decrease in the presence of iron. Also, extending the preliminary findings on markers of hepatic injury and inflammation would help ascertain the role of iron and fatty acids in inflammation.

7.8. Future Directions

The present study has given an interesting insight into understanding the relationship between iron and lipid metabolism and their roles in NAFLD. The reduction in cholesterol crystal formation due to the presence of iron in association with high fat was a novel finding, and future studies are warranted in order to investigate the mechanism by which iron regulates crystal formation. For example, a study in mice using different compositions of high fat and cholesterol and then investigating the cholesterol crystal formation in the presence or absence of iron would provide information on the role played by high fat and cholesterol on crystal formation. It will become clear if the added cholesterol is driving the crystal formation and if there is a relationship between the concentration of cholesterol in the diet and crystal formation. Measuring extrahepatic cholesterol, including plasma cholesterol, as well as the activity of hepatic cholesterol transporters will demonstrate whether iron plays a role in transporting cholesterol out of the liver. The use of iron chelators in these dietary models would also help explain if the iron in the diet is responsible for the decrease in cholesterol crystals and overall cholesterol biosynthesis. It would be informative to investigate the types of cholesterol crystals in the liver as it is documented that different shapes of crystals may form as a result of different lipid types [292] and this may give an insight into the role of different lipid types in NAFLD pathogenesis. The measurement of cholesterol biosynthesis and transport genes would also shed light on the role of iron in cholesterol biosynthesis and metabolism in the presence of high fat in NAFLD.

The present study investigated gene expression but not protein expression or activity. Investigating protein expression would demonstrate whether iron is involved in post-transcriptional regulation of the key genes and investigating activity would provide information about iron's role in post-translational regulation. In the present study, only a limited number of samples were used to perform immunohistochemistry analysis of the liver samples. Given that the results were suggestive of inflammatory changes, performing further analysis on a larger sample size will allow for statistically robust conclusions to be derived. If cholesterol crystals

were present in the same samples, this would also help us understand the mechanism of any toxicity related to cholesterol crystal formation.

In the *in vitro* studies, the role of iron and lipid loading was investigated to understand mitochondrial bioenergetics and how iron modulates lipid deposition. The 12 h time period did not prove to be sufficient to induce lipid loading in cells as another project in the laboratory has shown that there is an increase in the lipid content of the cell after 12 h of iron loading. Therefore, future experiments will involve extending the incubation times of both iron and lipid loading to help capture changes associated with mitochondrial bioenergetics in order to better explain how iron and lipid loading lead to changes in mitochondrial function in NAFLD.

Publications and Presentations

Abhishek K Singh, Cyril DS Mamotte, Vincent M Williams, Leon A Adams, Ross M Graham. Reduction in Hepatic Cholesterol Crystals in Mice Upon Dietary Iron Overload. (Manuscript under preparation) 2022.

Singh, A., Mamotte, C., Adams, L., & Graham, R. (2017). Investigation of mitochondrial function with iron and lipid loading in aml12 cells. *American Journal of Hematology*, 92(8), E402-E402.

Reduction in hepatic cholesterol crystals upon dietary iron overload in mice.
Oral presentation at AusIron- Australian Iron Network, QIMR Berghofer Institute, Brisbane, 2021.

Investigation of Iron and Lipid Metabolism in Non-alcoholic Fatty Liver Disease.
Oral presentation at Australian Society for Medical Research (ASMR) National Scientific Conference, Perth, 2019.

Investigation of Mitochondrial Function with Iron and Lipid Loading.
Poster presentation at 7th Congress of the International BioIron Society, UCLA, Los Angeles, 2017

References

1. Ray, K., *NAFLD—the next global epidemic*. Nature Reviews Gastroenterology & Hepatology, 2013. **10**: p. 621.
2. Anstee, Q.M., G. Targher, and C.P. Day, *Progression of NAFLD to diabetes mellitus, cardiovascular disease or cirrhosis*. Nature Reviews Gastroenterology & Hepatology, 2013. **10**: p. 330.
3. Bedogni, G., et al., *Prevalence of and risk factors for nonalcoholic fatty liver disease: the Dionysos nutrition and liver study*. Hepatology, 2005. **42**(1): p. 44-52.
4. Machado, M., P. Marques-Vidal, and H. Cortez-Pinto, *Hepatic histology in obese patients undergoing bariatric surgery*. Journal of Hepatology, 2006. **45**(4): p. 600-606.
5. Yki-Järvinen, H., *Non-alcoholic fatty liver disease as a cause and a consequence of metabolic syndrome*. The Lancet Diabetes & Endocrinology, 2014. **2**(11): p. 901-910.
6. Dongiovanni, P., et al., *Iron in fatty liver and in the metabolic syndrome: A promising therapeutic target*. Journal of Hepatology, 2011. **55**(4): p. 920-932.
7. Nelson, J.E., H. Klintworth, and K.V. Kowdley, *Iron metabolism in Nonalcoholic Fatty Liver Disease*. Curr Gastroenterol Rep, 2012. **14**(1): p. 8-16.
8. Sherman, A.R., *Lipogenesis in iron-deficient adult rats*. Lipids, 1978. **13**(7): p. 473-8.
9. Bartholmey, S.J. and A.R. Sherman, *Carnitine levels in iron-deficient rat pups*. J Nutr, 1985. **115**(1): p. 138-45.
10. Britton, L.J., V.N. Subramaniam, and D.H. Crawford, *Iron and non-alcoholic fatty liver disease*. World J Gastroenterol, 2016. **22**(36): p. 8112-22.
11. Rolo, A.P., J.S. Teodoro, and C.M. Palmeira, *Role of oxidative stress in the pathogenesis of nonalcoholic steatohepatitis*. Free Radic Biol Med, 2012. **52**(1): p. 59-69.
12. Minamiyama, Y., et al., *Iron restriction improves type 2 diabetes mellitus in Otsuka Long-Evans Tokushima fatty rats*. Am J Physiol Endocrinol Metab, 2010. **298**(6): p. E1140-9.
13. MacDonald, G.A., et al., *Lipid peroxidation in hepatic steatosis in humans is associated with hepatic fibrosis and occurs predominately in acinar zone 3*. J Gastroenterol Hepatol, 2001. **16**(6): p. 599-606.
14. Ahmed, U., P.S. Latham, and P.S. Oates, *Interactions between hepatic iron and lipid metabolism with possible relevance to steatohepatitis*. World J Gastroenterol, 2012. **18**(34): p. 4651-8.
15. Ingvorsen, C., N.A. Karp, and C.J. Lelliott, *The role of sex and body weight on the metabolic effects of high-fat diet in C57BL/6N mice*. Nutrition & Diabetes, 2017. **7**: p. e261.
16. Neuschwander-Tetri, B.A., *Nonalcoholic steatohepatitis and the metabolic syndrome*. Am J Med Sci, 2005. **330**(6): p. 326-35.
17. Adams, L.A., et al., *The natural history of nonalcoholic fatty liver disease: a population-based cohort study*. Gastroenterology, 2005. **129**(1): p. 113-21.
18. Charlton, M., *Nonalcoholic fatty liver disease: a review of current understanding and future impact*. Clin Gastroenterol Hepatol, 2004. **2**(12): p. 1048-58.
19. de Alwis, N.M. and C.P. Day, *Non-alcoholic fatty liver disease: the mist gradually clears*. J Hepatol, 2008. **48 Suppl 1**: p. S104-12.
20. Masuoka, H.C. and N. Chalasani, *Nonalcoholic fatty liver disease: an emerging threat to obese and diabetic individuals*. Ann N Y Acad Sci, 2013. **1281**: p. 106-22.
21. Neuschwander-Tetri, B.A. and S.H. Caldwell, *Nonalcoholic steatohepatitis: summary of an AASLD Single Topic Conference*. Hepatology, 2003. **37**(5): p. 1202-19.
22. Tominaga, K., et al., *Prevalence of fatty liver in Japanese children and relationship to obesity. An epidemiological ultrasonographic survey*. Dig Dis Sci, 1995. **40**(9): p. 2002-9.
23. Franzese, A., et al., *Liver involvement in obese children. Ultrasonography and liver enzyme levels at diagnosis and during follow-up in an Italian population*. Dig Dis Sci, 1997. **42**(7): p. 1428-32.

24. Armstrong, M.J., et al., *Extrahepatic complications of nonalcoholic fatty liver disease*. Hepatology, 2014. **59**(3): p. 1174-97.
25. Adams, L.A., *Nonalcoholic fatty liver disease and diabetes mellitus*. Endocr Res, 2007. **32**(3): p. 59-69.
26. Valenti, L., et al., *Iron depletion by phlebotomy improves insulin resistance in patients with nonalcoholic fatty liver disease and hyperferritinemia: evidence from a case-control study*. Am J Gastroenterol, 2007. **102**(6): p. 1251-8.
27. Valenti, L., et al., *A randomized trial of iron depletion in patients with nonalcoholic fatty liver disease and hyperferritinemia*. World J Gastroenterol, 2014. **20**(11): p. 3002-10.
28. Facchini, F.S., N.W. Hua, and R.A. Stoohs, *Effect of iron depletion in carbohydrate-intolerant patients with clinical evidence of nonalcoholic fatty liver disease*. Gastroenterology, 2002. **122**(4): p. 931-9.
29. Adams, L.A., et al., *The impact of phlebotomy in nonalcoholic fatty liver disease: A prospective, randomized, controlled trial*. Hepatology, 2015. **61**(5): p. 1555-64.
30. Ryan, J.D., et al., *Hepatic iron is the major determinant of serum ferritin in NAFLD patients*. Liver Int, 2018. **38**(1): p. 164-173.
31. Kowdley, K.V., et al., *Serum ferritin is an independent predictor of histologic severity and advanced fibrosis in patients with nonalcoholic fatty liver disease*. Hepatology, 2012. **55**(1): p. 77-85.
32. Day, C.P. and O.F. James, *Steatohepatitis: a tale of two "hits"?* Gastroenterology, 1998. **114**(4): p. 842-5.
33. Day, C.P., *From fat to inflammation*. Gastroenterology, 2006. **130**(1): p. 207-10.
34. Buzzetti, E., M. Pinzani, and E.A. Tsochatzis, *The multiple-hit pathogenesis of non-alcoholic fatty liver disease (NAFLD)*. Metabolism, 2016. **65**(8): p. 1038-48.
35. Anstee, Q.M. and C.P. Day, *The Genetics of Nonalcoholic Fatty Liver Disease: Spotlight on PNPLA3 and TM6SF2*. Semin Liver Dis, 2015. **35**(3): p. 270-90.
36. Podrini, C., et al., *Redox homeostasis and epigenetics in non-alcoholic fatty liver disease (NAFLD)*. Curr Pharm Des, 2013. **19**(15): p. 2737-46.
37. Ferreira, D.M., et al., *Revisiting the metabolic syndrome and paving the way for microRNAs in non-alcoholic fatty liver disease*. FEBS J, 2014. **281**(11): p. 2503-24.
38. Panera, N., et al., *MicroRNAs as controlled systems and controllers in non-alcoholic fatty liver disease*. World J Gastroenterol, 2014. **20**(41): p. 15079-86.
39. Jaenisch, R. and A. Bird, *Epigenetic regulation of gene expression: how the genome integrates intrinsic and environmental signals*. Nat Genet, 2003. **33 Suppl**: p. 245-54.
40. Yamaguchi, K., et al., *Inhibiting triglyceride synthesis improves hepatic steatosis but exacerbates liver damage and fibrosis in obese mice with nonalcoholic steatohepatitis*. Hepatology, 2007. **45**(6): p. 1366-74.
41. Sanyal, A.J., et al., *Nonalcoholic steatohepatitis: association of insulin resistance and mitochondrial abnormalities*. Gastroenterology, 2001. **120**(5): p. 1183-92.
42. Backhed, F., et al., *The gut microbiota as an environmental factor that regulates fat storage*. Proc Natl Acad Sci U S A, 2004. **101**(44): p. 15718-23.
43. Wang, Z., et al., *Gut flora metabolism of phosphatidylcholine promotes cardiovascular disease*. Nature, 2011. **472**(7341): p. 57-63.
44. Corbin, K.D. and S.H. Zeisel, *Choline metabolism provides novel insights into nonalcoholic fatty liver disease and its progression*. Curr Opin Gastroenterol, 2012. **28**(2): p. 159-65.
45. Lee, J.M., et al., *A nuclear-receptor-dependent phosphatidylcholine pathway with antidiabetic effects*. Nature, 2011. **474**(7352): p. 506-10.
46. Graham, R.M., et al., *Hepatic iron loading in mice increases cholesterol biosynthesis*. Hepatology, 2010. **52**(2): p. 462-71.
47. Chua, A.C., et al., *The regulation of cellular iron metabolism*. Crit Rev Clin Lab Sci, 2007. **44**(5-6): p. 413-59.

48. Abbaspour, N., R. Hurrell, and R. Kelishadi, *Review on iron and its importance for human health*. J Res Med Sci, 2014. **19**(2): p. 164-74.
49. Ganz, T. and E. Nemeth, *Regulation of iron acquisition and iron distribution in mammals*. Biochim Biophys Acta, 2006. **1763**(7): p. 690-9.
50. Wang, J. and K. Pantopoulos, *Regulation of cellular iron metabolism*. Biochem J, 2011. **434**(3): p. 365-81.
51. Papanikolaou, G. and K. Pantopoulos, *Iron metabolism and toxicity*. Toxicol Appl Pharmacol, 2005. **202**(2): p. 199-211.
52. Sola, M., *Bioinorganic chemistry: By I. Bertini, H.B. Gray, S.J. Lippard and J.S. Valentine, published by University Science Books, Mill Valley, CA, USA, 1994, 611 pp. US\$ 58, ISBN 0-935702-57-1 (Book Review)*. Inorganica Chimica Acta, 1995. **230**(1): p. 253-254.
53. Ponka, P., C. Beaumont, and D.R. Richardson, *Function and regulation of transferrin and ferritin*. Semin Hematol, 1998. **35**(1): p. 35-54.
54. Benkovic, S.A. and J.R. Connor, *Ferritin, transferrin, and iron in selected regions of the adult and aged rat brain*. J Comp Neurol, 1993. **338**(1): p. 97-113.
55. Skinner, M.K. and M.D. Griswold, *Secretion of testicular transferrin by cultured Sertoli cells is regulated by hormones and retinoids*. Biol Reprod, 1982. **27**(1): p. 211-21.
56. Graham, R.M., et al., *Liver iron transport*. World J Gastroenterol, 2007. **13**(35): p. 4725-36.
57. Young, S.P., S. Roberts, and A. Bomford, *Intracellular processing of transferrin and iron by isolated rat hepatocytes*. Biochem J, 1985. **232**(3): p. 819-23.
58. Halliday, J.W. and J. Searle, *Hepatic iron deposition in human disease and animal models*. Biometals, 1996. **9**(2): p. 205-9.
59. Dautry-Varsat, A., A. Ciechanover, and H.F. Lodish, *pH and the recycling of transferrin during receptor-mediated endocytosis*. Proc Natl Acad Sci U S A, 1983. **80**(8): p. 2258-62.
60. Anderson, E.R. and Y.M. Shah, *Iron homeostasis in the liver*. Compr Physiol, 2013. **3**(1): p. 315-30.
61. Kew, M.C., *Hepatic iron overload and hepatocellular carcinoma*. Liver cancer, 2014. **3**(1): p. 31-40.
62. Baldwin, D.A., D.M. De Sousa, and R.M. Von Wandruszka, *The effect of pH on the kinetics of iron release from human transferrin*. Biochim Biophys Acta, 1982. **719**(1): p. 140-6.
63. Zhang, D.L., M.C. Ghosh, and T.A. Rouault, *The physiological functions of iron regulatory proteins in iron homeostasis - an update*. Front Pharmacol, 2014. **5**: p. 124.
64. Muckenthaler, M.U., B. Galy, and M.W. Hentze, *Systemic iron homeostasis and the iron-responsive element/iron-regulatory protein (IRE/IRP) regulatory network*. Annu Rev Nutr, 2008. **28**: p. 197-213.
65. Mullner, E.W. and L.C. Kuhn, *A stem-loop in the 3' untranslated region mediates iron-dependent regulation of transferrin receptor mRNA stability in the cytoplasm*. Cell, 1988. **53**(5): p. 815-25.
66. Binder, R., et al., *Evidence that the pathway of transferrin receptor mRNA degradation involves an endonucleolytic cleavage within the 3' UTR and does not involve poly(A) tail shortening*. EMBO J, 1994. **13**(8): p. 1969-80.
67. Muckenthaler, M.U., et al., *A Red Carpet for Iron Metabolism*. Cell, 2017. **168**(3): p. 344-361.
68. Yoshinaga, M., et al., *Regnase-1 Maintains Iron Homeostasis via the Degradation of Transferrin Receptor 1 and Prollyl-Hydroxylase-Domain-Containing Protein 3 mRNAs*. Cell Rep, 2017. **19**(8): p. 1614-1630.
69. Bianchi, L., L. Tacchini, and G. Cairo, *HIF-1-mediated activation of transferrin receptor gene transcription by iron chelation*. Nucleic Acids Res, 1999. **27**(21): p. 4223-7.
70. Lok, C.N. and P. Ponka, *Identification of a hypoxia response element in the transferrin receptor gene*. J Biol Chem, 1999. **274**(34): p. 24147-52.
71. Miskimins, W.K., et al., *Cell proliferation and expression of the transferrin receptor gene: promoter sequence homologies and protein interactions*. J Cell Biol, 1986. **103**(5): p. 1781-8.

72. Seiser, C., S. Teixeira, and L.C. Kuhn, *Interleukin-2-dependent transcriptional and post-transcriptional regulation of transferrin receptor mRNA*. J Biol Chem, 1993. **268**(18): p. 13074-80.
73. Garrick, M.D., et al., *DMT1: a mammalian transporter for multiple metals*. Biometals, 2003. **16**(1): p. 41-54.
74. Mackenzie, B., et al., *Functional properties of multiple isoforms of human divalent metal-ion transporter 1 (DMT1)*. Biochem J, 2007. **403**(1): p. 59-69.
75. Gunshin, H., et al., *Cloning and characterization of a mammalian proton-coupled metal-ion transporter*. Nature, 1997. **388**(6641): p. 482-8.
76. Garrick, M.D., et al., *DMT1: which metals does it transport?* Biol Res, 2006. **39**(1): p. 79-85.
77. Knutson, M.D., *Non-transferrin-bound iron transporters*. Free Radic Biol Med, 2018.
78. Chua, A.C., et al., *Nontransferrin-bound iron uptake by hepatocytes is increased in the Hfe knockout mouse model of hereditary hemochromatosis*. Blood, 2004. **104**(5): p. 1519-25.
79. Trinder, D., et al., *Localisation of divalent metal transporter 1 (DMT1) to the microvillus membrane of rat duodenal enterocytes in iron deficiency, but to hepatocytes in iron overload*. Gut, 2000. **46**(2): p. 270-6.
80. Garrick, M.D., et al., *Comparison of mammalian cell lines expressing distinct isoforms of divalent metal transporter 1 in a tetracycline-regulated fashion*. Biochem J, 2006. **398**(3): p. 539-46.
81. Nemeth, E., et al., *Hepcidin regulates cellular iron efflux by binding to ferroportin and inducing its internalization*. Science, 2004. **306**(5704): p. 2090-3.
82. Ward, D.M. and J. Kaplan, *Ferroportin-mediated iron transport: expression and regulation*. Biochim Biophys Acta, 2012. **1823**(9): p. 1426-33.
83. Taylor, M., et al., *Hypoxia-inducible factor-2alpha mediates the adaptive increase of intestinal ferroportin during iron deficiency in mice*. Gastroenterology, 2011. **140**(7): p. 2044-55.
84. Knutson, M.D., et al., *Iron loading and erythrophagocytosis increase ferroportin 1 (FPN1) expression in J774 macrophages*. Blood, 2003. **102**(12): p. 4191-7.
85. Troadec, M.B., et al., *Induction of FPN1 transcription by MTF-1 reveals a role for ferroportin in transition metal efflux*. Blood, 2010. **116**(22): p. 4657-64.
86. Qian, Y., et al., *Estrogen contributes to regulating iron metabolism through governing ferroportin signaling via an estrogen response element*. Cell Signal, 2015. **27**(5): p. 934-42.
87. Abboud, S. and D.J. Haile, *A novel mammalian iron-regulated protein involved in intracellular iron metabolism*. J Biol Chem, 2000. **275**(26): p. 19906-12.
88. Donovan, A., et al., *Positional cloning of zebrafish ferroportin1 identifies a conserved vertebrate iron exporter*. Nature, 2000. **403**(6771): p. 776-81.
89. McKie, A.T., et al., *A novel duodenal iron-regulated transporter, IREG1, implicated in the basolateral transfer of iron to the circulation*. Mol Cell, 2000. **5**(2): p. 299-309.
90. Drakesmith, H., E. Nemeth, and T. Ganz, *Ironing out Ferroportin*. Cell Metab, 2015. **22**(5): p. 777-87.
91. Gubler, C.J., et al., *Studies on copper metabolism. III. The metabolism of iron in copper deficient swine*. Blood, 1952. **7**(11): p. 1075-92.
92. McDermott, J.A., et al., *Role of iron in the oxidase activity of ceruloplasmin*. Biochim Biophys Acta, 1968. **151**(3): p. 541-57.
93. Osaki, S., D.A. Johnson, and E. Frieden, *The mobilization of iron from the perfused mammalian liver by a serum copper enzyme, ferroxidase I*. J Biol Chem, 1971. **246**(9): p. 3018-23.
94. Sarkar, J., et al., *Role of ceruloplasmin in macrophage iron efflux during hypoxia*. J Biol Chem, 2003. **278**(45): p. 44018-24.
95. De Domenico, I., et al., *Ferroxidase activity is required for the stability of cell surface ferroportin in cells expressing GPI-ceruloplasmin*. EMBO J, 2007. **26**(12): p. 2823-31.

96. Jeong, S.Y. and S. David, *Glycosylphosphatidylinositol-anchored ceruloplasmin is required for iron efflux from cells in the central nervous system*. J Biol Chem, 2003. **278**(29): p. 27144-8.
97. Hilton, K.B. and L.A. Lambert, *Molecular evolution and characterization of hepcidin gene products in vertebrates*. Gene, 2008. **415**(1-2): p. 40-8.
98. Valore, E.V. and T. Ganz, *Posttranslational processing of hepcidin in human hepatocytes is mediated by the prohormone convertase furin*. Blood Cells Mol Dis, 2008. **40**(1): p. 132-8.
99. Bekri, S., et al., *Increased adipose tissue expression of hepcidin in severe obesity is independent from diabetes and NASH*. Gastroenterology, 2006. **131**(3): p. 788-96.
100. Liu, X.B., et al., *Regulation of hepcidin and ferroportin expression by lipopolysaccharide in splenic macrophages*. Blood Cells Mol Dis, 2005. **35**(1): p. 47-56.
101. Goodnough, L.T., E. Nemeth, and T. Ganz, *Detection, evaluation, and management of iron-restricted erythropoiesis*. Blood, 2010. **116**(23): p. 4754-61.
102. Nemeth, E. and T. Ganz, *Regulation of iron metabolism by hepcidin*. Annu Rev Nutr, 2006. **26**: p. 323-42.
103. Ramos, E., et al., *Evidence for distinct pathways of hepcidin regulation by acute and chronic iron loading in mice*. Hepatology, 2011. **53**(4): p. 1333-41.
104. Ilyin, G., et al., *Comparative analysis of mouse hepcidin 1 and 2 genes: evidence for different patterns of expression and co-inducibility during iron overload*. FEBS Lett, 2003. **542**(1-3): p. 22-6.
105. Nicolas, G., et al., *Lack of hepcidin gene expression and severe tissue iron overload in upstream stimulatory factor 2 (USF2) knockout mice*. Proc Natl Acad Sci U S A, 2001. **98**(15): p. 8780-5.
106. Pigeon, C., et al., *A new mouse liver-specific gene, encoding a protein homologous to human antimicrobial peptide hepcidin, is overexpressed during iron overload*. J Biol Chem, 2001. **276**(11): p. 7811-9.
107. Lou, D.Q., et al., *Functional differences between hepcidin 1 and 2 in transgenic mice*. Blood, 2004. **103**(7): p. 2816-21.
108. Lu, S., J. Seravalli, and D. Harrison-Findik, *Inductively coupled mass spectrometry analysis of biometals in conditional Hamp1 and Hamp1 and Hamp2 transgenic mouse models*. Transgenic Res, 2015. **24**(4): p. 765-73.
109. Khan, F.Z., et al., *Advances in hepatocellular carcinoma: Nonalcoholic steatohepatitis-related hepatocellular carcinoma*. World J Hepatol, 2015. **7**(18): p. 2155-61.
110. Lade, A., L.A. Noon, and S.L. Friedman, *Contributions of metabolic dysregulation and inflammation to nonalcoholic steatohepatitis, hepatic fibrosis, and cancer*. Curr Opin Oncol, 2014. **26**(1): p. 100-7.
111. Valenti, L., et al., *HFE genotype, parenchymal iron accumulation, and liver fibrosis in patients with nonalcoholic fatty liver disease*. Gastroenterology, 2010. **138**(3): p. 905-12.
112. Nelson, J.E., et al., *Relationship between the pattern of hepatic iron deposition and histological severity in nonalcoholic fatty liver disease*. Hepatology, 2011. **53**(2): p. 448-57.
113. Bonkovsky, H.L., et al., *Non-alcoholic steatohepatitis and iron: increased prevalence of mutations of the HFE gene in non-alcoholic steatohepatitis*. J Hepatol, 1999. **31**(3): p. 421-9.
114. George, D.K., et al., *Increased hepatic iron concentration in nonalcoholic steatohepatitis is associated with increased fibrosis*. Gastroenterology, 1998. **114**(2): p. 311-8.
115. Hubscher, S.G., *Iron overload, inflammation and fibrosis in genetic haemochromatosis*. J Hepatol, 2003. **38**(4): p. 521-5.
116. Zhou, Y., et al., *Iron overloaded polarizes macrophage to proinflammation phenotype through ROS/acetyl-p53 pathway*. Cancer Med, 2018. **7**(8): p. 4012-4022.
117. Pan, M., et al., *Lipid peroxidation and oxidant stress regulate hepatic apolipoprotein B degradation and VLDL production*. J Clin Invest, 2004. **113**(9): p. 1277-87.
118. Nakashima, T., et al., *Elevation of serum thioredoxin levels in patients with nonalcoholic steatohepatitis*. Hepatol Res, 2005. **33**(2): p. 135-7.

119. Messner, D.J., B.H. Rhieu, and K.V. Kowdley, *Iron overload causes oxidative stress and impaired insulin signaling in AML-12 hepatocytes*. *Dig Dis Sci*, 2013. **58**(7): p. 1899-908.
120. Ruddell, R.G., et al., *Ferritin functions as a proinflammatory cytokine via iron-independent protein kinase C zeta/nuclear factor kappaB-regulated signaling in rat hepatic stellate cells*. *Hepatology*, 2009. **49**(3): p. 887-900.
121. Chen, L., et al., *Iron causes interactions of TAK1, p21ras, and phosphatidylinositol 3-kinase in caveolae to activate IkkappaB kinase in hepatic macrophages*. *J Biol Chem*, 2007. **282**(8): p. 5582-8.
122. Tiniakos, D.G., *Nonalcoholic fatty liver disease/nonalcoholic steatohepatitis: histological diagnostic criteria and scoring systems*. *Eur J Gastroenterol Hepatol*, 2010. **22**(6): p. 643-50.
123. Sparks, J.D. and C.E. Sparks, *Insulin regulation of triacylglycerol-rich lipoprotein synthesis and secretion*. *Biochim Biophys Acta*, 1994. **1215**(1-2): p. 9-32.
124. Debeer, L.J., et al., *Lipolysis of hepatic triacylglycerol stores*. *FEBS Lett*, 1982. **140**(2): p. 159-64.
125. Patsch, W., S. Franz, and G. Schonfeld, *Role of insulin in lipoprotein secretion by cultured rat hepatocytes*. *J Clin Invest*, 1983. **71**(5): p. 1161-74.
126. Adeli, K. and A. Theriault, *Insulin modulation of human apolipoprotein B mRNA translation: studies in an in vitro cell-free system from HepG2 cells*. *Biochem Cell Biol*, 1992. **70**(12): p. 1301-12.
127. Sparks, J.D. and C.E. Sparks, *Insulin modulation of hepatic synthesis and secretion of apolipoprotein B by rat hepatocytes*. *J Biol Chem*, 1990. **265**(15): p. 8854-62.
128. Brasaemle, D.L., et al., *Adipose differentiation-related protein is an ubiquitously expressed lipid storage droplet-associated protein*. *J Lipid Res*, 1997. **38**(11): p. 2249-63.
129. Phillips, S.A., et al., *Adipocyte differentiation-related protein in human skeletal muscle: relationship to insulin sensitivity*. *Obes Res*, 2005. **13**(8): p. 1321-9.
130. Bosner, M.S., et al., *Percent cholesterol absorption in normal women and men quantified with dual stable isotopic tracers and negative ion mass spectrometry*. *J Lipid Res*, 1999. **40**(2): p. 302-8.
131. Caballero, F., et al., *Enhanced free cholesterol, SREBP-2 and StAR expression in human NASH*. *J Hepatol*, 2009. **50**(4): p. 789-96.
132. Ioannou, G.N., *The Role of Cholesterol in the Pathogenesis of NASH*. *Trends Endocrinol Metab*, 2016. **27**(2): p. 84-95.
133. Mari, M., et al., *Mitochondrial free cholesterol loading sensitizes to TNF- and Fas-mediated steatohepatitis*. *Cell Metab*, 2006. **4**(3): p. 185-98.
134. Van Rooyen, D.M., et al., *Hepatic free cholesterol accumulates in obese, diabetic mice and causes nonalcoholic steatohepatitis*. *Gastroenterology*, 2011. **141**(4): p. 1393-403, 1403 e1-5.
135. Ioannou, G.N., et al., *Hepatic cholesterol crystals and crown-like structures distinguish NASH from simple steatosis*. *J Lipid Res*, 2013. **54**(5): p. 1326-34.
136. Savard, C., et al., *Synergistic interaction of dietary cholesterol and dietary fat in inducing experimental steatohepatitis*. *Hepatology*, 2013. **57**(1): p. 81-92.
137. Ioannou, G.N., et al., *Cholesterol Crystals in Hepatocyte Lipid Droplets Are Strongly Associated With Human Nonalcoholic Steatohepatitis*. *Hepatol Commun*, 2019. **3**(6): p. 776-791.
138. Duewell, P., et al., *NLRP3 inflammasomes are required for atherogenesis and activated by cholesterol crystals*. *Nature*, 2010. **464**(7293): p. 1357-61.
139. Bacon, B.R., et al., *Nonalcoholic steatohepatitis: an expanded clinical entity*. *Gastroenterology*, 1994. **107**(4): p. 1103-9.
140. Aigner, E., et al., *Pathways underlying iron accumulation in human nonalcoholic fatty liver disease*. *Am J Clin Nutr*, 2008. **87**(5): p. 1374-83.
141. Sikorska, K., et al., *Liver steatosis correlates with iron overload but not with HFE gene mutations in chronic hepatitis C*. *Hepatobiliary Pancreat Dis Int*, 2013. **12**(4): p. 377-84.

142. Bacon, B.R., R. O'Neill, and C.H. Park, *Iron-induced peroxidative injury to isolated rat hepatic mitochondria*. J Free Radic Biol Med, 1986. **2**(5-6): p. 339-47.
143. Ohyashiki, T., T. Ohtsuka, and T. Mohri, *A change in the lipid fluidity of the porcine intestinal brush-border membranes by lipid peroxidation. Studies using pyrene and fluorescent stearic acid derivatives*. Biochim Biophys Acta, 1986. **861**(2): p. 311-8.
144. Curtis, M.T., D. Gilfor, and J.L. Farber, *Lipid peroxidation increases the molecular order of microsomal membranes*. Arch Biochem Biophys, 1984. **235**(2): p. 644-9.
145. Schachter, D., *Fluidity and function of hepatocyte plasma membranes*. Hepatology, 1984. **4**(1): p. 140-51.
146. Foretz, M., F. Foufelle, and P. Ferre, *Polyunsaturated fatty acids inhibit fatty acid synthase and spot-14-protein gene expression in cultured rat hepatocytes by a peroxidative mechanism*. Biochem J, 1999. **341** (Pt 2): p. 371-6.
147. Brunet, S., et al., *Dietary iron overload and induced lipid peroxidation are associated with impaired plasma lipid transport and hepatic sterol metabolism in rats*. Hepatology, 1999. **29**(6): p. 1809-17.
148. Fisher, A.L., et al., *Iron loading induces cholesterol synthesis and sensitizes endothelial cells to TNFalpha-mediated apoptosis*. J Biol Chem, 2021. **297**(4): p. 101156.
149. Drevon, C.A., S.C. Engelhorn, and D. Steinberg, *Secretion of very low density lipoproteins enriched in cholesteryl esters by cultured rat hepatocytes during simulation of intracellular cholesterol esterification*. J Lipid Res, 1980. **21**(8): p. 1065-71.
150. Padda, R.S., et al., *A high-fat diet modulates iron metabolism but does not promote liver fibrosis in hemochromatotic HJV(-)/(-) mice*. Am J Physiol Gastrointest Liver Physiol, 2015. **308**(4): p. G251-61.
151. McLachlan, S., et al., *Hamp1 mRNA and plasma hepcidin levels are influenced by sex and strain but do not predict tissue iron levels in inbred mice*. Am J Physiol Gastrointest Liver Physiol, 2017. **313**(5): p. G511-G523.
152. Wei, Y., et al., *Nonalcoholic fatty liver disease and mitochondrial dysfunction*. World J Gastroenterol, 2008. **14**(2): p. 193-9.
153. Atig, R.K., et al., *[Mitochondrial DNA: properties and applications]*. Arch Inst Pasteur Tunis, 2009. **86**(1-4): p. 3-14.
154. Fromenty, B., *Alteration of mitochondrial DNA homeostasis in drug-induced liver injury*. Food Chem Toxicol, 2020. **135**: p. 110916.
155. Rao, M.S. and J.K. Reddy, *PPARalpha in the pathogenesis of fatty liver disease*. Hepatology, 2004. **40**(4): p. 783-6.
156. Reddy, J.K. and T. Hashimoto, *Peroxisomal beta-oxidation and peroxisome proliferator-activated receptor alpha: an adaptive metabolic system*. Annu Rev Nutr, 2001. **21**: p. 193-230.
157. Jansen, G.A. and R.J. Wanders, *Alpha-oxidation*. Biochim Biophys Acta, 2006. **1763**(12): p. 1403-12.
158. Pessayre, D. and B. Fromenty, *NASH: a mitochondrial disease*. J Hepatol, 2005. **42**(6): p. 928-40.
159. Ibdah, J.A., et al., *Mice heterozygous for a defect in mitochondrial trifunctional protein develop hepatic steatosis and insulin resistance*. Gastroenterology, 2005. **128**(5): p. 1381-90.
160. Glick, D., et al., *BNIP3 regulates mitochondrial function and lipid metabolism in the liver*. Mol Cell Biol, 2012. **32**(13): p. 2570-84.
161. Kim, H.J., et al., *Liver-specific deletion of RORalpha aggravates diet-induced nonalcoholic steatohepatitis by inducing mitochondrial dysfunction*. Sci Rep, 2017. **7**(1): p. 16041.
162. Han, Y.H., et al., *RORalpha decreases oxidative stress through the induction of SOD2 and GPx1 expression and thereby protects against nonalcoholic steatohepatitis in mice*. Antioxid Redox Signal, 2014. **21**(15): p. 2083-94.

163. Ou, Z., et al., *Regulation of the human hydroxysteroid sulfotransferase (SULT2A1) by RORalpha and RORgamma and its potential relevance to human liver diseases*. Mol Endocrinol, 2013. **27**(1): p. 106-15.
164. Kim, E.J., et al., *Retinoic acid receptor-related orphan receptor alpha-induced activation of adenosine monophosphate-activated protein kinase results in attenuation of hepatic steatosis*. Hepatology, 2012. **55**(5): p. 1379-88.
165. Torti, S.V. and F.M. Torti, *Iron and cancer: more ore to be mined*. Nat Rev Cancer, 2013. **13**(5): p. 342-55.
166. Richardson, D.R., et al., *Mitochondrial iron trafficking and the integration of iron metabolism between the mitochondrion and cytosol*. Proc Natl Acad Sci U S A, 2010. **107**(24): p. 10775-82.
167. Nie, G., et al., *Overexpression of mitochondrial ferritin causes cytosolic iron depletion and changes cellular iron homeostasis*. Blood, 2005. **105**(5): p. 2161-7.
168. Petrat, F., H. de Groot, and U. Rauen, *Subcellular distribution of chelatable iron: a laser scanning microscopic study in isolated hepatocytes and liver endothelial cells*. Biochem J, 2001. **356**(Pt 1): p. 61-9.
169. Petrat, F., et al., *The chelatable iron pool in living cells: a methodically defined quantity*. Biol Chem, 2002. **383**(3-4): p. 489-502.
170. Glickstein, H., et al., *Intracellular labile iron pools as direct targets of iron chelators: a fluorescence study of chelator action in living cells*. Blood, 2005. **106**(9): p. 3242-50.
171. Chang, H.C., et al., *Reduction in mitochondrial iron alleviates cardiac damage during injury*. EMBO Mol Med, 2016. **8**(3): p. 247-67.
172. Grattagliano, I., et al., *Role of mitochondria in nonalcoholic fatty liver disease--from origin to propagation*. Clin Biochem, 2012. **45**(9): p. 610-8.
173. Nassir, F. and J.A. Ibdah, *Role of mitochondria in nonalcoholic fatty liver disease*. Int J Mol Sci, 2014. **15**(5): p. 8713-42.
174. Paul, B.T., et al., *Mitochondria and Iron: current questions*. Expert Rev Hematol, 2017. **10**(1): p. 65-79.
175. Breuer, W., S. Epsztejn, and Z.I. Cabantchik, *Iron acquired from transferrin by K562 cells is delivered into a cytoplasmic pool of chelatable iron(II)*. J Biol Chem, 1995. **270**(41): p. 24209-15.
176. Flatmark, T. and I. Romslo, *Energy-dependent accumulation of iron by isolated rat liver mitochondria. Requirement of reducing equivalents and evidence for a unidirectional flux of Fe(II) across the inner membrane*. J Biol Chem, 1975. **250**(16): p. 6433-8.
177. Lange, H., G. Kispal, and R. Lill, *Mechanism of iron transport to the site of heme synthesis inside yeast mitochondria*. J Biol Chem, 1999. **274**(27): p. 18989-96.
178. Hamdi, A., et al., *Erythroid cell mitochondria receive endosomal iron by a "kiss-and-run" mechanism*. Biochim Biophys Acta, 2016. **1863**(12): p. 2859-2867.
179. Sheftel, A.D., et al., *Direct interorganellar transfer of iron from endosome to mitochondrion*. Blood, 2007. **110**(1): p. 125-32.
180. Richardson, D.R., P. Ponka, and D. Vyoral, *Distribution of iron in reticulocytes after inhibition of heme synthesis with succinylacetone: examination of the intermediates involved in iron metabolism*. Blood, 1996. **87**(8): p. 3477-88.
181. Lutsenko, S., *Human copper homeostasis: a network of interconnected pathways*. Curr Opin Chem Biol, 2010. **14**(2): p. 211-7.
182. Shi, H., et al., *A cytosolic iron chaperone that delivers iron to ferritin*. Science, 2008. **320**(5880): p. 1207-10.
183. Muhlenhoff, U., et al., *Cytosolic monothiol glutaredoxins function in intracellular iron sensing and trafficking via their bound iron-sulfur cluster*. Cell Metab, 2010. **12**(4): p. 373-385.
184. Lane, D.J., et al., *Cellular iron uptake, trafficking and metabolism: Key molecules and mechanisms and their roles in disease*. Biochim Biophys Acta, 2015. **1853**(5): p. 1130-44.

185. Wolff, N.A., et al., *A role for divalent metal transporter (DMT1) in mitochondrial uptake of iron and manganese*. Sci Rep, 2018. **8**(1): p. 211.
186. Wolff, N.A., et al., *Evidence for mitochondrial localization of divalent metal transporter 1 (DMT1)*. FASEB J, 2014. **28**(5): p. 2134-45.
187. Wolff, N.A., et al., *Mitochondria represent another locale for the divalent metal transporter 1 (DMT1)*. Channels (Austin), 2014. **8**(5): p. 458-66.
188. Petrat, F., U. Rauen, and H. de Groot, *Determination of the chelatable iron pool of isolated rat hepatocytes by digital fluorescence microscopy using the fluorescent probe, phen green SK*. Hepatology, 1999. **29**(4): p. 1171-9.
189. Mackenzie, B., et al., *Divalent metal-ion transporter DMT1 mediates both H⁺-coupled Fe²⁺ transport and uncoupled fluxes*. Pflugers Arch, 2006. **451**(4): p. 544-58.
190. Shaw, G.C., et al., *Mitoferrin is essential for erythroid iron assimilation*. Nature, 2006. **440**(7080): p. 96-100.
191. Paradkar, P.N., et al., *Regulation of mitochondrial iron import through differential turnover of mitoferrin 1 and mitoferrin 2*. Mol Cell Biol, 2009. **29**(4): p. 1007-16.
192. Chen, W., et al., *Abcb10 physically interacts with mitoferrin-1 (Slc25a37) to enhance its stability and function in the erythroid mitochondria*. Proc Natl Acad Sci U S A, 2009. **106**(38): p. 16263-8.
193. Chen, W., H.A. Dailey, and B.H. Paw, *Ferrochelatase forms an oligomeric complex with mitoferrin-1 and Abcb10 for erythroid heme biosynthesis*. Blood, 2010. **116**(4): p. 628-30.
194. Gao, X., et al., *Mitochondrial DNA damage in iron overload*. J Biol Chem, 2009. **284**(8): p. 4767-75.
195. Jouihan, H.A., et al., *Iron-mediated inhibition of mitochondrial manganese uptake mediates mitochondrial dysfunction in a mouse model of hemochromatosis*. Mol Med, 2008. **14**(3-4): p. 98-108.
196. Furuhashi, M. and G.S. Hotamisligil, *Fatty acid-binding proteins: role in metabolic diseases and potential as drug targets*. Nat Rev Drug Discov, 2008. **7**(6): p. 489-503.
197. Casares, D., P.V. Escriba, and C.A. Rossello, *Membrane Lipid Composition: Effect on Membrane and Organelle Structure, Function and Compartmentalization and Therapeutic Avenues*. Int J Mol Sci, 2019. **20**(9).
198. Wojtczak, L. and P. Schonfeld, *Effect of fatty acids on energy coupling processes in mitochondria*. Biochim Biophys Acta, 1993. **1183**(1): p. 41-57.
199. Feldkamp, T., et al., *Evidence for involvement of nonesterified fatty acid-induced protonophoric uncoupling during mitochondrial dysfunction caused by hypoxia and reoxygenation*. Nephrol Dial Transplant, 2009. **24**(1): p. 43-51.
200. Cole, M.A., et al., *A high fat diet increases mitochondrial fatty acid oxidation and uncoupling to decrease efficiency in rat heart*. Basic Res Cardiol, 2011. **106**(3): p. 447-57.
201. Bernardi, P., *Mitochondrial transport of cations: channels, exchangers, and permeability transition*. Physiol Rev, 1999. **79**(4): p. 1127-55.
202. Penzo, D., et al., *Effects of fatty acids on mitochondria: implications for cell death*. Biochim Biophys Acta, 2002. **1555**(1-3): p. 160-5.
203. Ricchi, M., et al., *Differential effect of oleic and palmitic acid on lipid accumulation and apoptosis in cultured hepatocytes*. J Gastroenterol Hepatol, 2009. **24**(5): p. 830-40.
204. Li, Z., et al., *The lysosomal-mitochondrial axis in free fatty acid-induced hepatic lipotoxicity*. Hepatology, 2008. **47**(5): p. 1495-503.
205. Kidman, C.J., et al., *Tracking biochemical changes induced by iron loading in AML12 cells with synchrotron live cell, time-lapse infrared microscopy*. Biochem J, 2021. **478**(6): p. 1227-1239.
206. Herbison, C.E., et al., *The role of transferrin receptor 1 and 2 in transferrin-bound iron uptake in human hepatoma cells*. Am J Physiol Cell Physiol, 2009. **297**(6): p. C1567-75.

207. Crowe, A. and E.H. Morgan, *Iron and copper interact during their uptake and deposition in the brain and other organs of developing rats exposed to dietary excess of the two metals*. J Nutr, 1996. **126**(1): p. 183-94.
208. McDonald, C.J., et al., *Increased iron stores correlate with worse disease outcomes in a mouse model of schistosomiasis infection*. PLoS One, 2010. **5**(3): p. e9594.
209. Kohn-Gaone, J., et al., *Divergent Inflammatory, Fibrogenic, and Liver Progenitor Cell Dynamics in Two Common Mouse Models of Chronic Liver Injury*. Am J Pathol, 2016. **186**(7): p. 1762-1774.
210. Frezza, C., S. Cipolat, and L. Scorrano, *Organelle isolation: functional mitochondria from mouse liver, muscle and cultured fibroblasts*. Nat Protoc, 2007. **2**(2): p. 287-95.
211. Peng, K.Y., et al., *Mitochondrial dysfunction-related lipid changes occur in nonalcoholic fatty liver disease progression*. J Lipid Res, 2018. **59**(10): p. 1977-1986.
212. Degli Esposti, D., et al., *Mitochondrial roles and cytoprotection in chronic liver injury*. Biochem Res Int, 2012. **2012**: p. 387626.
213. Handa, P., et al., *Iron alters macrophage polarization status and leads to steatohepatitis and fibrogenesis*. J Leukoc Biol, 2019. **105**(5): p. 1015-1026.
214. Carlessi, R., et al., *GLP-1 receptor signalling promotes beta-cell glucose metabolism via mTOR-dependent HIF-1alpha activation*. Sci Rep, 2017. **7**(1): p. 2661.
215. Cheng, J., et al., *Mitochondrial Proton Leak Plays a Critical Role in Pathogenesis of Cardiovascular Diseases*. Adv Exp Med Biol, 2017. **982**: p. 359-370.
216. Divakaruni, A.S., et al., *Analysis and interpretation of microplate-based oxygen consumption and pH data*. Methods Enzymol, 2014. **547**: p. 309-54.
217. Brand, M.D. and D.G. Nicholls, *Assessing mitochondrial dysfunction in cells*. Biochem J, 2011. **435**(2): p. 297-312.
218. Datz, C., E. Muller, and E. Aigner, *Iron overload and non-alcoholic fatty liver disease*. Minerva Endocrinol, 2017. **42**(2): p. 173-183.
219. Moravcova, A., et al., *The effect of oleic and palmitic acid on induction of steatosis and cytotoxicity on rat hepatocytes in primary culture*. Physiol Res, 2015. **64 Suppl 5**: p. S627-36.
220. Chen, H.J., et al., *Response to iron overload in cultured hepatocytes*. Sci Rep, 2020. **10**(1): p. 21184.
221. Eynaudi, A., et al., *Differential Effects of Oleic and Palmitic Acids on Lipid Droplet-Mitochondria Interaction in the Hepatic Cell Line HepG2*. Front Nutr, 2021. **8**: p. 775382.
222. Leonard, S.S., G.K. Harris, and X. Shi, *Metal-induced oxidative stress and signal transduction*. Free Radic Biol Med, 2004. **37**(12): p. 1921-42.
223. Gluchowski, N.L., et al., *Lipid droplets and liver disease: from basic biology to clinical implications*. Nat Rev Gastroenterol Hepatol, 2017. **14**(6): p. 343-355.
224. Nobes, C.D., W.W. Hay, Jr., and M.D. Brand, *The mechanism of stimulation of respiration by fatty acids in isolated hepatocytes*. J Biol Chem, 1990. **265**(22): p. 12910-5.
225. Oexle, H., E. Gnaiger, and G. Weiss, *Iron-dependent changes in cellular energy metabolism: influence on citric acid cycle and oxidative phosphorylation*. Biochim Biophys Acta, 1999. **1413**(3): p. 99-107.
226. Esteve, S., et al., *Morphofunctional responses to anaemia in rat skeletal muscle*. J Anat, 2008. **212**(6): p. 836-44.
227. Ackrell, B.A., et al., *Effect of iron deficiency on succinate- and NADH-ubiquinone oxidoreductases in skeletal muscle mitochondria*. J Biol Chem, 1984. **259**(16): p. 10053-9.
228. Davies, K.J., et al., *Distinguishing effects of anemia and muscle iron deficiency on exercise bioenergetics in the rat*. Am J Physiol, 1984. **246**(6 Pt 1): p. E535-43.
229. Dranka, B.P., B.G. Hill, and V.M. Darley-Usmar, *Mitochondrial reserve capacity in endothelial cells: The impact of nitric oxide and reactive oxygen species*. Free Radic Biol Med, 2010. **48**(7): p. 905-14.

230. Hill, B.G., et al., *Integration of cellular bioenergetics with mitochondrial quality control and autophagy*. Biol Chem, 2012. **393**(12): p. 1485-1512.
231. Motlagh Scholle, L., et al., *Palmitate but Not Oleate Exerts a Negative Effect on Oxygen Utilization in Myoblasts of Patients with the m.3243A>G Mutation: A Pilot Study*. Life (Basel), 2020. **10**(9).
232. Chen, X., et al., *Oleic acid protects saturated fatty acid mediated lipotoxicity in hepatocytes and rat of non-alcoholic steatohepatitis*. Life Sci, 2018. **203**: p. 291-304.
233. Courselaud, B., et al., *Strain and gender modulate hepatic hepcidin 1 and 2 mRNA expression in mice*. Blood Cells Mol Dis, 2004. **32**(2): p. 283-9.
234. Krijt, J., et al., *Different expression pattern of hepcidin genes in the liver and pancreas of C57BL/6N and DBA/2N mice*. J Hepatol, 2004. **40**(6): p. 891-6.
235. McDonald, C.J., et al., *Parenteral vs. oral iron: influence on hepcidin signaling pathways through analysis of Hfe/Tfr2-null mice*. Am J Physiol Gastrointest Liver Physiol, 2014. **306**(2): p. G132-9.
236. Corradini, E., et al., *Serum and liver iron differently regulate the bone morphogenetic protein 6 (BMP6)-SMAD signaling pathway in mice*. Hepatology, 2011. **54**(1): p. 273-84.
237. Fleming, R.E., et al., *Mouse strain differences determine severity of iron accumulation in Hfe knockout model of hereditary hemochromatosis*. Proc Natl Acad Sci U S A, 2001. **98**(5): p. 2707-11.
238. Rishi, G., E.S. Secondes, and V. Nathan Subramaniam, *Hemochromatosis: Evaluation of the dietary iron model and regulation of hepcidin*. Biochim Biophys Acta Mol Basis Dis, 2018. **1864**(8): p. 2550-2556.
239. Sohal, R.S., et al., *Effect of age and caloric restriction on bleomycin-chelatable and nonheme iron in different tissues of C57BL/6 mice*. Free Radic Biol Med, 1999. **27**(3-4): p. 287-93.
240. den Elzen, W.P., et al., *Plasma hepcidin levels and anemia in old age. The Leiden 85-Plus Study*. Haematologica, 2013. **98**(3): p. 448-54.
241. Reddy, J.K. and M.S. Rao, *Lipid metabolism and liver inflammation. II. Fatty liver disease and fatty acid oxidation*. Am J Physiol Gastrointest Liver Physiol, 2006. **290**(5): p. G852-8.
242. Ward, D.M. and S.M. Cloonan, *Mitochondrial Iron in Human Health and Disease*. Annu Rev Physiol, 2019. **81**: p. 453-482.
243. Volani, C., et al., *Dietary iron loading negatively affects liver mitochondrial function*. Metallomics, 2017. **9**(11): p. 1634-1644.
244. Handa, P., et al., *Iron overload results in hepatic oxidative stress, immune cell activation, and hepatocellular ballooning injury, leading to nonalcoholic steatohepatitis in genetically obese mice*. Am J Physiol Gastrointest Liver Physiol, 2016. **310**(2): p. G117-27.
245. Zheng, Q., et al., *Iron overload promotes mitochondrial fragmentation in mesenchymal stromal cells from myelodysplastic syndrome patients through activation of the AMPK/MFF/Drp1 pathway*. Cell Death Dis, 2018. **9**(5): p. 515.
246. Solsona-Vilarrasa, E., et al., *Cholesterol enrichment in liver mitochondria impairs oxidative phosphorylation and disrupts the assembly of respiratory supercomplexes*. Redox Biol, 2019. **24**: p. 101214.
247. Hou, Y., et al., *Estrogen regulates iron homeostasis through governing hepatic hepcidin expression via an estrogen response element*. Gene, 2012. **511**(2): p. 398-403.
248. MacKenzie, E.L., K. Iwasaki, and Y. Tsuji, *Intracellular iron transport and storage: from molecular mechanisms to health implications*. Antioxid Redox Signal, 2008. **10**(6): p. 997-1030.
249. Casey, J.L., et al., *Iron-responsive elements: regulatory RNA sequences that control mRNA levels and translation*. Science, 1988. **240**(4854): p. 924-8.
250. Begrich, K., et al., *Mitochondrial adaptations and dysfunctions in nonalcoholic fatty liver disease*. Hepatology, 2013. **58**(4): p. 1497-507.

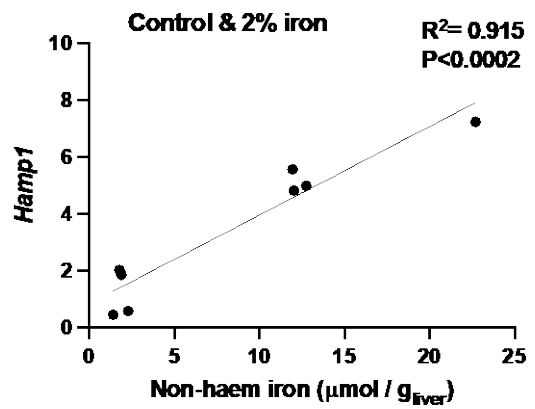
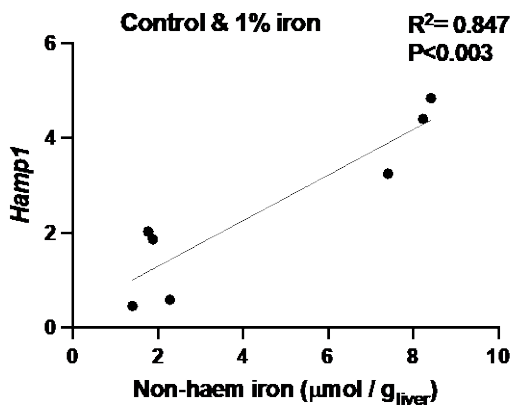
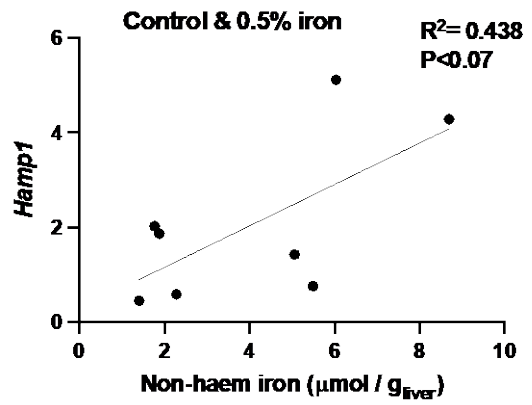
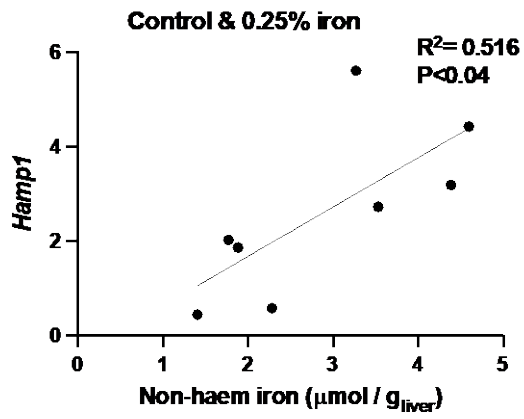
251. Huang, J., et al., *Iron overload and diabetes risk: a shift from glucose to Fatty Acid oxidation and increased hepatic glucose production in a mouse model of hereditary hemochromatosis*. *Diabetes*, 2011. **60**(1): p. 80-7.
252. Kremastinos, D.T. and D. Farmakis, *Iron overload cardiomyopathy in clinical practice*. *Circulation*, 2011. **124**(20): p. 2253-63.
253. Milic, S., et al., *The Role of Iron and Iron Overload in Chronic Liver Disease*. *Med Sci Monit*, 2016. **22**: p. 2144-51.
254. Masarone, M., et al., *Role of Oxidative Stress in Pathophysiology of Nonalcoholic Fatty Liver Disease*. *Oxid Med Cell Longev*, 2018. **2018**: p. 9547613.
255. Mohamed, M. and J. Phillips, *Hereditary haemochromatosis*. *BMJ*, 2016. **353**: p. i3128.
256. Adams, P.C., et al., *The relationship between iron overload, clinical symptoms, and age in 410 patients with genetic hemochromatosis*. *Hepatology*, 1997. **25**(1): p. 162-6.
257. Newton, J.L., *Systemic symptoms in non-alcoholic fatty liver disease*. *Dig Dis*, 2010. **28**(1): p. 214-9.
258. Newton, J.L., et al., *Fatigue in non-alcoholic fatty liver disease (NAFLD) is significant and associates with inactivity and excessive daytime sleepiness but not with liver disease severity or insulin resistance*. *Gut*, 2008. **57**(6): p. 807-13.
259. BRANISSO, P.P.F., et al., *Iron-Overload Evaluation by Noninvasive Methods in Patients with Nonalcoholic Fatty Liver Disease, Overweight, and Hyperferritinemia*. *Diabetes*, 2018. **67**(Supplement 1): p. 292-LB.
260. Arguello, G., et al., *Recent insights on the role of cholesterol in non-alcoholic fatty liver disease*. *Biochim Biophys Acta*, 2015. **1852**(9): p. 1765-78.
261. Wan, X., et al., *Role of NLRP3 Inflammasome in the Progression of NAFLD to NASH*. *Can J Gastroenterol Hepatol*, 2016. **2016**: p. 6489012.
262. Bloomer, S.A. and K.E. Brown, *Iron-Induced Liver Injury: A Critical Reappraisal*. *Int J Mol Sci*, 2019. **20**(9).
263. Atarashi, M., et al., *[The role of iron overload in the progression of nonalcoholic steatohepatitis (NASH)]*. *Nihon Yakurigaku Zasshi*, 2019. **154**(2): p. 61-65.
264. Atarashi, M., et al., *Dietary Iron Supplementation Alters Hepatic Inflammation in a Rat Model of Nonalcoholic Steatohepatitis*. *Nutrients*, 2018. **10**(2).
265. Robinson, M.W., C. Harmon, and C. O'Farrelly, *Liver immunology and its role in inflammation and homeostasis*. *Cell Mol Immunol*, 2016. **13**(3): p. 267-76.
266. Schuster, S., et al., *Triggering and resolution of inflammation in NASH*. *Nat Rev Gastroenterol Hepatol*, 2018. **15**(6): p. 349-364.
267. Barisani, D., et al., *Hepcidin and iron-related gene expression in subjects with Dysmetabolic Hepatic Iron Overload*. *J Hepatol*, 2008. **49**(1): p. 123-33.
268. Katsarou, A., et al., *Tissue-Specific Regulation of Ferroportin in Wild-Type and HJV^{-/-} Mice Following Dietary Iron Manipulations*. *Hepatol Commun*, 2021. **5**(12): p. 2139-2150.
269. Nsiah-Sefaa, A. and M. McKenzie, *Combined defects in oxidative phosphorylation and fatty acid beta-oxidation in mitochondrial disease*. *Biosci Rep*, 2016. **36**(2).
270. Kamijo, T., et al., *Structural analysis of cDNAs for subunits of human mitochondrial fatty acid beta-oxidation trifunctional protein*. *Biochem Biophys Res Commun*, 1994. **199**(2): p. 818-25.
271. Carpenter, K., R.J. Pollitt, and B. Middleton, *Human liver long-chain 3-hydroxyacyl-coenzyme A dehydrogenase is a multifunctional membrane-bound beta-oxidation enzyme of mitochondria*. *Biochem Biophys Res Commun*, 1992. **183**(2): p. 443-8.
272. Schonfeld, P. and L. Wojtczak, *Short- and medium-chain fatty acids in energy metabolism: the cellular perspective*. *J Lipid Res*, 2016. **57**(6): p. 943-54.
273. Lombard, M., E. Chua, and P. O'Toole, *Regulation of intestinal non-haem iron absorption*. *Gut*, 1997. **40**(4): p. 435-9.
274. Dupic, F., et al., *Duodenal mRNA expression of iron related genes in response to iron loading and iron deficiency in four strains of mice*. *Gut*, 2002. **51**(5): p. 648-53.

275. Camberlein, E., et al., *Hepcidin induction limits mobilisation of splenic iron in a mouse model of secondary iron overload*. *Biochim Biophys Acta*, 2010. **1802**(3): p. 339-46.
276. Wang, F., et al., *Genetic variation in Mon1a affects protein trafficking and modifies macrophage iron loading in mice*. *Nat Genet*, 2007. **39**(8): p. 1025-32.
277. da Silva-Santi, L.G., et al., *Liver Fatty Acid Composition and Inflammation in Mice Fed with High-Carbohydrate Diet or High-Fat Diet*. *Nutrients*, 2016. **8**(11).
278. Schreck, R., et al., *Dithiocarbamates as potent inhibitors of nuclear factor kappa B activation in intact cells*. *J Exp Med*, 1992. **175**(5): p. 1181-94.
279. Das, S.K., et al., *Resveratrol mediates therapeutic hepatic effects in acquired and genetic murine models of iron-overload*. *Liver Int*, 2016. **36**(2): p. 246-57.
280. Brown, K.E., et al., *Chronic iron overload stimulates hepatocyte proliferation and cyclin D1 expression in rodent liver*. *Transl Res*, 2006. **148**(2): p. 55-62.
281. Subramanian, S., et al., *Dietary cholesterol exacerbates hepatic steatosis and inflammation in obese LDL receptor-deficient mice*. *J Lipid Res*, 2011. **52**(9): p. 1626-35.
282. Brown, K.E., et al., *Effect of vitamin E supplementation on hepatic fibrogenesis in chronic dietary iron overload*. *Am J Physiol*, 1997. **272**(1 Pt 1): p. G116-23.
283. Park, C.H., et al., *Pathology of dietary carbonyl iron overload in rats*. *Lab Invest*, 1987. **57**(5): p. 555-63.
284. Nielsen, P. and H.C. Heinrich, *Metabolism of iron from (3,5,5-trimethylhexanoyl)ferrocene in rats. A dietary model for severe iron overload*. *Biochem Pharmacol*, 1993. **45**(2): p. 385-91.
285. Bacon, B.R., et al., *Hepatic lipid peroxidation in vivo in rats with chronic iron overload*. *J Clin Invest*, 1983. **71**(3): p. 429-39.
286. Asare, G.A., et al., *Iron-free neoplastic nodules and hepatocellular carcinoma without cirrhosis in Wistar rats fed a diet high in iron*. *J Pathol*, 2006. **208**(1): p. 82-90.
287. Brown, K.E., et al., *Effect of iron overload and dietary fat on indices of oxidative stress and hepatic fibrogenesis in rats*. *Liver Int*, 2003. **23**(4): p. 232-42.
288. Shi, Z., A.E. Wakil, and D.C. Rokey, *Strain-specific differences in mouse hepatic wound healing are mediated by divergent T helper cytokine responses*. *Proc Natl Acad Sci U S A*, 1997. **94**(20): p. 10663-8.
289. Li, X., et al., *Isocaloric Pair-Fed High-Carbohydrate Diet Induced More Hepatic Steatosis and Inflammation than High-Fat Diet Mediated by miR-34a/SIRT1 Axis in Mice*. *Sci Rep*, 2015. **5**: p. 16774.
290. Ioannou, G.N., et al., *Cholesterol crystallization within hepatocyte lipid droplets and its role in murine NASH*. *J Lipid Res*, 2017. **58**(6): p. 1067-1079.
291. Bozaykut, P., et al., *Endoplasmic reticulum stress related molecular mechanisms in nonalcoholic steatohepatitis*. *Mech Ageing Dev*, 2016. **157**: p. 17-29.
292. Varsano, N., et al., *Two polymorphic cholesterol monohydrate crystal structures form in macrophage culture models of atherosclerosis*. *Proc Natl Acad Sci U S A*, 2018. **115**(30): p. 7662-7669.
293. Wang, L., et al., *Nonalcoholic fatty liver disease experiences accumulation of hepatic liquid crystal associated with increasing lipophagy*. *Cell Biosci*, 2020. **10**: p. 55.
294. Velazquez, K.T., et al., *Prolonged high-fat-diet feeding promotes non-alcoholic fatty liver disease and alters gut microbiota in mice*. *World J Hepatol*, 2019. **11**(8): p. 619-637.
295. Chua, A.C., et al., *Iron uptake from plasma transferrin by a transferrin receptor 2 mutant mouse model of haemochromatosis*. *J Hepatol*, 2010. **52**(3): p. 425-31.
296. Nunez, M.T., et al., *Iron supply determines apical/basolateral membrane distribution of intestinal iron transporters DMT1 and ferroportin 1*. *Am J Physiol Cell Physiol*, 2010. **298**(3): p. C477-85.
297. Ahmed, U. and P.S. Oates, *Dietary fat level affects tissue iron levels but not the iron regulatory gene HAMP in rats*. *Nutr Res*, 2013. **33**(2): p. 126-35.

298. Krammer, J., et al., *Overexpression of CD36 and acyl-CoA synthetases FATP2, FATP4 and ACSL1 increases fatty acid uptake in human hepatoma cells*. *Int J Med Sci*, 2011. **8**(7): p. 599-614.
299. Ho, C.M., et al., *Accumulation of free cholesterol and oxidized low-density lipoprotein is associated with portal inflammation and fibrosis in nonalcoholic fatty liver disease*. *J Inflamm (Lond)*, 2019. **16**: p. 7.
300. Shu, F., et al., *Cholesterol Crystal-Mediated Inflammation Is Driven by Plasma Membrane Destabilization*. *Front Immunol*, 2018. **9**: p. 1163.
301. Prasnicka, A., et al., *Iron overload reduces synthesis and elimination of bile acids in rat liver*. *Sci Rep*, 2019. **9**(1): p. 9780.
302. Liu, H., et al., *Cholesterol 7alpha-hydroxylase protects the liver from inflammation and fibrosis by maintaining cholesterol homeostasis*. *J Lipid Res*, 2016. **57**(10): p. 1831-1844.
303. Liang, H., et al., *Effect of iron on cholesterol 7alpha-hydroxylase expression in alcohol-induced hepatic steatosis in mice*. *J Lipid Res*, 2017. **58**(8): p. 1548-1560.
304. Kohn-Gaone, J., et al., *The role of liver progenitor cells during liver regeneration, fibrogenesis, and carcinogenesis*. *Am J Physiol Gastrointest Liver Physiol*, 2016. **310**(3): p. G143-54.
305. Fujita, N. and Y. Takei, *Iron overload in nonalcoholic steatohepatitis*. *Adv Clin Chem*, 2011. **55**: p. 105-32.
306. Philippe, M.A., R.G. Ruddell, and G.A. Ramm, *Role of iron in hepatic fibrosis: one piece in the puzzle*. *World J Gastroenterol*, 2007. **13**(35): p. 4746-54.
307. Walter, P.B., et al., *Iron deficiency and iron excess damage mitochondria and mitochondrial DNA in rats*. *Proc Natl Acad Sci U S A*, 2002. **99**(4): p. 2264-9.
308. Kitamura, N., et al., *Iron supplementation regulates the progression of high fat diet induced obesity and hepatic steatosis via mitochondrial signaling pathways*. *Sci Rep*, 2021. **11**(1): p. 10753.
309. Parks, E., H. Yki-Jarvinen, and M. Hawkins, *Out of the frying pan: dietary saturated fat influences nonalcoholic fatty liver disease*. *J Clin Invest*, 2017. **127**(2): p. 454-456.
310. Sullivan, S., *Implications of diet on nonalcoholic fatty liver disease*. *Curr Opin Gastroenterol*, 2010. **26**(2): p. 160-4.
311. Liu, L., et al., *Low-Level Saturated Fatty Acid Palmitate Benefits Liver Cells by Boosting Mitochondrial Metabolism via CDK1-SIRT3-CPT2 Cascade*. *Dev Cell*, 2020. **52**(2): p. 196-209 e9.
312. Sorrentino, P., et al., *Liver iron excess in patients with hepatocellular carcinoma developed on non-alcoholic steato-hepatitis*. *J Hepatol*, 2009. **50**(2): p. 351-7.
313. Marmur, J., et al., *Hepcidin levels correlate to liver iron content, but not steatohepatitis, in non-alcoholic fatty liver disease*. *BMC Gastroenterol*, 2018. **18**(1): p. 78.
314. Modares Mousavi, S.R., et al., *Correlation between Serum Ferritin Level and Histopathological Disease Severity in Non-alcoholic Fatty Liver Disease*. *Middle East J Dig Dis*, 2018. **10**(2): p. 90-95.
315. Nassir, F., et al., *Regulation of mitochondrial trifunctional protein modulates nonalcoholic fatty liver disease in mice*. *J Lipid Res*, 2018. **59**(6): p. 967-973.
316. Zhou, T., et al., *Mst1 inhibition attenuates non-alcoholic fatty liver disease via reversing Parkin-related mitophagy*. *Redox Biol*, 2019. **21**: p. 101120.
317. Tan, T.C., et al., *Excess iron modulates endoplasmic reticulum stress-associated pathways in a mouse model of alcohol and high-fat diet-induced liver injury*. *Lab Invest*, 2013. **93**(12): p. 1295-312.
318. Gill, D., et al., *Associations of genetically determined iron status across the phenome: A mendelian randomization study*. *PLoS Med*, 2019. **16**(6): p. e1002833.
319. Tabas, I., *Consequences of cellular cholesterol accumulation: basic concepts and physiological implications*. *J Clin Invest*, 2002. **110**(7): p. 905-11.

320. Ioannou, G.N., et al., *Cholesterol-lowering drugs cause dissolution of cholesterol crystals and disperse Kupffer cell crown-like structures during resolution of NASH*. *J Lipid Res*, 2015. **56**(2): p. 277-85.

Appendix A



Appendix B

Control diet

Calculated Nutritional Parameters	
Protein	20.0%
Total Fat	8.6%
Total Digestible Carbohydrate	55.5%
Crude Fibre	4.7%
AD Fibre	4.7%
Digestible Energy	16.6 MJ / Kg
% Total calculated digestible energy from lipids	19.0%
% Total calculated digestible energy from protein	20.2%

High fat diet

Calculated Nutritional Parameters	
Protein	19.0%
Total Fat	21.0%
Crude Fibre	4.7%
AD Fibre	4.7%
Digestible Energy	19.4 MJ / Kg
% Total calculated digestible energy from lipids	40.0%
% Total calculated digestible energy from protein	17.0%



This is a License Agreement between Abhishek Kumar Singh ("User") and Copyright Clearance Center, Inc. ("CCC") on behalf of the Rightsholder identified in the order details below. The license consists of the order details, the Marketplace Permissions General Terms and Conditions below, and any Rightsholder Terms and Conditions which are included below.

All payments must be made in full to CCC in accordance with the Marketplace Permissions General Terms and Conditions below.

Order Date	14-Mar-2023	Type of Use	Republish in a thesis/dissertation
Order License ID	1333375-1	Publisher Portion	ANNUAL REVIEWS Image/photo/illustration
ISSN	1545-1585		

LICENSED CONTENT

Publication Title	Annual review of physiology	Country	United States of America
Author/Editor	American Physiological Society (1887-)	Rightsholder	Annual Reviews, Inc.
Date	01/01/1939	Publication Type	e-Journal
Language	English	URL	http://arjournals.annualreviews.org/loi/physiol

REQUEST DETAILS

Portion Type	Image/photo/illustration	Distribution	Worldwide
Number of Images / Photos / Illustrations	1	Translation	Original language of publication
Format (select all that apply)	Electronic	Copies for the Disabled?	No
Who Will Republish the Content?	Academic institution	Minor Editing Privileges?	No
Duration of Use	Life of current edition	Incidental Promotional Use?	No
Lifetime Unit Quantity	Up to 44,999	Currency	AUD
Rights Requested	Main product and any product related to main product		

NEW WORK DETAILS

Title	Dr	Institution Name	Curtin University
Instructor Name	Ross Graham	Expected Presentation Date	2023-03-31

ADDITIONAL DETAILS

Order Reference Number	N/A	The Requesting Person/Organization to Appear on the License	Abhishek Kumar Singh
-------------------------------	-----	--	----------------------



This is a License Agreement between Abhishek Kumar Singh ("User") and Copyright Clearance Center, Inc. ("CCC") on behalf of the Rightsholder identified in the order details below. The license consists of the order details, the Marketplace Permissions General Terms and Conditions below, and any Rightsholder Terms and Conditions which are included below.

All payments must be made in full to CCC in accordance with the Marketplace Permissions General Terms and Conditions below.

Order Date	14-Mar-2023	Type of Use	Republish in a thesis/dissertation
Order License ID	1333375-1	Publisher Portion	ANNUAL REVIEWS Image/photo/illustration
ISSN	1545-1585		

LICENSED CONTENT

Publication Title	Annual review of physiology	Country	United States of America
Author/Editor	American Physiological Society (1887-)	Rightsholder	Annual Reviews, Inc.
Date	01/01/1939	Publication Type	e-Journal
Language	English	URL	http://arjournals.annualreviews.org/loi/physiol

REQUEST DETAILS

Portion Type	Image/photo/illustration	Distribution	Worldwide
Number of Images / Photos / Illustrations	1	Translation	Original language of publication
Format (select all that apply)	Electronic	Copies for the Disabled?	No
Who Will Republish the Content?	Academic institution	Minor Editing Privileges?	No
Duration of Use	Life of current edition	Incidental Promotional Use?	No
Lifetime Unit Quantity	Up to 44,999	Currency	AUD
Rights Requested	Main product and any product related to main product		

NEW WORK DETAILS

Title	Dr	Institution Name	Curtin University
Instructor Name	Ross Graham	Expected Presentation Date	2023-03-31

ADDITIONAL DETAILS

Order Reference Number	N/A	The Requesting Person/Organization to Appear on the License	Abhishek Kumar Singh
-------------------------------	-----	--	----------------------